THE STRUCTURE OF THE ELECTRICAL DOUBLE LAYER AT THE METAL–SOLUTION INTERFACE

M. A. V. DEVANATHAN AND B. V. K. S. R. A. TILAK

Central Electrochemical Research Institute, Karaikudi 3, India

Received March 8, 1965

CONTENTS

I. Introduction 635
II. Thermodynamics 636
A. Ideally Polarizable Interfaces 636
B. Nonpolarizable Interfaces 636
III. Adsorption of Ions at the Mercury–Solution Interface under Ideally Polarizable Conditions 637
A. Methods of Evaluating the Components of Charge 637
B. Differential Capacity at Ideally Polarizable Interfaces 641
C. Differential Capacity at Nonpolarizable Interfaces 643
D. Nature of Specific Adsorption 644
E. Structure of the Electrical Double Layer 646
F. Inner Layer Capacity in the Absence of Specific Adsorption 650
G. Esin and Markov Effect 650
H. Ionic Isotherms 651
I. Capacitance Humps 653
J. The Minimum Capacity and the Cathodic Branch of the Differential Capacity Curves 654
IV. Adsorption of Organic Molecules at the Mercury–Solution Interface 655
A. Methods Used for the Evaluation of the Surface Excess of Organic Molecules 655
B. Potential Due to Permanent Dipoles at the Metal–Solution Interface 659
C. Theory of the Adsorption of Neutral Molecules 659
D. Isotherms for Organic Adsorption 661
E. Quantitative Theories of the Effect of the Electric Field on Adsorption 662
F. Adsorption of Organic Ions at the Mercury–Solution Interface 665
G. Role of Water at the Interface 667
V. Adsorption of Ions at the Mercury–Solution Interface in Nonaqueous Solvents 667
A. Organic Solvents (Bulk Dielectric Constant < 80) 668
B. Organic Solvents (Bulk Dielectric Constant > 80) 669
C. Inorganic Solvents 669
VI. Adsorption on Solid Metals in Aqueous Media 670
A. Electrocapillary Properties 670
B. Differential Capacity Studies 670
C. Determination of Point of Zero Charge on Solid Metals 671
D. Organic Adsorption 673
E. Isotherms for Organic Adsorption 674
VII. Electrical Double Layer in Molten Salts 675
A. Solid Metals 675
B. Liquid Metals 675
C. Electrocapillary Studies of Alloys and Amalgams (in Molten and Aqueous Media) 677
VIII. Nature and Significance of the Potential of the Electrocapillary Maximum 677
IX. Glossary of Symbols 679
X. References 680

I. INTRODUCTION

Since the classical review (127) of the electrical double layer by Grahame in 1947, several partial reviews (44, 55, 96, 105, 117, 132, 255, 260) have been published. The first by Parsons (255) in 1954 dealt with the problem of electrical potential differences in dissimilar media in great detail, owing to its importance in double layer theory. Recent advances in the thermodynamic treatment of interfaces were discussed, and the structural aspects were treated with emphasis on the specific adsorption of ions. A later review (260) also by Parsons in 1961 was concerned largely with the effects of the structure of the double layer on the kinetics of electrode process and the kinetics of adsorption of organic molecules. Frumkin's "Palladium Medal Address" (96) in 1960 is also concerned mainly with the effects of the electrical double layer on electrode kinetics. But a substantial portion deals with methods of determining the point of zero charge on solid metals. Frumkin's reviews (91, 93, 95, 97–99, 101, 104) and also a recent brief survey by Damaskin (44) provide references to the extensive

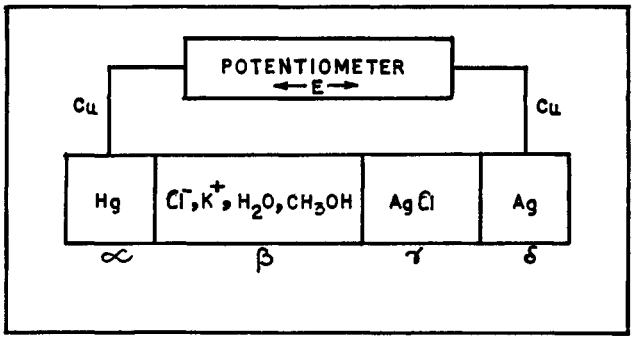

Figure 1.—Scheme for the ideally polarizable electrode system.

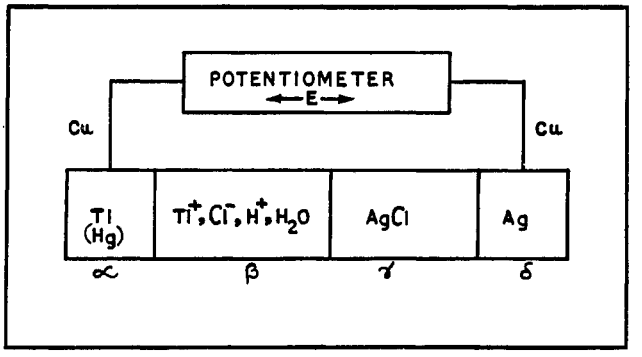

Figure 2.—Scheme for the nonpolarizable electrode system.

Soviet literature on interfacial phenomena. The adsorption of organic compounds at the metal solution interface is the subject of a very recent review by Frumkin and Damaskin (105). The structure of the electrical double layer at a semiconductor–electrolyte interface has been surveyed by Green (148), Gerischer (116), and Devanathan (60).

The present work is concerned with the adsorption of ions and organic molecules at the metal–solution interface and its theoretical treatment. The structure of the double layer at metal–nonaqueous solution interfaces and metal–molten salt interfaces is also discussed.

II. THERMODYNAMICS

Metal–solution interfaces can be classified into (i) ideally polarizable interfaces and (ii) nonpolarizable interfaces. The basis of the distinction arises from the absence or presence of a potential-determining ion, common to both sides of the interface. If a common ion is absent as is in the case of Hg–KCl(aq), then it is called an ideally polarizable interface. The characteristic of such an interface is that the potential difference across it can be altered at will with the aid of a suitable external circuit. In the case of nonpolarizable interfaces, *e.g.*, $Hg–Hg_2(NO_3)_2$, there is one ion common to both the phases, and the potential difference across the interface is determined by the Nernst equation and can be varied only by altering the chemical composition of the phases.

A. IDEALLY POLARIZABLE INTERFACES

The thermodynamic properties of ideally polarizable electrodes are adequately described by the electrocapillary equation which may be derived (a) by using thermodynamic cycles (40–42) and (b) by the direct application of the Gibbs adsorption equation (56, 146, 183, 265). Previous treatments (146, 183), which did not consider the reference electrode and the potentiometer as an essential part of the ideally polarizable electrode system, suffer from the disadvantage of containing a term involving the difference of inner potentials of the metal and the solution phase, in the basic electrocapillary equation

$$d\gamma + S_s\,dT = -q^\beta\,d(\phi^\beta - \phi^\alpha) + \Sigma\Gamma_i\,d\mu_i \quad \text{(Eq. 1)}$$

This restricts the application of Eq. 1 to systems in which there is no appreciable change in the solvent composition, and it cannot be used for mixtures of solvents. However, when one considers the entire system (Figure 1), an application of the concept of electrochemical equilibrium at every interface (except at the polarizable interface) yields the corresponding equation

$$d\gamma + S_s\,dT = -q^\alpha\,dE^- - \Gamma^\beta_{K^+}\,\partial\mu^\beta_{KCl} - \Gamma_{H_2O}\,\partial\mu_{H_2O} - \Gamma_{CH_3OH}\,\partial\mu_{CH_3OH} \quad \text{(Eq. 2)}$$

It may be noted that the equilibrium between phases α and β is not across the ideally polarizable interface but through a chain of nonpolarizable interfaces constituting the rest of the circuit. Or, in other words, there is no thermodynamic equilibrium directly across the interface, but only electrostatic, hydrostatic, and thermal equilibrium as in the case of a perfect condenser. The detailed derivation of Eq. 2 is given elsewhere (56, 255, 265).

B. NONPOLARIZABLE INTERFACES

The electrocapillary properties of nonpolarizable interfaces can also be treated in a similar manner. The system chosen is represented in Figure 2.

The Gibbs adsorption equation for the interface at constant temperature and pressure is

$$d\gamma = -\Gamma^\alpha_{Tl^+}\,d\bar{\mu}^\alpha_{Tl^+} - \Gamma^\alpha_{Hg_2^{2+}}\,d\bar{\mu}^\alpha_{Hg_2^{2+}} - \Gamma_{e_0}\,d\mu^\alpha_{e_0} - \Gamma^\beta_{Tl^+}\,d\bar{\mu}^\beta_{Tl^+} - \Gamma^\beta_{H^+}\,d\bar{\mu}^\beta_{H^+} - \Gamma^\beta_{Cl^-}\,d\bar{\mu}^\beta_{Cl^-} - \Gamma^\beta_{H_2O}\,d\mu^\beta_{H_2O} \quad \text{(Eq. 3)}$$

By following the electrochemical equilibria at each interface and imposing the condition of electroneutrality of the interface, it can be shown that

$$d\gamma = -(\Gamma^\alpha_{Tl^+} + \Gamma^\beta_{Tl^+})\,d\mu^\alpha_{Tl} - \Gamma^\alpha_{Hg_2^{2+}}\,d\mu^\alpha_{Hg} - \Gamma^\beta_{H^+}\,d\mu^\beta_{HCl} - \Gamma^\beta_{H_2O}\,d\mu^\beta_{H_2O} + (q^\beta - \Gamma^\beta_{Tl^+}\mathfrak{F})\,dE \quad \text{(Eq. 4)}$$

This is the basic electrocapillary equation for a nonpolarizable or reversible electrode system. A general derivation has been given by Mohilner (231).

For the above system, there is a unique potentiometer setting for every concentration of the potential-determining species. Any alteration in the potential will cause electrolysis. Since there is equilibrium directly across the interface, using the condition

$$\mu^{\alpha}_{Tl^+} = \mu^{\beta}_{Tl^+} \qquad \text{(Eq. 5)}$$

and noting that the Nernst equation gives

$$\mathfrak{F}\, dE = d\mu^{\beta}_{TlCl} \qquad \text{(Eq. 6)}$$

substitution of Eq. 5 and 6, in Eq. 3, gives an equation identical with Eq. 4. Thus for nonpolarizable electrodes, it is not necessary to consider the external circuit and the reference electrode.

If the amalgam concentration and HCl concentration are constant, one obtains the analog of Lippman's equation for reversible electrodes, *i.e.*

$$\left(\frac{\partial\gamma}{\partial E}\right)_{d\mu^{\alpha}_{Tl},\ \mu_{HCl},\ T,\ P\ldots} = (q^{\beta} - \Gamma^{\beta}_{Tl^+}\mathfrak{F}) = (\Gamma^{\beta}_{H^+} - \Gamma^{\beta}_{Cl^-})\mathfrak{F} \qquad \text{(Eq. 7)}$$

But when $a_{Tl^+} << a_{HCl}$, $\Gamma^{\beta}_{Tl^+}$ is likely to be very small compared to $\Gamma^{\beta}_{H^+}$ and hence

$$\left(\frac{\partial\gamma}{\partial E}\right)_{\mu^{\alpha}_{Tl},\ \mu_{HCl}\ldots} = q^{\beta} \qquad \text{(Eq. 8)}$$

Significant information on the structure of electrical double layer at nonpolarizable interfaces can be obtained with the aid of Eq. 4. Studies (184) have been made only for Hg in contact with $Hg_2(NO_3)_2$, HNO_3 and $Hg_2(ClO_4)_2$, $HClO_4$. These lead to the conclusion that nitrate ion is more adsorbed than ClO_4^- on mercury. This result, however, only confirms well-known facts and has not thrown any new light on the structure of nonpolarizable interfaces.

III. Adsorption of Ions at the Mercury–Solution Interface under Ideally Polarizable Conditions

A. Methods of Evaluating the Components of Charge

The following are at present the three methods available for obtaining the ionic surface concentrations.

1. Thermodynamic Method

According to the basic electrocapillary equation

$$\left(\frac{\partial\gamma}{\partial\mu_a}\right)_{E^{\pm}} = -\Gamma^{\pm} + \Gamma_{H_2O}\left(\frac{x_{salt}}{x_{H_2O}}\right) \qquad \text{(Eq. 9)}$$

For solutions of moderate concentrations, $\Gamma_{H_2O}(x_{salt}/x_{H_2O})$ can be neglected, and Eq. 9 yields the absolute value of surface concentration of the ion directly as a function of potential.

In order to plot Γ^- *vs.* q_M, q_M has to be obtained by graphical differentiation of the electrocapillary curve, which will invariably introduce errors of about ± 0.5 μc. near the point of zero charge and ± 1 μc. in the extremes. Figure 3 gives an example of a family of such curves. Alternatively one can obtain the charge and the interfacial tension data from the differential capacity curves by the application of the well-known thermodynamic relations

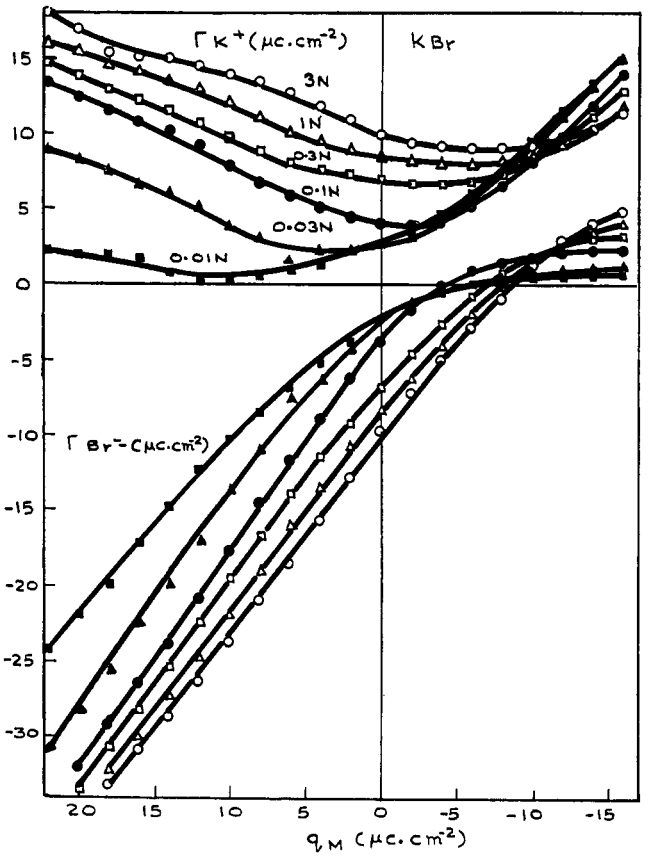

Figure 3.—Surface excess ($\Gamma_k{}^+$ and $\Gamma_{Br}{}^-$ in μc./cm.^{2}) curves on mercury for K^+ and Br^- ions from KBr solutions as a function of charge on the metal (q_M) at 25° (from the thermodynamic data of Peries (269)).

$$\iint_{E_{e.c.m}}^{E} C\, d^2E = \int_{E_{e.c.m}}^{E} q_M\, dE = \gamma_{e.c.m} - \gamma \qquad \text{(Eq. 10)}$$

The coordinates of e.c.m., *i.e.*, $E_{e.c.m}$ and $\gamma_{e.c.m}$ should be known in advance for the integration to be performed. Thus, from the charge curves obtained from differential capacity data, and $\Gamma^{\pm}$'s at constant E, one can minimize errors in the plots of $\Gamma^{\pm}$ *vs.* q_M. To avoid the above tedious procedure, Parsons (256) has formulated a new function

$$\xi^{\pm} = \gamma + q_M E^{\pm} \qquad \text{(Eq. 11)}$$

which when graphically differentiated gives directly the surface excess values at constant q_M.

$$\left(\frac{\partial\xi^{\pm}}{\partial\mu_a}\right)_{q_M} = \frac{\partial(\gamma + q_M E^{\pm})}{\partial\mu_a} = -\Gamma^{\pm} \qquad \text{(Eq. 12)}$$

This method can yield accurate Γ^+ values only when the q_M values are derived from the differential capacity data.

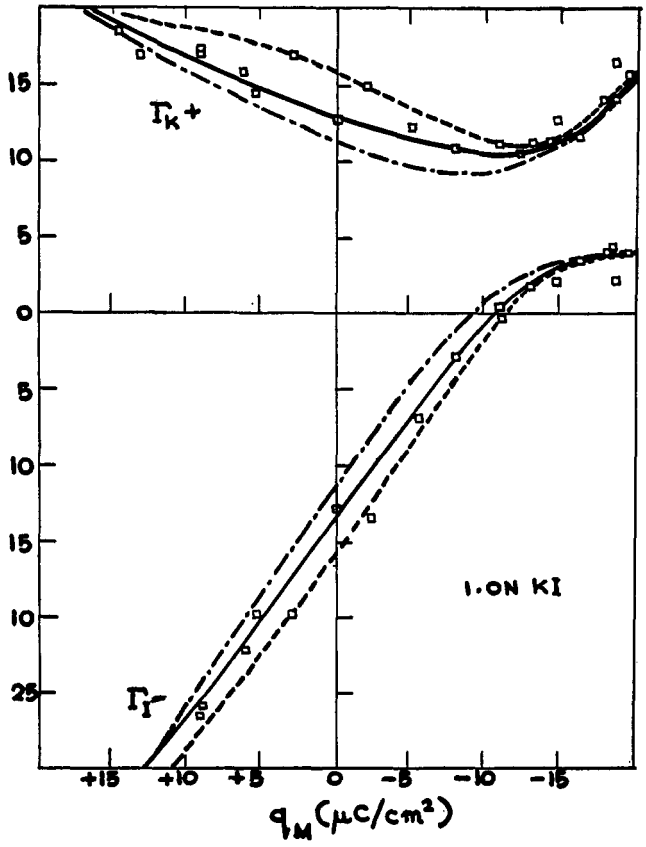

Figure 4.—Comparison of the components of charge (Γ_{K^+} and Γ_{I^-} in $\mu c./cm.^2$) evaluated by different methods for K^+ and I^- ions from 1.0 N KI solution on mercury at 25° (reproduced from ref. 62). —, thermodynamic data; ——, Grahame's method; -·-·-· Devanathan's method.

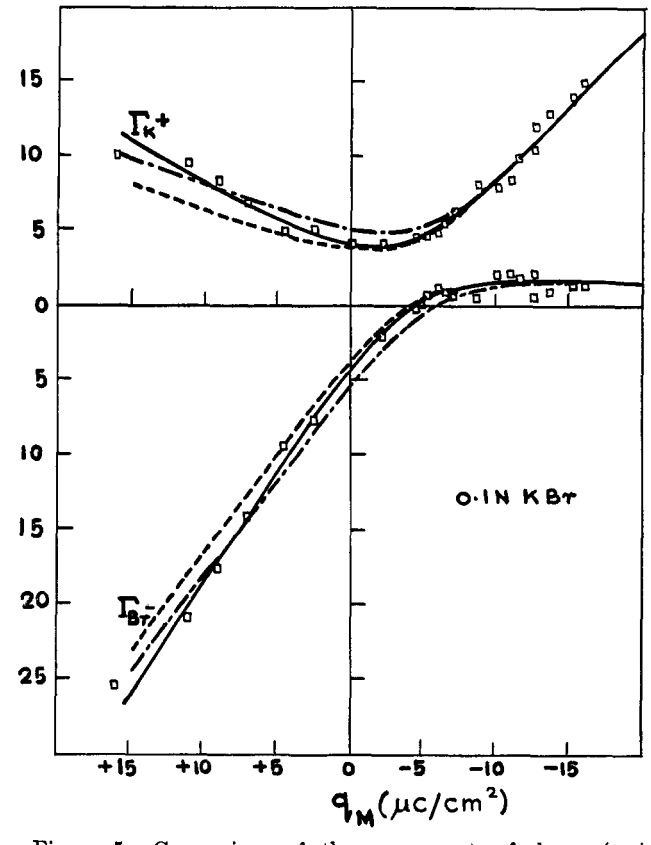

Figure 5.—Comparison of the components of charge (Γ_{K^+} and Γ_{Br^-} in $\mu c./cm.^2$) evaluated by different methods for K^+ and Br^- ions from 0.1 N KBr solution on mercury at 25° (reproduced from ref. 62). Symbols are the same as in Figure 4.

Thus the above methods require the knowledge of $E^{\pm}$ for graphical differentiation and computation of $\xi^{\pm}$. But it is not possible to obtain always a suitable reference electrode which is reversible to one of the ions in solution. Even if available, complications will come in at high concentrations. These difficulties have been surmounted by the elegant thermodynamic treatment due to Frumkin (92). If, in electrocapillary measurements, a reference electrode is used, its potential can be expressed in terms of an electrode reversible to one of the ions in solution (for 1:1 electrolytes) as

$$E_{ref} = E^{\pm} \pm \frac{RT}{\mathfrak{F}} \ln a_{\pm} + \text{constant} \quad \text{(Eq. 13)}$$

$$= E^{\pm} \pm \frac{1}{2\mathfrak{F}} \mu_a + \text{constant} \quad \text{(Eq. 14)}$$

This constant includes the liquid junction potential. The uncertainty due to liquid junction potentials has been overexaggerated. If one grants its constancy or neglects it (usually it is less than 1 mv. with a salt bridge), then the derivative $(\partial\gamma/\partial\mu_a)_{E_{ref}}$ is

$$\left(\frac{\partial\gamma}{\partial\mu_a}\right)_{E_{re}} = \left(\frac{\partial\gamma}{\partial\mu_a}\right)_{E^{\pm}} + \left(\frac{\partial\gamma}{\partial E^{\pm}}\right)_{\mu_a}\left(\frac{\partial E^{\pm}}{\partial\mu_a}\right)_{E_{ref}} \quad \text{(Eq. 15)}$$

Since

$$\left(\frac{\partial\gamma}{\partial E^{\pm}}\right)_{\mu_a} = -q_M = \mathfrak{F}(\Gamma^+ - \Gamma^-) \quad \text{(Eq. 16)}$$

by substitution from Eq. 16, 14, and 9, Eq. 15 can be written as

$$\left(\frac{\partial\gamma}{\partial\mu_a}\right)_{E_{ref}} = \frac{1}{2}(\Gamma^+ + \Gamma^-) + \Gamma_{H_2O}\left(\frac{x_{salt}}{x_{H_2O}}\right) \quad \text{(Eq. 17)}$$

Thus from Eq. 16 and 17, components of charge can be evaluated. This method is particularly useful (110) in concentrated solutions.

2. *Grahame's Capacity Method*

From the thermodynamic theory of the ideally polarizable electrode, it can be shown (145) that

$$-\frac{dC_+}{dE} = Z_+\nu_+\mathfrak{F}\left(\frac{\partial C}{\partial\mu_a}\right)_{E^-} \quad \text{(Eq. 18)}$$

$$C_+ = \int\left(\frac{dC_+}{dE}\right)dE + K \quad \text{(Eq. 19)}$$

$$Z^+\mathfrak{F}\Gamma_+ = -\int C_+\,dE + K' \quad \text{(Eq. 20)}$$

Actual values of the integration constants K or K' (or C_+ or Γ^+ at any value of E) should be known for carrying out the integration. They can be obtained

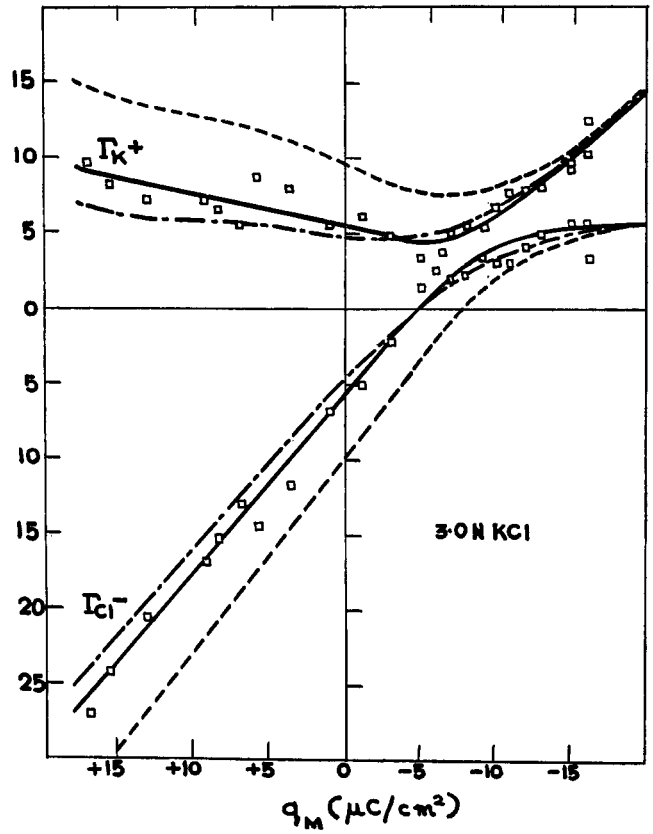

Figure 6.—Comparison of the components of charge (Γ_{K^+} and Γ_{Cl^-} in μc./cm.²) evaluated by different methods for K^+ and Cl^- ions from 3.0 *N* KCl solution on mercury at 25° (reproduced from ref. 62). Symbols are the same as in Figure 4.

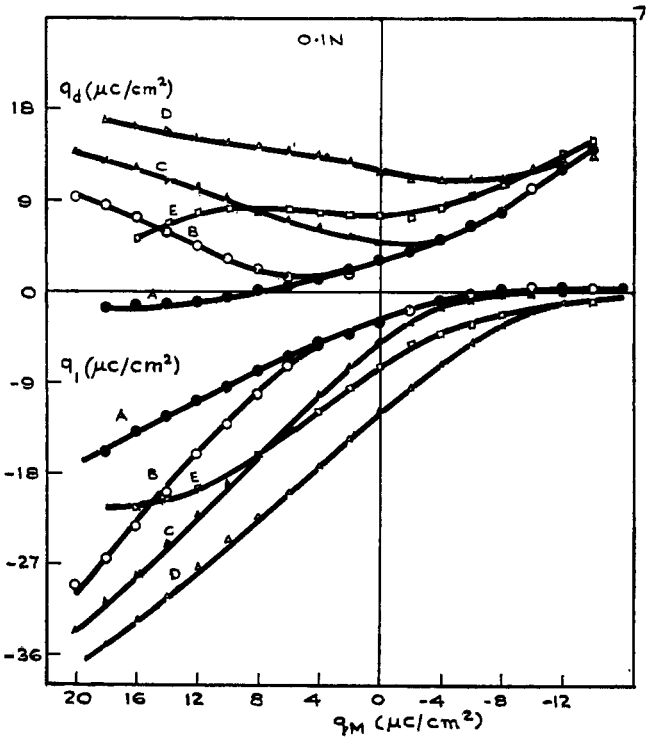

Figure 7.—Comparison of the variation of specifically adsorbed charge (q_i in μc./cm.²) with q_M (in μc./cm.²) on mercury (from 0.1 *N* solutions in the case of halides at 25° and 0.0847 *M* of sodium benzene-*m*-disulfonate solutions at 20°) for various anions. A, KF (from the data of Devanathan (57)); B, KCl; C, KBr; D, KI (from the thermodynamic data of Peries (269)); and E, for benzene-*m*-disulfonate ion (the thermodynamic data evaluated (68) from the data of Parry and Parsons (254)).

either from electrocapillary data or by using the diffuse layer theory. Grahame used the latter in assuming that since the anions are completely repelled from the interface at $E = \approx -1.2$ v., the capacity $C+$ can be calculated from diffuse layer theory. Thus by experimentally measuring $(\partial C/\partial \mu_a)_{E^-}$, Γ^+ values are evaluated by integration.

The values calculated (136, 138, 143, 281) by the above method are found to be in reasonable agreement with thermodynamic values for iodide solutions but in the case of chloride solutions (281), the disagreement is as high as 90% for 3 *N* KCl (62). This conclusion is also substantiated by electrocapillary studies in concentrated chloride solutions (110).

This discrepancy stems from two major disadvantages. First, the computation of $C+$ from diffuse layer theory breaks down when there is strong specific adsorption of cations as in the case of, *e.g.*, tetraalkyl salts or Cs^+ ions. Second, as Grahame himself had pointed out, the double integration of $(\partial C/\partial \mu_a)_{E^-}$ calls for an exceptionally high degree of accuracy in the experimental determination because small experimental errors are magnified enormously. The experimental error in $(\partial C/\partial \mu_a)_E$ is large when the specific adsorption of anions is not strong as is in the case of chloride solutions.

3. *Devanathan's Model Method*

This method (57) is based on a postulated structure of the electrical double layer and can be used to evaluate the surface excesses from differential capacity data at single concentrations. It has been shown (57, 62) that the Γ^+ values obtained by the model method are in excellent agreement with the thermodynamic values for halide ions and for benzene-*m*-disulfonate (69) ions. The details of this method will be discussed in a later section.

A comparison of the surface excesses obtained by the above three methods are shown in Figures 4, 5, and 6.

4. *Direct Methods*

By labeling one of the ions of the electrolyte with radioactive isotopes, it is possible to measure the surface excess of ions directly. Such studies (6–8, 172–174) have been carried out on platinum, but not on mercury.

From the ionic surface concentrations obtained by the above methods, it is possible (127, 130) to evaluate the quantity of specifically adsorbed charge q_i, from the diffuse layer theory, if only one ionic species is specifically adsorbed.

Instead, one can calculate surface pressure Φ (256) from the ξ function using

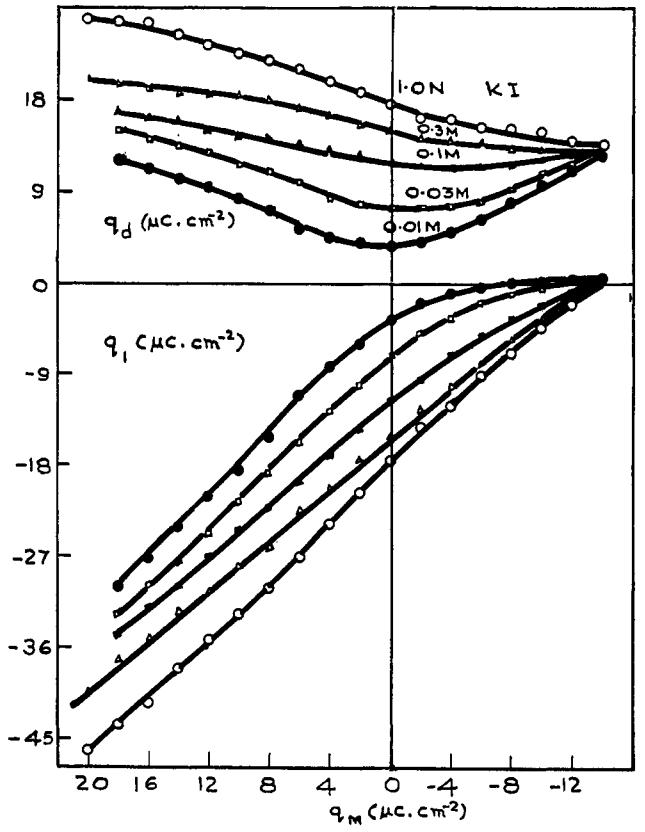

Figure 8.—Variation of q_1 (in μc./cm.²) with q_M (in μc./cm.²) for various concentrations of KI at 25° (from the thermodynamic data of Peries (269)).

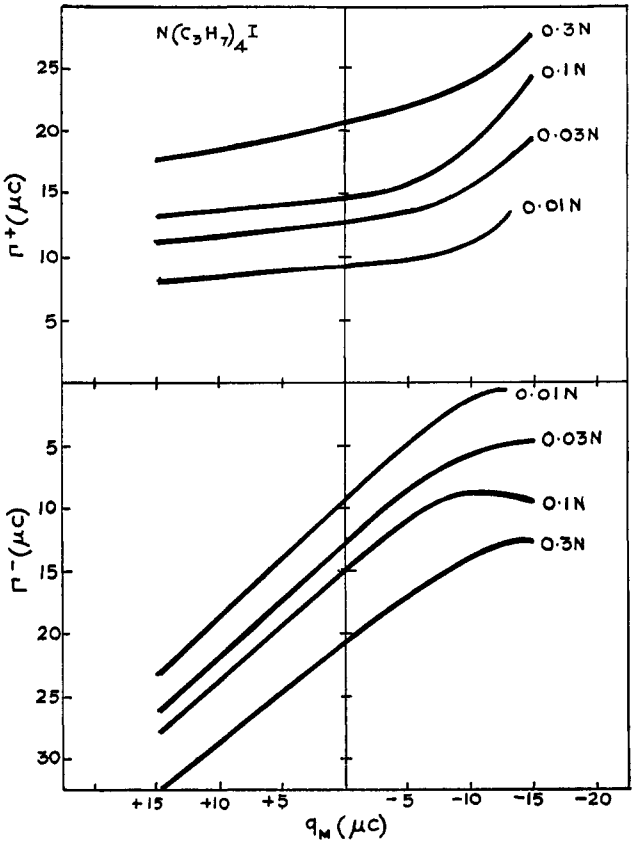

Figure 9.—Surface excess (in μc./cm.²) curves for tetrapropylammonium iodide at 25° (reproduced from ref. 63).

$$\xi^+ - \xi_0^+ + I = \Phi \ (q_M = \text{constant}) \quad \text{(Eq. 21)}$$

where

$$I = \int_{-\infty}^{\mu_a} \Gamma^-_{\text{diffuse}} \, d\mu_a$$

and ξ_0^+ is the value of ξ^+ when $C = 0$, and differentiate when q_1 is obtained directly

$$\left(\frac{d\Phi}{d\mu_a}\right)_{q_M} = -q_1 \quad \text{(Eq. 22)}$$

A knowledge of the specifically adsorbed charge is necessary for understanding the structure of the electrical double layer and the nature of specific adsorption. Very few systems have been systematically studied to obtain the q_1 values as a function of q_M. The specific adsorption behavior observed from the q_1 curves, evaluated by the thermodynamic method, are given below for four types of systems.

Inorganic Anions.—The q_1 *vs.* q_M curves (65, 269) for the Cl^-, Br^-, and I^- in their potassium salt solutions are given in Figures 7 and 8. It can be seen from the above figures that normally the operative range of the charge of the metal (q_M) is between +25 to −20 μc./cm.². Further the following general trends have been noticed from such figures.

i. The specific adsorption of the anions increases with (a) increasing concentration, (b) increasing positive charge on the metal, and (c) increasing size of the anion (Figure 7), the order being F^-, $H_2PO_4^- < OH^- < Cl^-$, NO_3^-, ClO_4^-, IO_3^-, $BrO_3^- < Br^- < SCN^- < I^-$.

ii. An inflexion is observed in the q_1 *vs.* q_M curve on the anodic side of the e.c.m., and the value of $q_{M,\text{inflexion}}$ is dependent on the concentration and the nature of the anion.

iii. Irrespective of the size, all the anions are desorbed at $q_M = -12$ to -13 μc./cm.² or ≈ -1.2 v. (*vs.* n.c.e.) in not too concentrated solutions and in the absence of specific adsorption of cations.

It may be mentioned here that electrocapillary studies (108, 160, 161) carried out with very concentrated solutions of HCl, HBr, and H_2SO_4 (3 to >10 *N*) show anomalies on the cathodic side of the e.c.m. Normally the diffuse layer theory holds for most of the ions in aqueous solutions as shown by Γ^+ being positive, and Γ^- becoming equal to the limiting repulsion value at extreme cathodic polarization. For these acids in moderate concentrations Γ^+ decreases with increasing negative charge and becomes negative as the concentration is increased to ≈ 10 *N*. Similar anomalies are observed in the presence of organic cations (10) in strong acid solutions. No satisfactory explanation has yet been advanced for this phenomenon.

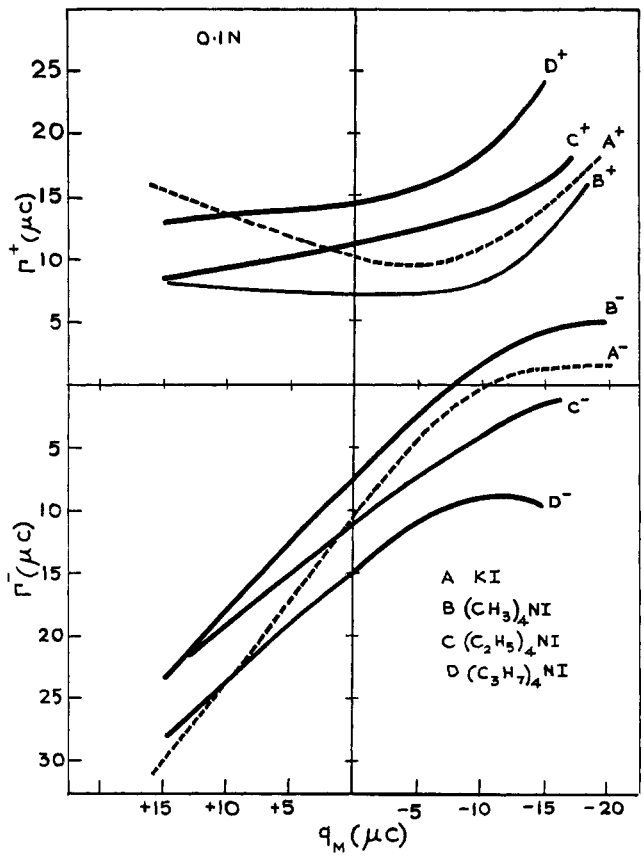

Figure 10.—Surface excess (in μc./cm.²) curves for various tetraalkyl salts on mercury from 0.1 *N* solutions at 25° (reproduced from ref. 63).

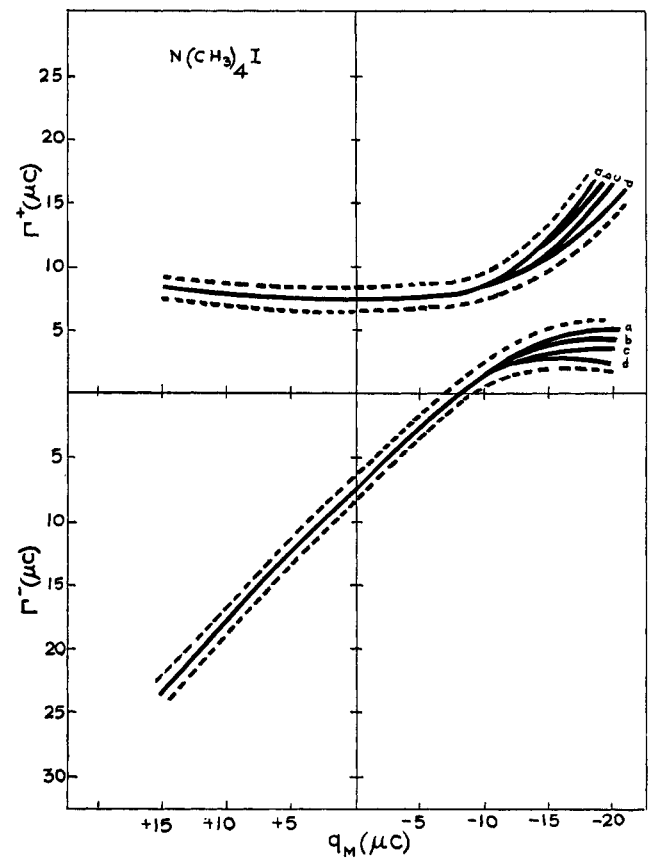

Figure 11.—Surface excess data (in μc./cm.²) of tetramethylammonium ion on mercury at various concentrations at 25°. a, 0.2 *N*; b, 0.1 *N*; c, 0.03 *N*; d, 0.01 *N*; dashed lines represent the limits of error (reproduced from ref. 63).

Organic Anions.—The only system studied in detail (254) is that of Hg in contact with sodium benzene-*m*-disulfonate solutions. These organic anions appear to behave in the same way as halide ions except in that nearly a unit coverage is attained at large q_M.

Inorganic Cations.—Surface excess data are very scarce on this subject. But from differential capacity and electrocapillary data (52, 94, 103, 113, 115, 129, 304, 309), it has been inferred (97, 110) that the adsorbability increases in the order $Li^+ < Na^+ < K^+ < Rb^+ < Cs^+ < Tl^+$. It is also observed that polyvalent cations La^{3+}, Al^{3+} (290) are also specifically adsorbed as anion–cation complexes of lower oxidation states, *e.g.*, LaI^{2+}, $LaCl^{2+}$.

Organic Cations.—The surface excess plots for tetraalkylammonium ions adsorbed from tetraalkylammonium iodide solutions (63, 84) are given in Figures 9, 10, and 11. Here also the specific adsorption increases with increasing concentration, increasing negative charge on the metal, and increasing size of the cation (Figure 10); $(CH_3)_4N^+ < (C_2H_5)_4N^+ < (C_3H_7)_4N^+$.

The interesting features noticed in the above study are:

i. In the case of tetramethyl salts, the $(CH_3)_4N^+$ and I^- ions are specifically adsorbed on either side of the e.c.m. and appear to be independent of the concentration of $(CH_3)_4NI$ in the range studied, within the limits of experimental error.

ii. On the negative side of the e.c.m., the adsorption of $(CH_3)_4N^+$ is smaller than that of K^+. Possible causes for the anomaly have been discussed elsewhere (63, 84).

These tetraalkyl salts when studied as added substances to a supporting electrolyte get desorbed at extreme negative polarization. This behavior is marked when the number of carbon atoms exceeds three (51, 105, 244).

Aromatic and heterocyclic cations (11, 15, 36, 120) also exhibit specific adsorption on either side of the e.c.m. (see Figure 12).

B. DIFFERENTIAL CAPACITY AT IDEALLY POLARIZABLE INTERFACES

The fine structure of the electrical double layer can be best studied by differential capacity measurements. To understand the capacity data, it is necessary to know the pattern of the differential capacity curve when there is no specific adsorption. From Γ^- curves for the alkali halides it is known that at −12 to −13 μc./cm.² there is no specific adsorption of anions and the capacity of the electrical double layer is ≈ 16.2

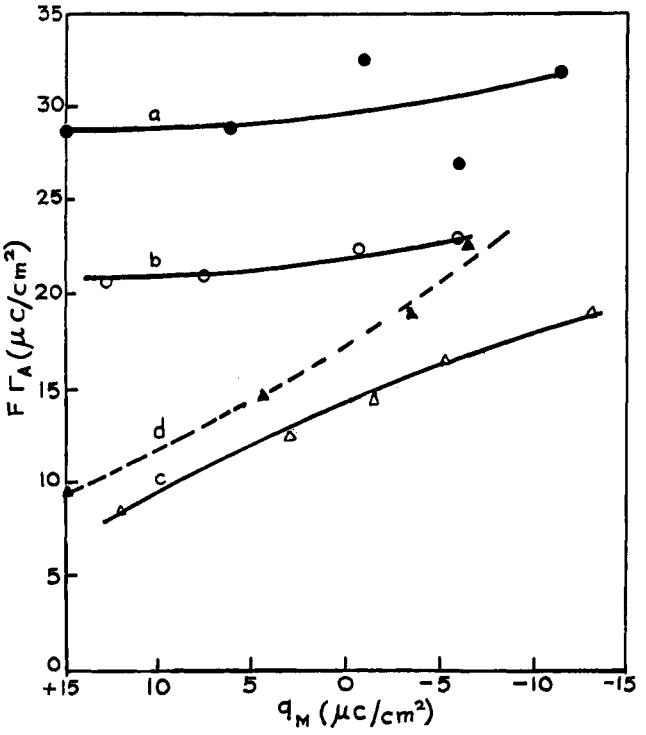

Figure 12.—Surface excess (in μc./cm.^{2}) data of aromatic cations on mercury (from the data of Conway and Barradas, (ref. 11, 36). a, 2-aminopyridinium ion; b, anilinium ion; c, pyridinium ion; d, piperidinium ion.

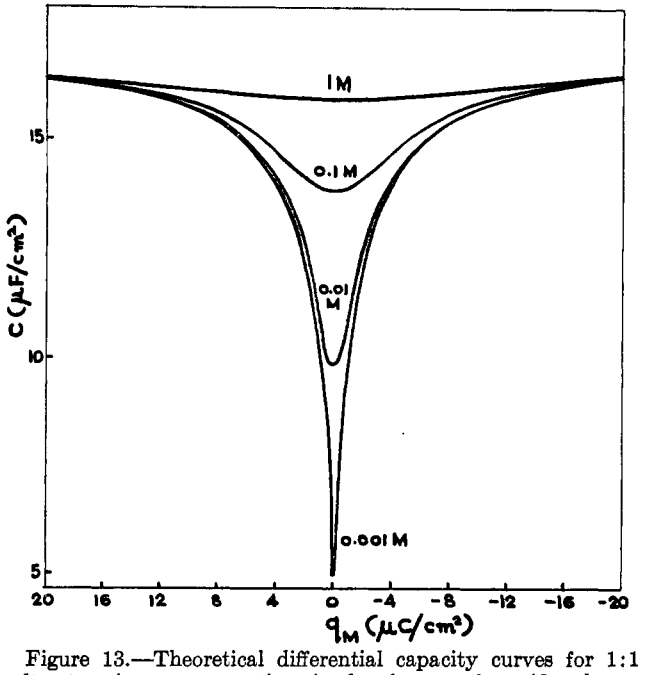

Figure 13.—Theoretical differential capacity curves for 1:1 salts at various concentrations in the absence of specific adsorption.

μf./cm.^{2}. When allowance is made for the diffuse layer capacity using

$$\frac{1}{C} = \frac{1}{C_H} + \frac{1}{C_d} \qquad \text{(Eq. 23)}$$

C_H is found to be 17.1 μf./cm.^{2}. This value can be assumed to be the solvent capacity. Independent

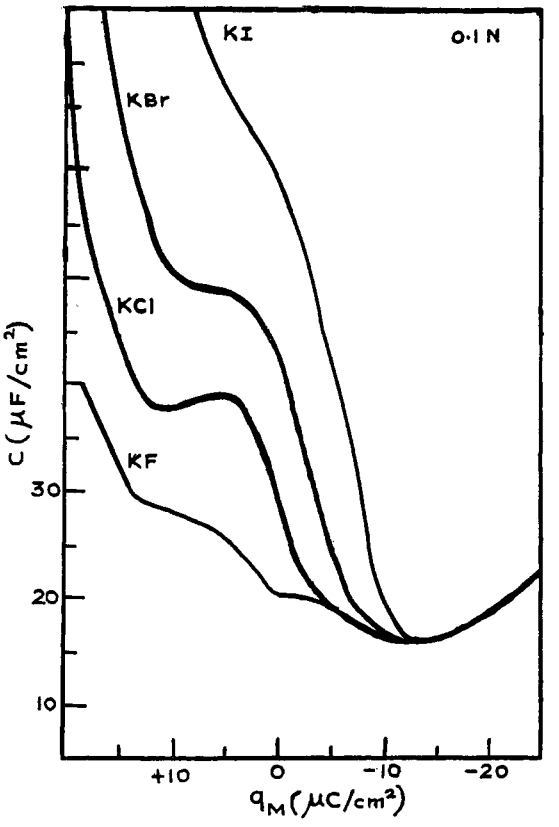

Figure 14.—Differential capacity curves of potassium halides from 0.1 N solutions as a function of charge on the metal, at 25° (reproduced from ref. 57).

evidence confirming the 17.1 μf. also comes from the capacity measurements on platinum (66). A constant capacity of 17 μf. can therefore be regarded as the base capacity in the absence of specific adsorption provided the distance of closest approach of both ionic species exceeds 3.8 Å. and is constant with potential. If 17 μf./cm.^{2} is a constant value in the absence of specific adsorption, then the effect of dilution on the capacity curves can be schematically represented as in Figure 13. The experimental curves, for example, for potassium halides (128, 131) are different as seen in Figures 14 and 15. Thus it is seen that the capacity is $\approx$16 μf./cm.^{2} at $q_M = -12$ to -13 μc./cm.^{2} and increases with increasing positive charge on the metal. Typical curves for various anions are given in Figure 14. It can be noticed that all the capacity curves coincide at 16.1 μf./cm.^{2} corresponding to a q_M of ≈ -12 μc./cm.^{2}.

Another characteristic feature is the presence of a *hump* near the e.c.m. (mostly on the anodic side). The hump is pronounced with planar molecules like NO_3^- and not with pyramidal molecules (229, 305) like ClO_3^-, BrO_3^-, and IO_3^- or with Cl^-, Br^-, and I^-. Thus it is dependent on the structure and the polarizability of the anion. Further the hump decreases with increasing temperature as shown in Figures 16 and 17 (133, 135). Another interesting point (18) is that

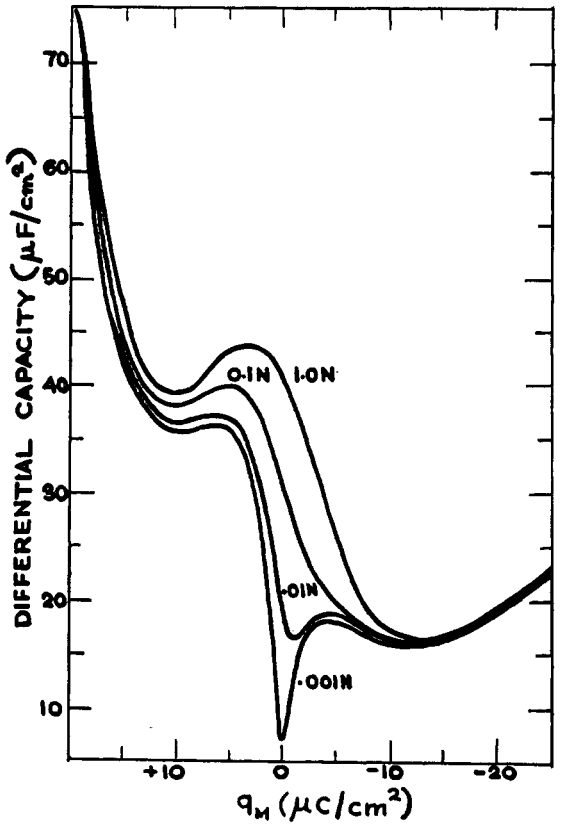

Figure 15.—Differential capacity curves for various concentrations of KCl as a function of q_M on mercury at 25° (reproduced from ref. 57).

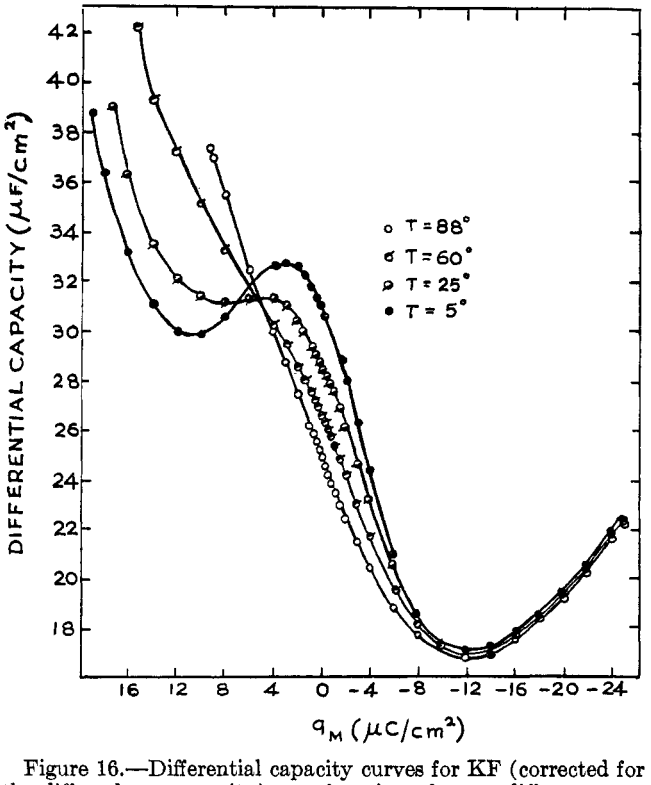

Figure 16.—Differential capacity curves for KF (corrected for the diffuse layer capacity) as a function of q_M at different temperatures (reproduced from ref. 133 with the permission of the editors).

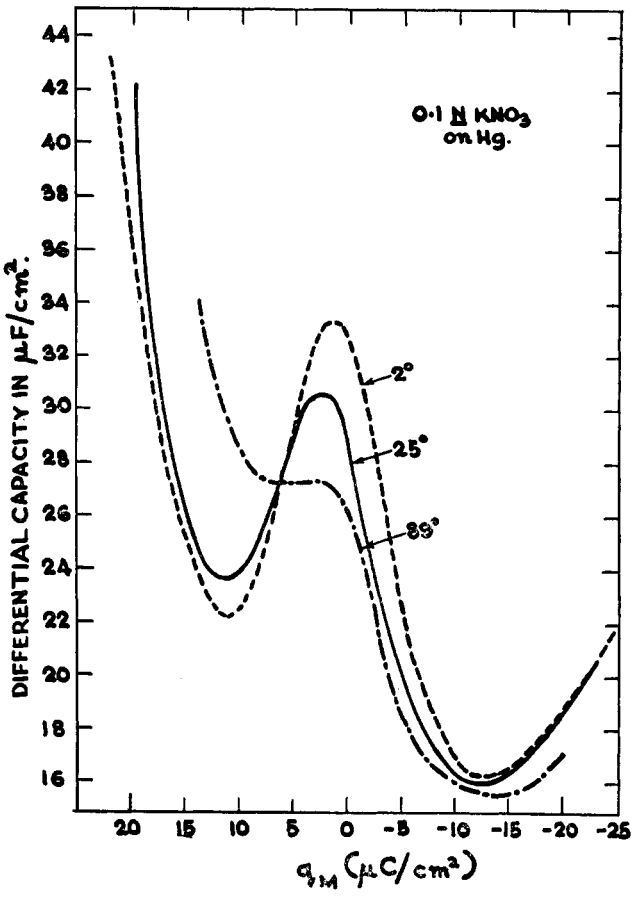

Figure 17.—Differential capacity curves of 0.1 N KNO_3 on mercury at different temperatures as a function of q_M (reproduced from ref. 135 with the permission of the editors).

the humps occur at the same value of charge at which the inflexion in the q_1 *vs.* q_M curve occurs (Figure 18). The charge at which the hump occurs (20) becomes less positive as (i) q_1 increases and (ii) the ionic radius increases.

C. DIFFERENTIAL CAPACITY AT NONPOLARIZABLE INTERFACES

Some studies have been made on silver iodide (216, 251) and silver sulfide sols (85, 162) by computing the surface concentration by direct methods (see section IV-A-2) and hence the surface charge density. It may be pointed out that the potential scale is calculated from the concentration of the potential-determining ions in the bulk of the solution (obtained by any analytical method) with the aid of the Nernst equation. By differentiating the surface charge-density curves, the differential capacity curves have been constructed and are found to be similar to the differential capacity curves of Hg in aqueous electrolyte solutions. Since the absolute area of the sol is not known, the effective area is obtained assuming that the true capacity is the same as that at the Hg–solution interface in very dilute solution, when the diffuse layer controls the over-all capacity (see Figure 19). By varying the electrolyte

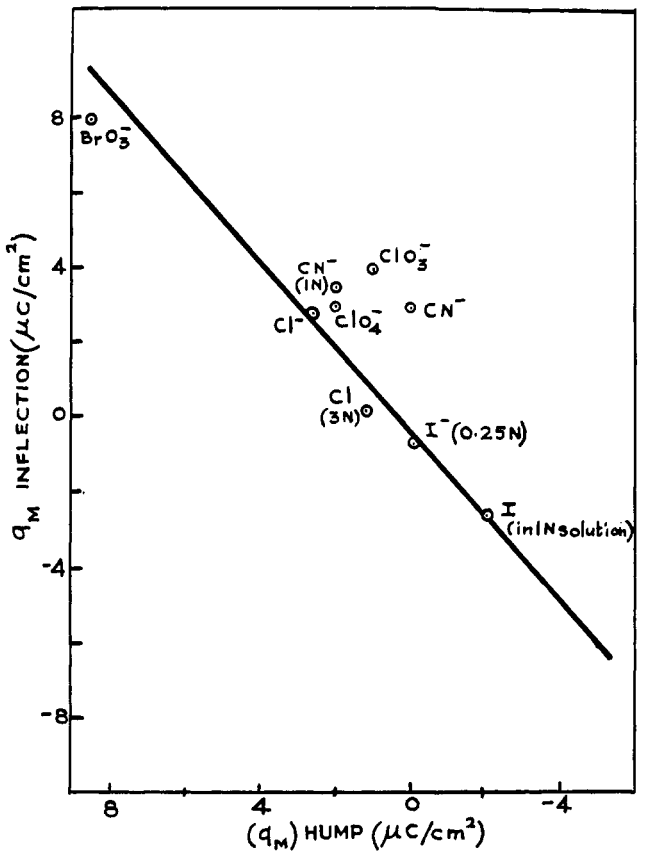

Figure 18.—Plot of the charge on the metal at which the inflexion on the thermodynamically evaluated components of specifically adsorbed charge occurs ($q_{M,\text{inflexion}}$) *vs.* the charge on the metal at which the hump in the capacity curves ($q_{M,\text{hump}}$) occurs (reproduced from ref. 18).

concentration (see section VI-C-3), the zero charge point has been located from the capacity minima. The capacity curves have been found (162) to be dependent on the method of preparation of the sol. Thus the capacity curves on the silver sulfide sols prepared by silver amine method in sodium acetate solution shows the characteristic hump (see sections III-A and III-I),

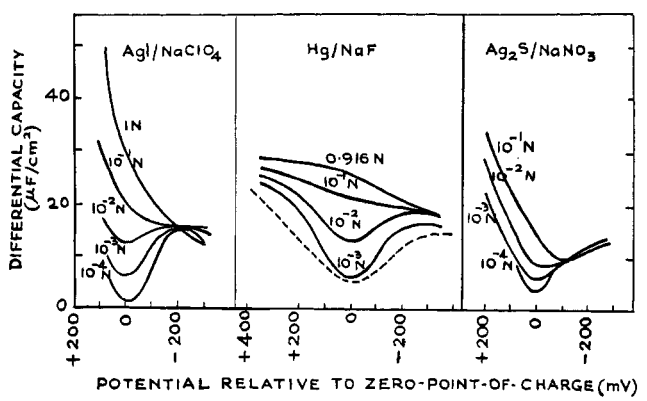

Figure 19.—Comparison of the differential capacity curves for mercury in NaF with the capacity curves on nonpolarizable systems AgI–$NaClO_4$ and Ag_2S–$NaNO_3$ (reproduced from ref. 162).

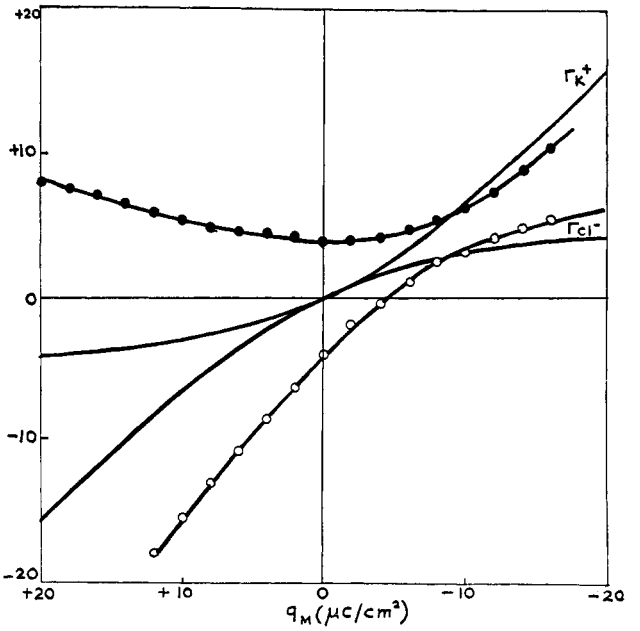

Figure 20.—Comparison of the surface excess data calculated for conditions of no specific adsorption at 25° (full lines) with the experimentally determined values (from the data of Peries (269)) for K^+ and Cl^- from 1.0 *N* KCl solutions.

whereas the silver sulfide sols prepared by other methods show the normal pattern. The former has been attributed to the adsorption of acetate ions. Capacity curves calculated on the basis of diffuse layer theory have been found to agree with the observed curves. This has been assumed to be due to the absence of specific adsorption as suggested by Grahame. However, this conclusion does not appear to be correct (see sections III-E and III-F). But one significant result of the above studies is that the structure of the double layer at nonpolarizable interfaces appears to be not very different from that at ideally polarizable interfaces.

D. NATURE OF SPECIFIC ADSORPTION

Under conditions of no specific adsorption, the base capacity for, *e.g.*, Hg–KCl should be 17.1 μf./cm.^{2} over a wide potential range, and correspondingly the components of charge are as shown in Figure 20. The experimentally observed components of charge for KCl are also given in the above figure for the sake of comparison. The disparity in the anodic region is quite marked and points to greater adsorption of chloride ion on the anodic side of the e.c.m. This behavior has been termed specific adsorption or superequivalent adsorption (103).

The energetics of specific adsorption have been explained in terms of covalent forces (127, 128, 136, 144) between Hg and the halide ion and electrostatic forces. If the idea of covalent binding is correct, adsorbability (20) should increase with increasing bond strength of the Hg–X bond. But what is observed is an inverse

correlation (see Table I). Further it is very difficult to envisage covalent binding between mercury and positively charged ions, especially organic cations.

TABLE I

ADSORBABILITY AND SOME PROPERTIES OF THE IONS AND Hg-ION BONDS

Ion	Adsorbability at q_M = 10 μc./cm.², μc./cm.²	Bond strength, kcal. mole⁻¹ (ref. 20)	Hydration numbers (ref. 17)	% covalent character of the Hg-ion bond (ref. 67)
F^-	9.5	32	4	34
Cl^-	14.6	23	1	74
Br^-	19.2	17	1	82
I^-	29.2	7	1	91

The following facts (20) should now be noted for further discussion. (i) For halide ions, the adsorbability increases with increase in the cube root of the radius of the anion (Figure 21). (ii) For the same radius at a given charge, $q_{i,\text{anions}} \approx x q_{i,\text{cation}}$ where x is 3 or 4 (see Figure 21). (iii) When the ion size is small, the heat of hydration is high (Figure 22) and the primary hydration number large.

The trend seems to be that the smaller, heavily hydrated ions are less specifically adsorbed than larger ions which are devoid of their hydration sheaths. Thus it appears that loss of the hydration sheath, at least in the direction of the metal, is a *necesssary condition for specific adsorption.* From this point of view, one can understand (a) the greater adsorbability of anions over the cations, the basis being that, for the same radius, cations have larger heats of hydration than anions and (b) the weak specific adsorption of ions whose radius is less than 1.41 Å., since such ions are strongly hydrated.

The above concept of specific adsorption and its relation to solvation predicts that for the same cation, the larger the energy of hydration of the anion, the larger is the solubility of the salt and therefore its solubility product. Thus the relationship between solubility product and specific adsorbability cited (127, 128, 144) in connection with the explanation of specific adsorption of ions in terms of covalent forces can be explained on the basis of electrostatic forces between ions "bereft" of their hydration sheaths and the metal.

The above electrostatic explanation of specific adsorption or superequivalent adsorption is in accordance with the suggestion of Devanathan (57) that the specifically adsorbed ions should be regarded as being merely dehydrated in the direction of the metal. However, the above definition does not specify the nature of bonding. On the hydration model, the equivalent adsorption (20) or no specific adsorption means that both ionic species with their hydration sheaths intact are in contact with the metal, their mean electrical centers constituting the outer Helmholtz or Gouy plane.

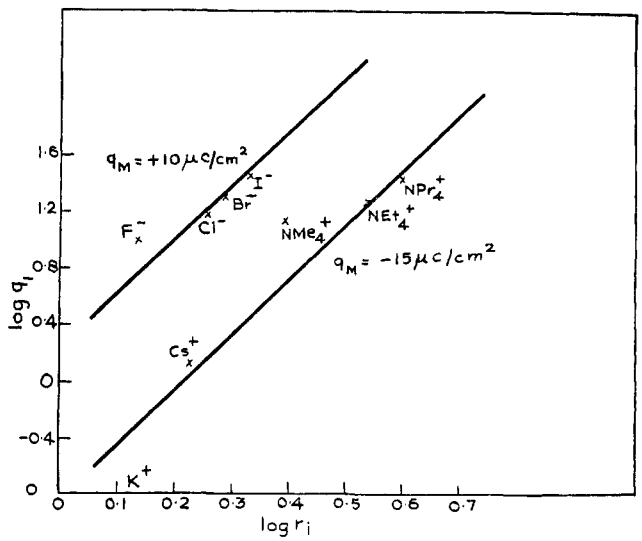

Figure 21.—Specific adsorbability (q_i) plotted against the ionic radius (r_i) for some cations and anions (logarithmic scale) (reproduced from ref. 20).

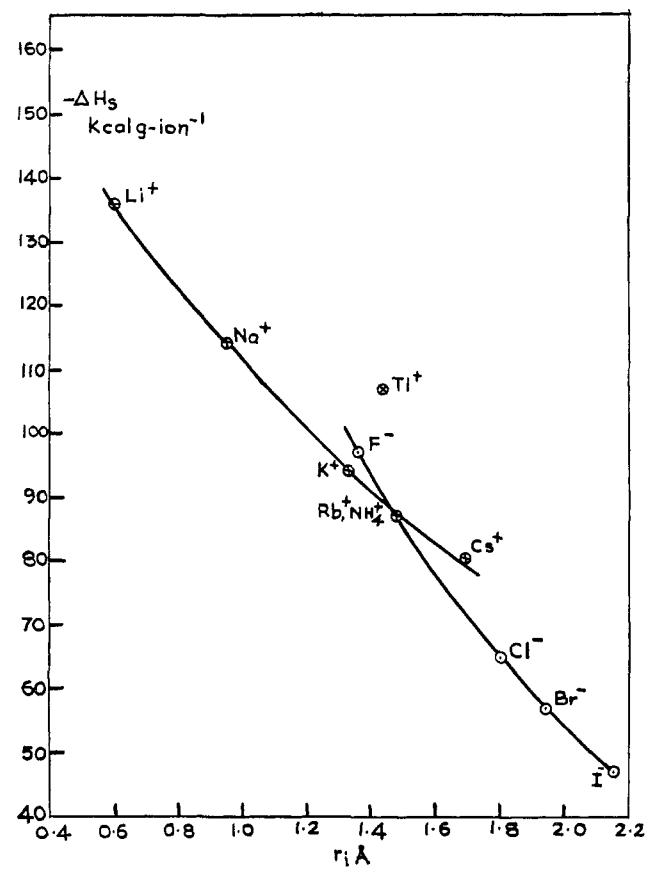

Figure 22.—Heat of hydration ($-\Delta H_s$) plotted against the ionic radius (r_i) for cations and anions (reproduced from ref. 20).

Taking into account the interactions between the metal–ion, metal–water, and ion–water, calculations of free energy have been made in great detail (2). The results also confirm the notion that the forces involved in the specific adsorption do not involve cova-

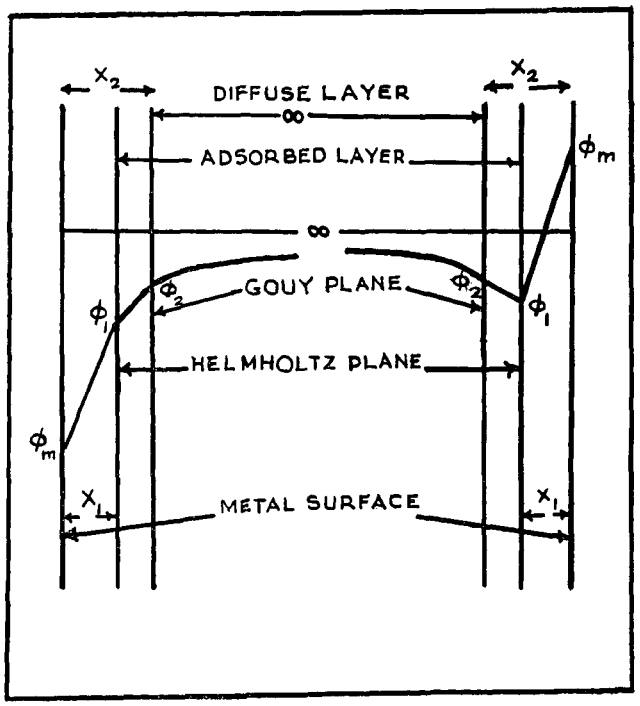

Figure 23.—Diagrammatic representation of the potential distribution in the double layer (reproduced from ref. 57).

lent bonding. But this conclusion is not final since all interatomic interactions cannot be covered in a nonquantum mechanical calculation.

The electrostatic model, however, predicts the same behavior for all metals. Recent studies in this laboratory (66) on platinum carried out under high-purity conditions show that the capacity is nearly constant at ≈ 20 μf./cm.^{2} over a wide potential range with chloride, bromide, and iodide solutions. (This result is contrary to the ones reported earlier (273, 274). Even though the later workers have found capacitance variation with potential, the order of increasing specific adsorbability observed is in the wrong direction and can be attributed to the presence of reducible species like oxygen.)

This result shows that a purely electrostatic approach to specific adsorption is inadequate and indicates the existence of non-Coulombic interactions between the metal and the ion. It has been pointed out (20) that covalent binding is not responsible for specific adsorption as specific adsorbability increases with decreasing bond strength of the Hg–X bond. This conclusion is not justified since the bond strength refers to the sum total of Coulombic and non-Coulombic interactions. Instead, a comparison with the percentage covalent character calculated from the electronegativities (267) shows (see Table I) the adsorbability to increase with increasing percentage covalent character of the Hg–X bond. Thus for specific adsorption, *ease of dehydration of the ion is a necessary condition, and a covalent ion–metal bond is the sufficient condition.*

E. STRUCTURE OF THE ELECTRICAL DOUBLE LAYER

Consistent with the ideas of specific adsorption discussed earlier, Grahame distinguished (127, 128) two different planes, one for specifically adsorbed ions and the other for the hydrated ions which are not specifically adsorbed. The plane corresponding to the "locus of the electrical centers of a layer of adsorbed ions" has been termed the inner Helmholtz plane and the nonspecifically adsorbed ions with their hydration shells have been located at a slightly greater distance from the metal, at the outer Helmholtz plane or Gouy plane. Starting from the Gouy plane, the diffuse layer extends into the interior of the solution. However, these concepts have been used only qualitatively.

1. Devanathan's Model

Devanathan (57) has proposed a model for aqueous solutions which enables the location of these planes from known ionic and molecular dimensions and has developed a quantitative theory. The main postulates of the theory are that (i) the specifically adsorbed ions occupy the inner Helmholtz plane, (ii) the solvated cations or anions remain at the Gouy plane, (iii) the region between the inner Helmholtz plane and the Gouy plane is forbidden for occupancy by any ion, and (iv) χ potentials due to water dipoles and electron overlap are assumed to be either negligibly small or constant. The model is shown diagramatically in Figure 23.

The total charge per unit area can be written as

$$q = q_1 + q_d \qquad \text{(Eq. 24)}$$

As there is no charge between metal and inner Helmholtz plane, the potential at the inner Helmholtz plane is

$$\phi_M - \phi_1 = q/K_{m-1} \qquad \text{(Eq. 25)}$$

where $K_{m-1} = \epsilon/4\pi x_1$. Similarly, the potential of the outer Helmholtz plane is

$$\phi_1 - \phi_2 = q_d/K_{1-2} \qquad \text{(Eq. 26)}$$

where

$$K_{1-2} = \epsilon/4\pi(x_2 - x_1) \qquad \text{(Eq. 27)}$$

Differentiating Eq. 25, one obtains

$$\frac{d\phi_M}{dq} = \frac{1}{C} = \frac{1}{K_{m-1}} + \frac{d\phi_1}{dq} \qquad \text{(Eq. 28)}$$

By evaluating $d\phi_1/dq$ from Eq. 26, and substituting in Eq. 28, the expression for the differential capacity is

$$\frac{d\phi_M}{dq} = \frac{1}{C} = \frac{1}{K_{m-1}} + \left(\frac{1}{K_{1-2}} + \frac{1}{C_d}\right)\left(1 - \frac{dq_1}{dq}\right) \qquad \text{(Eq. 29)}$$

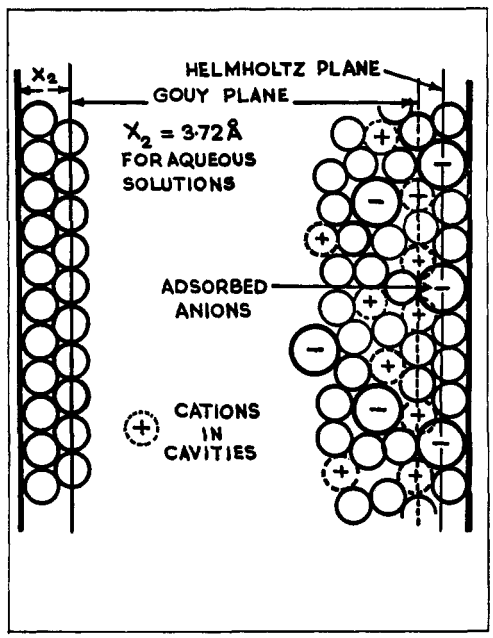

Figure 24.—Schematic representation of the population of double layer by ions (reproduced from ref. 57).

or

$$\left(1 - \frac{dq_1}{dq}\right) = \frac{\frac{1}{C} - \frac{1}{K_{m-1}}}{\frac{1}{C_d} + \frac{1}{K_{1-2}}} \qquad \text{(Eq. 30)}$$

From this equation, the complete differential capacity curve has been explained in terms of the variation of specifically adsorbed charge with charge on the metal.

The salient points are: (i) at $q_M = -12$ to -13 μc./cm.^{2}, dq_1/dq is zero and q_1 is zero. Hence the measured capacity is

$$\frac{1}{C} = \frac{1}{K_{m-1}} + \frac{1}{K_{1-2}} + \frac{1}{C_d} \qquad \text{(Eq. 31)}$$

The $(1/K_{m-1} + 1/K_{1-2})$ term has been called the solvent capacity (K_s) as it depends on the ϵ and x_2 of the solvent, according to the identity

$$\frac{\epsilon}{4\pi x_2} = \frac{1}{K_{m-1}} + \frac{1}{K_{1-2}} \qquad \text{(Eq. 32)}$$

This means that in the absence of specific adsorption, the inner Helmholtz plane cannot be located. The value for K_s is 17.1 μf./cm.^{2} (see section III-B, Eq. 23). Since the Gouy plane is taken as locus of centers of the second layer of water molecules corresponding to the sites occupied by cations, which are usually smaller than the water molecules (assuming close-packing of water molecules taking the Bernal and Fowler's values of 1.41 Å. for the radius of the water molecule), the value of x_2 is found to be 3.72 Å. (see Figure 24). From the values of x_2 and K_s, ϵ has been found to be 7.19.

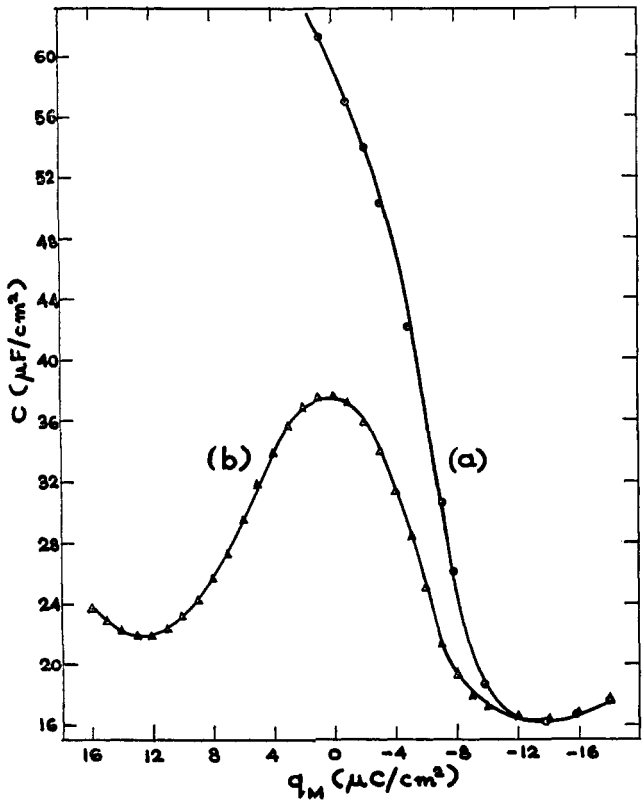

Figure 25.—Differential capacity curves for mercury as a function of charge on the metal. (a) for 0.1 N KI at 25° (from the data of Grahame (136)); (b) for 0.0847 M sodium benzene-m-disulfonate at 20° (from the data of Parry and Parsons (254)).

(ii) In the presence of specific adsorption, dq_1/dq is finite and the capacity always increases with increasing q. When dq_1/dq exceeds unity, the differential capacity rises rapidly to infinity (when $1/K_{m-1}$ is equal to $(1/K_{1-2} + 1/C_d)(1 - dq_1/dq)$), *i.e.*, when the ideally polarizable system is converted into a nonpolarizable or reversible system. The variation of C with q is dependent on the numerical magnitude of dq_1/dq. If the rate of variation is high, then one should expect capacity to increase rapidly to a high value. But if the rate is low because of geometrical restrictions, then the C *vs.* q_M curve should come down to 16 μf./cm.^{2} on the anodic side also, before faradaic reaction sets in. The former behavior can be noticed in iodide and the latter in benzene-m-disulfonate solutions (Figure 25).

(iii) According to Eq. 29, in dilute solutions, the capacity of the electrical double layer is governed by the diffuse layer capacity. The minimum or the dip in the differential capacity curves should be observed at the point of zero charge when specific adsorption is absent and the position of the dip gets shifted to other values of q_M in the presence of specific adsorption.

For evaluating the components of charge (q_1), C_d, K_{m-1}, and K_{1-2} should be known. C_d can of course be calculated from the theory of the diffuse layer. Knowing K_s to be 17.1 μf./cm.^{2} and x_1 as equal to the crystallographic radius of the adsorbed ion, K_{m-1}

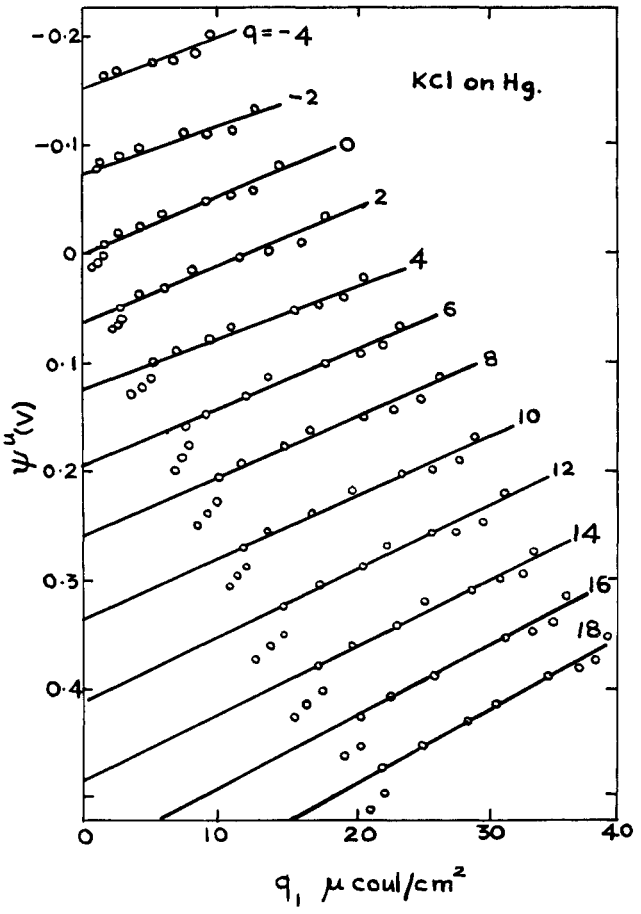

Figure 26.—Potential drop in the compact layer (ψ^u) plotted against the specifically adsorbed charge (q_1) at constant q_M for KCl on mercury (reproduced from ref. 143).

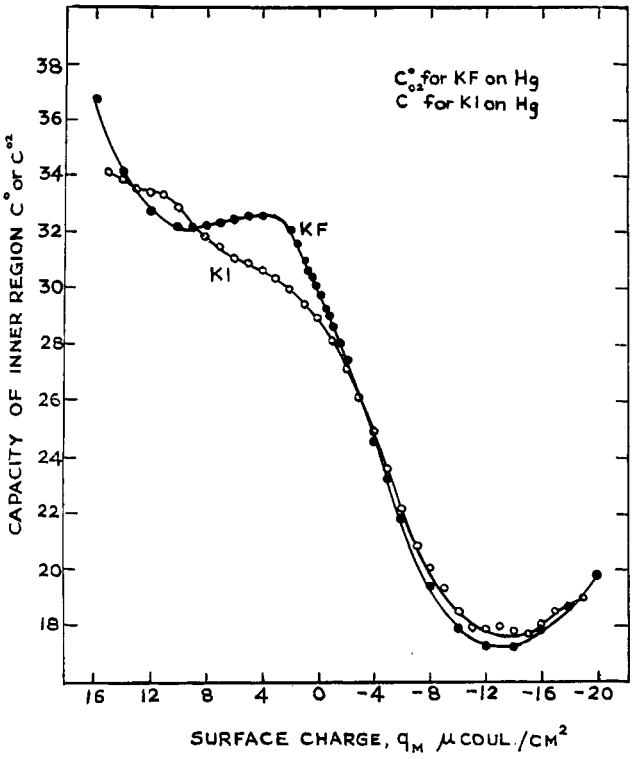

Figure 27.—The inner layer capacity (C^{02}) of KI and the differential capacity curve, corrected for the diffuse layer capacity (C^0) for KF as a function of q_M (reproduced from ref. 138 with the permission of the editors).

and K_{1-2} can be calculated. By the method of successive approximations, assuming in the beginning that C_d is negligible, values of q_1 accurate to ± 0.1 μc. can be calculated from Eq. 21 or 22. Such calculations were carried out for KI, KCl, KBr, and KF and the values compared with the thermodynamic values. The agreement was found to be very good. Equation 30 also provides a method for calculating the potential at the inner Helmholtz plane, since

$$\phi_1 = \frac{q_d}{K_{1-2}} + \frac{2kT}{ze_0} \sinh^{-1} \frac{q_d}{2A} \qquad \text{(Eq. 33)}$$

where A^2 is equal to $DkTn_0/2\pi$.

The above theory assumes that specific adsorption of only one type of ion is operative in the given charge range and the dielectric constant is unchanged. Thus the increase in capacity beyond -12 μc./cm.² is attributed to cation adsorption. However, the above theory has to be extended to accommodate the simultaneous adsorption of anions and cations in order to interpret the complex behavior observed, for example, in the case of tetraalkyl salts (51, 63, 84).

Two main criticisms (44) have been leveled against the above theory and they are (i) the theory ignores the discrete nature of specifically adsorbed ionic charge. But it should be pointed that discrete effects are not involved when dealing with C *vs.* q curves as these are macroscopic quantities. Micropotentials are relevant only for a discussion of the potential seen by the particle which is to be adsorbed (see section III-H). (ii) The minimum of the capacity curve at -13 μc./cm.², which is the starting point for the integration of dq_1/dq curves, is the point at which there is no specific adsorption. This has been regarded as an assumption of the theory by Damaskin, whereas it is an experimental fact which is deduced from an inspection of the thermodynamic surface excess data. Thus there appears to be no valid criticism of the above model of the electrical double layer.

2. *Grahame's Method*

Grahame adopted a different approach for obtaining the inner layer parameters (136, 138). From the experimentally measured values of potentials for various q_M's, ϕ_2 and a constant (0.488 v. to correct for the potential difference at the e.c.m. of an unadsorbed electrolyte) are subtracted to obtain ψ^u. The potential difference across the compact layer in the absence of specific adsorption, ψ^{02}, is evaluated as follows.

As shown in section III-A-2, q_1 is evaluated from capacitance data. It is found from a plot of ψ^u *vs.* q_1 at constant q_M that when q_1 exceeds ≈ 5 μc./cm.²,

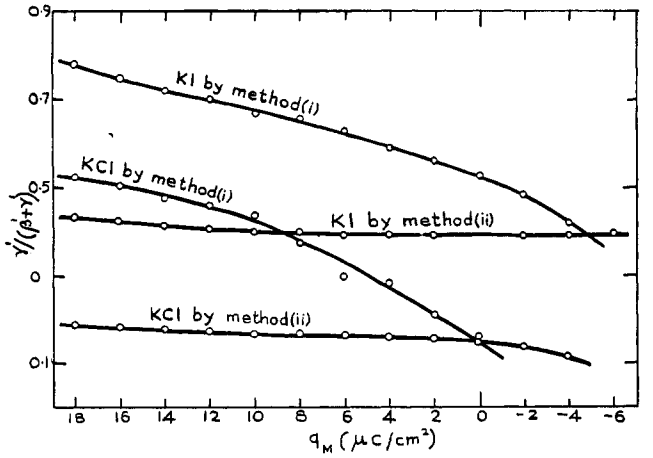

Figure 28.—$\gamma'/(\gamma' + \beta')$ evaluated by different methods for KI and KCl as a function of q_M (reproduced from ref. 143).

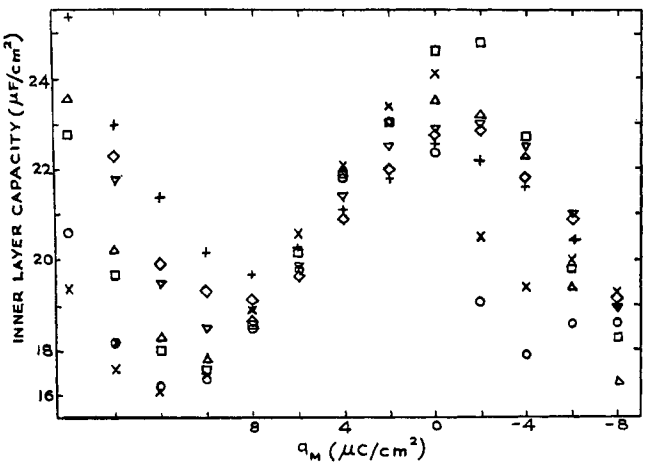

Figure 29.—Inner layer capacity in the case of benzene-*m*-disulfonate ion as a function of q_M at 20°. ×, 8.47 × 10^{-3} *M*; ○, 0.0169 *M*; □, 0.0423 *M*; ▽, 0.0847 *M*; △, 0.169 *M*; ◇, 0.423 *M*; +, 0.847 *M* (reproduced from ref. 254).

a family of parallel straight lines is obtained (Figure 26). This constant gradient is $(\partial\psi^u/\partial q_1)q_M$. The intercepts on the potential axis can now be plotted against q_M. The gradient for a particular value of q_M gives $(\partial\psi^u/\partial q_M)q_1$. Grahame regards the $(\partial\psi^u/\partial q_M)q_1$ as identical with $(\partial\psi^u/\partial_M)_{q_1\to 0}$ and hence regards it as a measure of the differential capacity of the inner layer in the absence of specific adsorption denoted C^{02}. Such a graph for KI is given in Figure 27 along with the differential capacity curve (corrected for the diffuse layer capacity) for KF.

From C^{02}, ψ^{02} is calculated through the identity

$$\psi^{02} = \int_0^{q_M} \frac{1}{C^{02}}\, dq_M \qquad \text{(Eq. 34)}$$

the integration constant at $q_M = 0$ being zero.

Now the potential drop between the outer Helmholtz plane and the inner Helmholtz plane (ψ^V) can be obtained from

$$\psi^V = \psi^u - \psi^{02} = -\frac{4\pi q_1 \gamma'}{\epsilon} \qquad \text{(Eq. 35)}$$

Assuming that a change in ψ^u is due to a change in ψ^V only, it is inferred from $(\partial\psi^u/\partial q_1)q_M$ curves that γ'/ϵ is independent of q_1 but is a function of q_M.

ψ_1^A, the potential of the inner Helmholtz plane relative to the outer Helmholtz plane, *i.e.*, $\phi_1 - \phi_2$, as a function of q_M is evaluated from ϕ_1 which is obtained from the following equation assuming an exponential adsorption isotherm. (The equation has also been derived by an independent method (206) from a discrete picture of the double layer.)

$$\frac{d\psi^V}{d\ln a_\pm} = \frac{1}{\frac{RT}{\mathfrak{F}\psi^V} - \frac{d\phi_1}{d\psi^V}} \left(\frac{RT}{\mathfrak{F}}\right) \frac{\left(1 + d\ln\frac{\gamma'}{\epsilon}\right)}{d\ln a_\pm}$$

(at constant q_M) (Eq. 36)

The inner layer parameters $\gamma'/(\beta'+\gamma')$ can now be found from the above potentials in two different ways. (i) The ratio of ψ_1^A/ψ^u gives the value of $\gamma'/(\beta' + \gamma')$ at different q_M's, since ψ_1^A is assumed to be proportional to γ' and ψ^u to $(\gamma' + \beta')$. (ii) Since

$$\left(\frac{\partial\psi^V}{\partial q_1}\right)_{q_M} = -\frac{4\pi\gamma'}{\epsilon} = \lambda' \qquad \text{(Eq. 37)}$$

and ψ^{02} can be expressed as

$$\psi^{02} = -\frac{4\pi q_M(\beta' + \gamma')}{\epsilon} \qquad \text{(Eq. 38)}$$

it is clear from the above two relationships that

$$\frac{\lambda' q_M}{\psi^{02}} = \frac{\gamma'}{\beta' + \gamma'} \qquad \text{(Eq. 39)}$$

The values of $\gamma'/(\beta' + \gamma')$ obtained by the two methods are not the same (see Figure 28) for KI and KCl solutions. The second method shows $\gamma'/(\beta' + \gamma')$ to be constant with q_M, and this has been explained as due to a simultaneous change in γ' and ϵ. The γ'/ϵ values are found to be smaller for Br^- than for iodide, contrary to what one would expect from a knowledge of the crystallographic radii.

The inner layer parameters have been obtained for the following systems by the above method, *i.e.*, for KI (138), KCl (143), and sodium benzene-*m*-disulfonate (254). This procedure is open to the following objections.

(i) From the constancy of C^{02} with q_1 and the plots of C^{02} for KI and KF, it has been deduced that the field due to anions does not affect the field in the inner region due to charge on the metal. Some alteration may be expected if the anion forms a covalent complex with mercury. Thus, this conclusion, if correct, provides evidence against covalent binding. Further, the postulate that C^{02} is indeed characteristic

of the inner layer properties is not supported by experiment (see Figures 27 and 29). Instead of one curve, different curves are obtained depending on the specific adsorption characteristics on the anodic side although the position on the cathodic side is more or less the same. Of particular interest is the curve for benzene-*m*-disulfonate solution where C^{02} comes back to 16 μf./cm.^{2} on the extreme anodic side. The fact that the C^{02} varies from electrolyte to electrolyte shows that it is not a measure of the capacity of the compact layer in the absence of specific adsorption.

This error originates in the linear extrapolation of the ψ^u *vs.* q_1 curves. An inspection of Figure 26 shows that, in all cases, the ψ^u *vs.* q_1 curve, though linear above 5 μc./cm.^{2}, does not intersect the q_1 axis sharply. Consequently

$$\left(\frac{\partial\psi^u}{\partial q_M}\right)_{q_1>5\mu c} \neq \left(\frac{\partial\psi^u}{\partial q_M}\right)_{q_1\to 0} \qquad \text{(Eq. 40)}$$

thereby invalidating the extrapolation. The latter value should be around 17 μf./cm.^{2} and independent of q_M. Therefore, the ψ^{02} values calculated using Eq. 34 are not characteristic of the compact layer in the absence of specific adsorption.

(ii) It has been mentioned earlier that $\gamma'/(\beta' + \gamma')$ is obtained from the ratio of ψ_1^A/ψ^u, assuming that the potential drop across the compact layer is linear. This assumption of a linear drop is also accepted by others (206, 207) and is equally open to the following criticism. The assumption of a linear drop in the inner layer, in the presence of specifically adsorbed charge, violates Poisson's equation since the charge density of the inner Helmholtz plane is not zero. Even when the coverage is 1% and the linearity taken as an approximation (189), it must be noted that the deviation from linearity is itself a direct measure of the charge density of the inner Helmholtz plane. Thus it appears that the anomalies observed in $\gamma'/(\gamma' + \beta')$ and log K'' (K'' is a constant related to the specific adsorption potential in the isotherm used by Grahame) are consequences of the above incorrect assumption.

F. INNER LAYER CAPACITY IN THE ABSENCE OF SPECIFIC ADSORPTION

A knowledge of the inner layer parameters is necessary for any discussion on the structural aspect of the double layer. One such basic parameter is the inner layer capacity in the absence of specific adsorption. This parameter can be evaluated as follows.

The measured capacity can be separated into the compact layer capacity and diffuse layer capacity with the help of Eq. 23, where C_d can be calculated from the diffuse layer theory. When specific adsorption is absent, the capacity at high concentration is taken as equal to the inner layer capacity, and, with the aid of Eq. 23, capacity curves have been theoretically calculated for dilute solutions and compared with experimental curves, in the case of NaF solutions (127, 131). The good agreement led Grahame to infer that the capacity curve in NaF solution is the inner layer capacitance curve in the absence of specific adsorption. Another variation of the above method (268) for showing the absence of specific adsorption is to plot $1/C$ *vs.* $1/C_d$ when a line of unit gradient with an intercept $1/C^{02}$ should be obtained at constant q_M. It has been shown (268) that with NaOH solutions for cathodic values of q_M, this equation is apparently obeyed but breaks down completely on the anodic side indicating specific adsorption. The viewpoint of Devanathan is discussed in sections III-B and III-D. According to him, the base capacity is 17.1 μf./cm.^{2} (*i.e.*, capacity in the absence of specific adsorption).

The main difference in the above two models is that Devanathan assumes that the base capacity is constant at 17.1 μf./cm.^{2} and does not change with change in the q_M, whereas Grahame assumes that the base capacity varies with q_M from a value of 17.1 μf./cm.^{2} at $q_M = -13$ μc./cm.^{2} to $\sim$33–34 μf./cm.^{2} at $q_M = \sim+10$ μc./cm.^{2} as shown in Figure 27. The latter picture is very difficult to understand because an increase in capacity in the absence of specific adsorption can be attributed only to either a decrease in the Helmholtz layer thickness or an increase in the dielectric constant of water with increase in field strength. The change in the dielectric constant cannot be assumed since the dielectric constant should be maximum at the e.c.m. and should decrease on either side of the e.c.m. The other alternative is to invoke changes in the thickness of compact layer due to electrostriction. Such an approach has been proposed (213, 214) to explain the small increase in the cathodic capacity but, on the anodic side, once again the rapid rise defies explanation based on the above concept and has been attributed to the specific adsorption of fluoride ions. Thus from the above discussion and the ones previously mentioned, it appears that the base capacity should be a constant value, independent of charge on the metal, in the absence of specific adsorption. What all the specific adsorption does is only to force the ions into the compact layer thereby increasing the capacity as given by Eq. 29. This confirms the model proposed by Devanathan.

G. ESIN AND MARKOV EFFECT (82, 132)

The variation of the potential of the electrocapillary maximum (measured with reference to a constant reference electrode) with concentration of the electrolyte at a rate greater than $RT/\mathfrak{F}$ is called the Esin and Markov effect. From a rigorous thermodynamic analysis, it (92, 257) has been shown that for 1:1 electrolytes

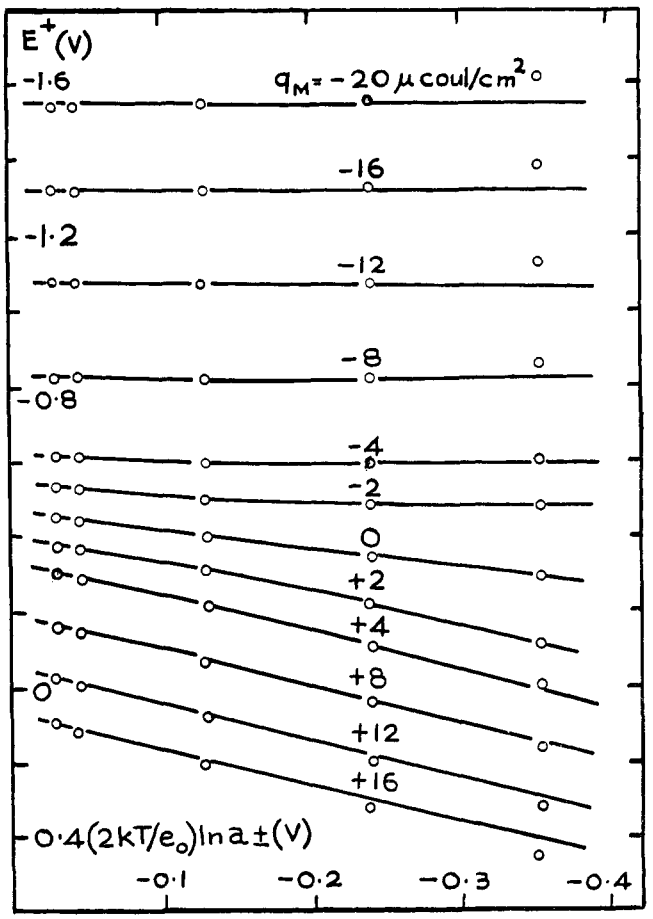

Figure 30.—The Esin and Markov effect in the absence of specific adsorption. Points are experimental values of Grahame for NaF. Lines are calculated and fitted at highest concentration (reproduced from ref. 257).

$$\left(\frac{\partial E^{\pm}}{\partial \ln a_{\pm}}\right)_{q_M} = \frac{2kT}{z_+e_0}\left(\frac{\partial q_1}{\partial q_M}\right)_{a\pm} \text{ or } \left(\frac{\partial E^{\pm}}{\partial \mu_a}\right)_{q_M} = \left(\frac{\partial q_1}{\partial q_M}\right)_{\mu_a} \quad \text{(Eq. 41)}$$

It can be seen from Eq. 41 that the Esin and Markov effect should be observed at all the values of q_M and depends on the variation of q_1 with q_M. It has been pointed out (257) that if there is no specific adsorption then the value $(d\Gamma^-/dq_M)$ can be evaluated from the diffuse layer theory alone. Under these conditions, the Esin–Markov coefficients $(\partial E^{\pm}/\partial \mu_a)_{q/M}$ are: (i) when $q_d = 0$

$$\left(\frac{\partial \Gamma^-}{\partial q_M}\right)_{\mu_a} = -1/2 \quad \text{(Eq. 42)}$$

(ii) when only anions are in the diffuse layer, *i.e.*, $q_d/2A << -1$

$$\left(\frac{\partial \Gamma^-}{\partial q_M}\right)_{\mu_a} = -1 \quad \text{(Eq. 43)}$$

and (iii) when only cations are in the diffuse layer, *i.e.*, $q_d/2A >> 1$

$$\left(\frac{\partial \Gamma^-}{\partial q_M}\right)_{\mu_a} \to 0 \quad \text{(Eq. 44)}$$

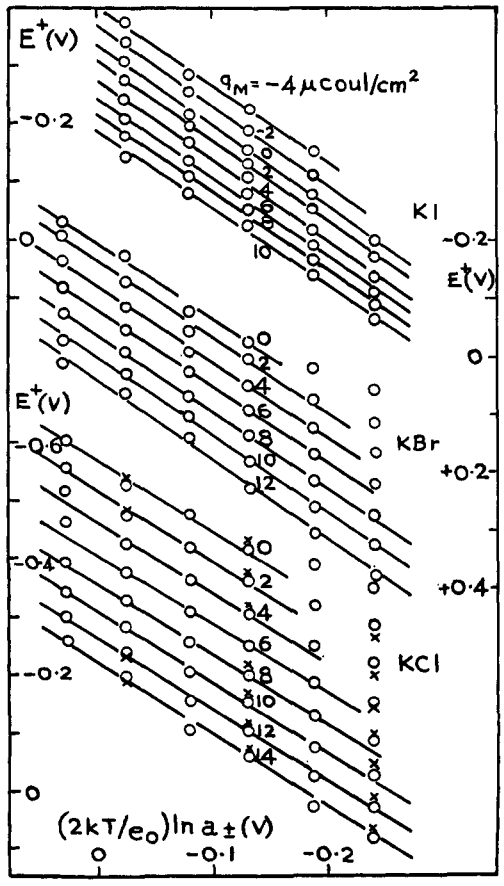

Figure 31.—The Esin and Markov effect in the presence of specific adsorption. O, electrocapillary results of Devanathan and Peries; ×, capacity results of Grahame (reproduced from ref. 257).

It should be noted here that the E_{ref} (at e.c.m.) is not a function of concentration in the absence of specific adsorption; therefore, conformity to the above prediction is a proof of the absence of specific adsorption (see Figure 30). For halide solutions which exhibit specific adsorption, the Esin and Markov coefficients (Figure 31) have been found to be 1.36, 1.35, and 1.22 for KI, KBr, and KCl, respectively. These slopes are the same as the slopes obtained from the linear segments of the q_1 *vs.* q_M curves.

$(\partial E/\partial \ln a_{\pm})_{q/M}$ can also be expressed as

$$\left(\frac{\partial E}{\partial \ln a_{\pm}}\right)_{q_M} = \left(\frac{\partial E}{\partial q_1}\right)_{q_M}\left(\frac{\partial q_1}{\partial \ln a_{\pm}}\right)_{q_M} \quad \text{(Eq. 45)}$$

The first term can be regarded as the specific adsorption capacity. The second term is the adsorption isotherm. Hence a knowledge of the proper adsorption isotherm will enable the evaluation of the Esin and Markov coefficients.

H. IONIC ISOTHERMS

Stern (289) proposed an isotherm, which is similar to Langmuir's for the specifically adsorbed ions

$$n_i = n_0 \exp\left[\frac{z\mathfrak{F}}{RT}(\Phi' - \phi_1)\right] \quad \text{(Eq. 46)}$$

Here Φ' denotes the nonelectrostatic forces of ionic adsorption in terms of an equivalent potential. Critical analyses of the above equation have been made by many workers (see references in 44, 60, 255) to show its inadequacy in explaining the adsorption characteristics of various ions. But Esin and Shikov (83) and Ershler (80) have recognized, upon a suggestion from Frumkin (89), that the above equation would be correct if ϕ_1 is evaluated properly. They have distinguished between macropotential ψ, which is regarded as the measured potential difference, and micropotential ψ_a, which is the potential "seen" by the adsorbing ion. The former potential is assumed to be the same as that which will exist if the ions are uniformly smeared out in the classical electrostatic sense, whereas the micropotential is the potential at the adsorption site due to discrete charges, *viz.*, the ions and their images in the solution, arranged in a hexagonal pattern. Esin and Shikov have estimated the ratio of micro- and macropotential and found it to be $0.74\delta/r$. Ershler made improvements in the model by considering the image of the ion in the solution as an ion cloud. Later Grahame (139) obtained the same result by considering the multiple reflection of the dipoles in the metal and in the solution. The ratio obtained by Grahame is

$$\frac{\psi_a}{\psi} = 0.805\frac{r}{\delta}\left[\sqrt{0.27566 + (\delta/r)^2} - \sqrt{0.27566}\right] \qquad \text{(Eq. 47)}$$

When δ/r is less than 0.2

$$\frac{\psi_a}{\psi} = 0.766\left(\frac{\delta}{r}\right) - 0.697\left(\frac{\delta}{r}\right)^3 \qquad \text{(Eq. 48)}$$

This value is nearly the same as obtained by Esin and Shikov.

The Esin and Markov effect was first proposed for the variations of $E^{\pm}$ with ln a_s at the e.c.m. only. But as shown by Parsons, it is a property that should be observed at all values of q_M. But Eq. 48, predicts variations in the Esin and Markov coefficients with q_M due to changes in r, contrary to the experimental observation that the Esin and Markov coefficient for halides is practically constant at ~1.23 provided $q_1 >$ 5 μc./cm.^{2}. Further the value of δ is variable from ion to ion and this should also result in a variation of the coefficients. However, as pointed out earlier, the Esin and Markov coefficient is independent of the nature of any ion. This difficulty appears to be due to the fact that the experimentally measurable potential is not the macropotential but a smoothed out or continuous charge-distribution potential, denoted by Grahame ψ_{cont} (139). This ratio ψ_a/ψ_{cont} has already been evaluated by Grahame to be equal to 0.805. The value of ψ_a/ψ_{cont} approaches unity at high coverages or for large δ/r.

Parsons (256, 261), by comparing the effective surface pressure due to specifically adsorbed ions with several isotherms, has found that the square root and Amagat isotherms are obeyed by the ions. Later he fitted Temkin's (254, 257, 261) and a modified Helfand, Frisch, and Lebowitz's isotherm (263) for the adsorption of iodide and benzene-*m*-disulfonate ions. However, by fitting the isotherms, none of the parameters controlling the specific adsorption, especially the free energy, have been obtained as a function of charge in order to understand the type of bonding between the metal and the ion. Since surface pressure is merely a difference of surface tensions, it is a quantity not particularly structure sensitive, like the electrocapillary curve.

Bockris, *et al.* (20), by taking into account the interaction of the specifically adsorbed ions with their images and their immediate neighbors, have developed an exponential isotherm which qualitatively agrees with the experiment.

It should be noted that Devanathan obtained the dq_1/dq_M values from the capacity curves, but did not formulate any isotherm. Recently (68) a simple isotherm has been evaluated for the ions. The basic isotherm is the same as is assumed by Grahame and is

$$n_i = \frac{a_i N \delta_i}{1000} \exp\left[\frac{\Delta G}{kT} - \frac{\phi_1}{kT}\right] \qquad \text{(Eq. 49)}$$

a_i has been shown to be equal to $c^{2/R'}$ (68) where R' is a ratio defined below. The potential ϕ_1 is not the simple electrostatic potential as has been assumed by previous workers. It is the resultant of two opposing factors: the first is the potential at the inner Helmholtz plane arising from the charge on the metal and the second is the potential at the adsorption site due to the already adsorbed anions which will tend to repel the adsorbing ion. Hence this value is the micropotential. These two potentials should be separately evaluated.

ϕ_1 in the absence of specific adsorption is given by

$$\phi_1 = \frac{4\pi q_M (x_2 - x_1)}{\epsilon} + \phi_2 \qquad \text{(Eq. 50)}$$

The specifically adsorbed ions contribute a continuous potential $4\pi q_1(x_2 - x_1)/\epsilon$. Therefore the micropotential sensed by the adsorbing anions is given by

$$\frac{4\pi q_1 (x_2 - x_1)}{\epsilon} R'$$

where R' is the ratio of the micro- to the continuous potential. Noting that

$$\frac{4\pi q_1 (x_2 - x_1)}{\epsilon} = \frac{1}{K_{1-2}} \qquad \text{(Eq. 51)}$$

the isotherm can be put in the form

$$q_1 = e_0 n_i = \frac{a_i \mathfrak{F} \delta_i}{1000} \exp\left[\frac{-\Delta G}{kT} + \frac{e_0 q_M}{kTK_{1-2}} - \frac{q_1 e_0 R'}{kTK_{1-2}} + \frac{\phi_2 e_0}{kT}\right] \qquad \text{(Eq. 52)}$$

Taking logarithms and denoting e_0/kTK_{1-2} as B'

$$\ln q_1 = \ln a_i + \ln\left(\frac{\mathfrak{F}\delta_i}{1000}\right) - \frac{\Delta G}{kT} + B'q_M - B'R'q_1 + \frac{\phi_2 e_0}{kT} \quad \text{(Eq. 53)}$$

If $q_1 > 5$ μc./cm.^{2}, then the variation of ln q_1 is negligibly small and hence the equation can be written as

$$q_1 \cong \left(\frac{1}{B'R'}\right)\ln a_i + \left(\frac{1}{B'R'}\right)\ln\left(\frac{\mathfrak{F}\delta_i}{1000}\right) - \frac{\Delta G}{B'R'kT} + \frac{q_M}{R'} + \frac{\phi_2 e_0}{B'R'kT} \quad \text{(Eq. 54)}$$

From this we deduce that, since ϕ_2 is small and practically constant

$$\left(\frac{\partial q_1}{\partial \ln a_i}\right)_{q_M} = \frac{1}{B'R'} \quad \text{(Eq. 55)}$$

and

$$\left(\frac{\partial q_1}{\partial q_M}\right)_c = \frac{1}{R'} \quad \text{(Eq. 56)}$$

Since R' is equal to 0.805 (139) when δ/r is <0.2, it follows that $dq_1/dq_M = 1.26$, independent of the nature of the anion which had been observed for eight different anions by Parsons (257). This now explains the constancy of the slope of dq_1/dq_M at 1.25. Further the Esin and Markov coefficient $(\partial E^{\pm}/\partial\mu_a)_{q_M}$ is also given by $1/R'$ according to Eq. 41 and 56.

Thus the simple isotherm explains very satisfactorily the shape of the q_1 *vs.* q_M, q_1 *vs.* ln $a_{\pm}$, and $dE^{\pm}/d \ln a_{\pm}$ plots.

An idea about the nature of forces controlling the specific adsorption can now be obtained by evaluating ΔG. On plotting $q_1 + (\phi_2 e_0/B'R'kT)$ against log C at constant q_M, straight lines are obtained. A plot of the intercepts at $a = 1$ against q_M gives a straight line of gradient equal to zero (see Figure 32). This means that the value of ΔG is independent of q_M. In other words, the variation of free energy of adsorption can be accounted completely by electrostatic interactions. The magnitude of the standard free energy of adsorption or the intrinsic adsorbability as shown by the height of the parallel lines is characteristic of the anion and follows the order $Cl^- < Br^- < I^-$, *i.e.*, the order of increasing covalent character of the ions. The intrinsic adsorbability is thus governed (67) by the ion-metal covalent binding forces. Thus if the substrate cannot form covalent complexes with the ion, then, even though the ion is free of its hydration sheaths, there will not be any specific adsorption as appears to be the case with platinum.

I. CAPACITANCE HUMPS

It has been pointed out in section III-B that one of the features of the capacitance curves is the presence of a hump. Grahame (135) studied the temperature dependence of the capacity curves and found that the hump decreases with increase in temperature. This observation led him to infer that the hump is due to a pseudo-crystalline "ice-like" layer of water molecules which melts as the temperature is increased.

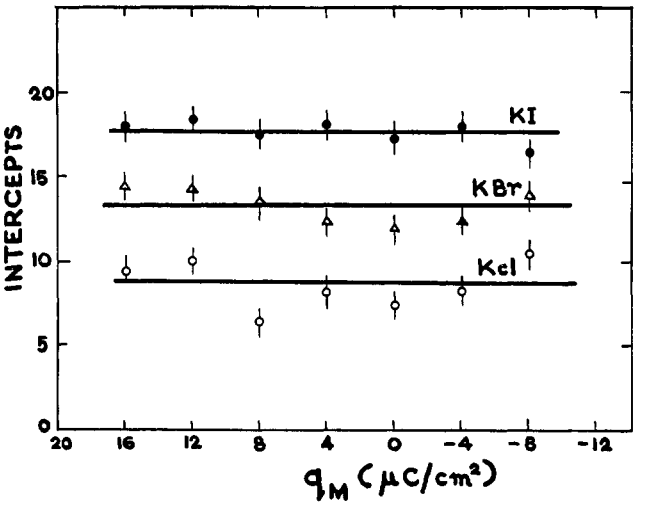

Figure 32.—Variation of log $(\mathfrak{F}\delta_i/1000) - (\Delta G/kT)$, the intercept, with the charge on the metal for various anions.

Watts-Tobin (307) and Mott and Watts-Tobin (233), in an attempt to explain the hump, have proposed that at the electrode surface there are two types of water molecules, one with the oxygen end towards the metal and the other with the hydrogen end towards the electrode, both at an angle of $\cos^{-1}(1/\sqrt{3})$ to the normal to the surface. Expressing the mean moment of each water dipole as $\mu_w \tanh \mu_w x/kT$, they obtained the following relationship between q_M and ψ_{m-2} (in the absence of specific adsorption).

$$q_M = -\frac{\psi_{m-2}k_0}{4\pi x_2} + \frac{N_d\mu_w}{x_2}\tanh\frac{\mu_w x}{kT} \quad \text{(Eq. 57)}$$

Thus they expect the hump near the electrocapillary maximum (*i.e.*, at a potential where the field in the inner region is zero) where the orientation of water molecules changes over resulting in dielectric unsaturation. In the presence of specific adsorption, they predict the hump to be on the anodic side of the electrocapillary maximum and more pronounced because the resultant μ_w is larger as the compact layer widens with the entry of a larger ion. However, it must be pointed out that if the Helmholtz layer is widened by anions, the hump will tend to be broader but will not shift away from the electrocapillary maximum. An increase in the height of the hump is possible only if μ_w increases faster than the increase in the thickness of compact layer. Even assuming a dipole chain model (307), it is difficult to visualize an increase in the effective μ_w because the dipole moment per unit length of the chain must be constant.

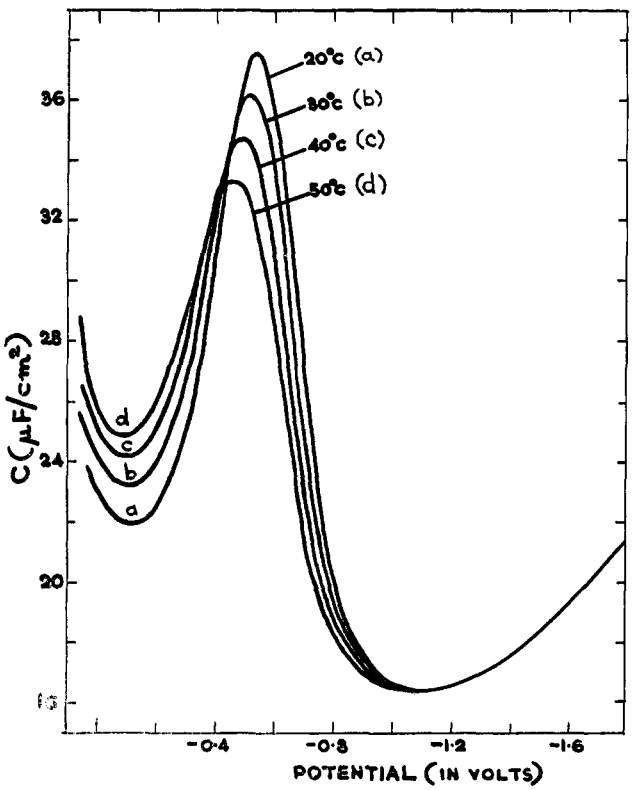

Figure 33.—Differential capacity curves of mercury in 0.0847 *M* sodium benzene-*m*-disulfonate solution at various temperatures (reproduced from ref. 254).

Another consequence of the above theory is that the location of the hump should be independent of the nature of the anion and concentration. But this is contrary to what is observed (see section III-B). Further Watts-Tobin's model implies that in the measured potentials, the contribution due to water dipoles is ≈ 1 v. and should take place within ± 0.2 v. from the electrocapillary maximum. Such a large change in χ_{dipole} would have given rise to several effects especially in electrode kinetics, which could not have gone undetected. A fundamental weakness in Watts-Tobin's model is that each water molecule is assumed to respond only to the field uninfluenced by neighboring water molecules. Such a behavior is possible only in the gas phase, but in the highly condensed liquid film such an assumption is unwarranted.

According to Schwartz, Damaskin, and Frumkin (286), the hump is due to the "delay in the adsorption of anions," the delay being caused by the reorientation of water molecules in the vicinity of the ion and hence a contribution to dE/dq_M and hence to the capacitance. They also expect (a) the hump to be more conspicuous with F^- (as it is more hydrated) than with iodide (which is less hydrated) and (b) the hump to disappear as the temperature is increased since the increase in temperature decreases hydratability and adsorbability. The above theory which is equivalent to an application of Watts-Tobin's treatment to the water molecules only in the vicinity of the specifically adsorbed ion cannot explain humps on the far anodic side (+6 μc.) in the case of BrO_3^- ion and also the hump in the case of benzene-*m*-disulfonate ion which does not disappear as the temperature is increased (see Figure 33).

Bockris, Devanathan, and Muller (20) have suggested that the hump in the capacitance curves is a consequence of an inflexion in the q_1 *vs.* q_M curves, *i.e.*, due to the term dq_1/dq_M (see Eq. 29). The inflexion is attributed to the lateral repulsions between the adjacent anions in the Helmholtz layer. From the isotherm, a simple calculation has shown that the hump should occur at

$$q_M = \frac{1}{A'}\left(\frac{2}{3}\log\frac{4}{3B''} - \log m + \frac{4}{3}\right) \quad \text{(Eq. 58)}$$

where $A' = 4\pi e_0 r_i/\epsilon kT$, $B'' = Me_0^2 r_i^2 \pi^{1/2}/4\epsilon kT$, and $m = 2r_i n_0$. This treatment appears to be qualitatively in accordance with the experiment.

The point at which the inflexion should occur, *i.e.*, the point at which dq_1/dq_M is maximum can be obtained in case of simple ions from Eq. 54. According to this $dq_1/dq_M = 1/R'$. But R' is a function of q_1 since the micropotential varies with the ratio δ/r. When δ/r is <0.2, it tends to 0.805, but as δ/r increases to 1, R' will tend to become 1 (see Table I in ref. 139). Thus at a particular value of q_1, the value of R' will start increasing. Around this point, therefore, dq_1/dq_M is a maximum. Since the position of the hump is dependent on q_1, it follows that with dilution, the position of the hump shifts towards the anodic side since a larger q_M is required to attain the same value of q_1. With organic anions of large area, the simple isotherm suggested will have to be modified to take into account their finite size. This will result in a S-shaped isotherm, with coverage approaching unity on the anodic side. Consequently dq_1/dq_M will have a maximum value at $\theta = 0.5$ and will be zero at $\theta = 0$ and $\theta = 1$. Therefore, according to Eq. 29, a distinct hump should be noticed at $\theta = 0.5$ and the capacity should come down to the base capacity value, namely 17 μf./cm.². Such a hump will not disappear with increasing temperature (see Figure 33). The behavior of benzene-*m*-disulfonic acid is in excellent agreement with these predictions.

J. THE MINIMUM CAPACITY AND THE CATHODIC BRANCH OF THE DIFFERENTIAL CAPACITY CURVES

As pointed out earlier, all the differential capacity curves for aqueous solutions coincide at one unique point, *i.e.*, at −12 to −13 μc./cm.², the capacity value being 17.1 μf./cm.². Since this minimum is independent of the nature of the anion as well as dilution, it can be inferred that it is characteristic of the solvent only. Hence the dielectric property of water can be derived at this point. From a simple calculation, it

is found (57) that the dielectric constant is 7.19, assigning a distance of 3.72 Å. for the compact layer. This value appears to be a reasonable one because from dielectric constant measurements in the microwave region (275, 287), a value of 6 is obtained for H_2O, corresponding to atom and electron polarizations only. This implies that at the interface, the water molecules have lost orientational freedom. This could arise if the electric field is sufficiently strong to cause dielectric saturation (213, 214) or if the chemisorption forces are sufficiently strong to hold the water molecules at a particular orientation irrespective of the field strength. As for values other than 6 to 7 quoted in the literature for water in the inner region, there appears to be no justification for their use.

At $q_M = -13$ μc./cm.^{2}, it is known that all the cations are in the diffuse layer, and the capacitance minimum is independent of the nature of the cation, the variation being less than 2%. It is obvious that if the dielectric constant beyond the outer Helmholtz plane is very much larger than 7, *i.e.*, ~79, then all hydrated cations whose centers lie beyond 3.72 Å. will exhibit the same capacity as that of the compact layer in the absence of specific adsorption. Thus the essential requirement for the constancy of the capacity is that the dielectric constant should increase rapidly with distance. The rate of this variation has been discussed by several authors (20, 38, 213, 232). In such discussions, the choice of the distance of the outer Helmholtz plane is an important point. The model of Bockris, Devanathan, and Muller (20) assumes too large a distance for the centers of hydrated ions which gives rise to difficulties concerning the mechanism of electrodeposition and dissolution. It therefore appears that the previously estimated distance of 3.72 Å. in which the ion is separated from the metal by one water molecule is more reasonable for the Helmholtz layer. This conclusion is also arrived at independently (110) by plotting salt excess *vs.* bulk concentration and then evaluating the slope of that curve. The value obtained is 3.3 Å. which is in close agreement with 3.72. Å. deduced for Devanathan's model (57).

Beyond -13 μc./cm.^{2}, the capacity increases rather slowly. MacDonald suggested (213) that this is due to electrostriction since on the basis of his model the water is already dielectrically saturated. But according to Eq. 29, this increase must be regarded as due to the specific adsorption of cations. On this basis, the rate of increase must be greater for less hydrated cations as is observed. This gradation has been confirmed independently from electrode kinetic data (see references in 112).

It may be noted that the range available for specific adsorption of cations is much less than for anions. This is due to the fact that the hydration energy for cations is much larger than for anions of the same radii. Consequently, specific adsorption of cations is restricted to a small range on the extreme cathodic side.

IV. Adsorption of Organic Molecules at the Mercury–Solution Interface

A. Methods Used for the Evaluation of the Surface Excess of Organic Molecules

1. Thermodynamic Method

From the basic electrocapillary equation

$$\partial\gamma = -q_M \, dE - \Gamma_{org} \, \partial\mu_{org} \qquad \text{(Eq. 59)}$$

Γ_{org} can be obtained, at constant E, by graphical differentiation as in the case of ions (see section III-A) from electrocapillary data. Γ_{org} can also be obtained, at constant q_M, from surface pressure (259) data obtained from interfacial tension measurements, by differentiation of Φ with respect to μ_{org} using

$$\Phi = \xi^b - \xi = \gamma^b - \gamma - q_M(E^b - E) = \Gamma_{org} \, d\mu_{org} \qquad \text{(Eq. 60)}$$

2. Direct Method

This method involves the measurement of difference in bulk concentration upon adsorption. By making the ratio of the area of the electrode to the volume of the solution large, it is possible by physico-chemical methods of analysis, *e.g.*, potentiometry and spectrophotometry (10, 37, 39), to determine Γ_{org} directly. Hitherto, this method has been applied to study adsorption on solids at their electrocapillary maximum.

However, recently a radiotracer technique has been perfected (14) for the *in situ* determination of Γ_{org} at different potentials. This method consists in lowering a Geiger–Muller counter with its window covered with a thin foil of the electrode material and measuring the change in the number of counts, as the electrode contacts the solution, at a particular potential. Since the β-rays must penetrate the electrode foil to the Geiger–Muller counter, the metal foil should be as thin as possible and be free of pinholes. This restricts the use of the above method to gold.

A modification (151) of the above method consists in sending a metallic tape through the solution containing the labeled species and measuring its radioactivity after adsorption when a thin film of solution of approximately 2 μ is left on the metal. This has a wider applicability and is used for studying organic adsorption (21, 22, 149, 150, 308) on a number of solid metals.

3. Nonthermodynamic Approaches

These are concerned mainly with the calculation of Γ_{org} or θ from the differential capacity curves (Figures 34 and 35) studied in the presence of organic compounds.

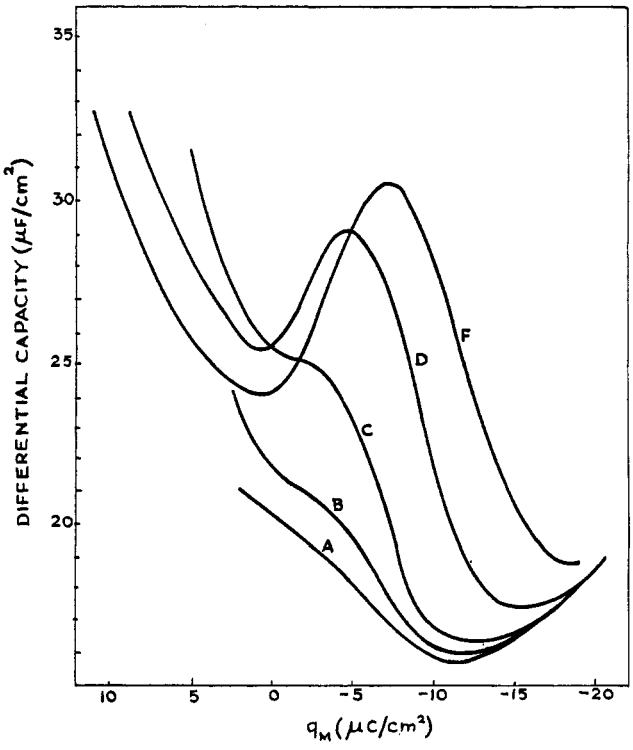

Figure 34.—Differential capacity curves (at 1025 c.p.s.) of thiourea in 0.1 N NaF on mercury, as a function of q_M. A, 0; B, 10^{-3} M; C, 10^{-2} M; D, 10^{-1} M; E, 0.5 M (from the data of Schapink, *et al.* (283)).

a. Frumkin's Method

In the case of aliphatic compounds, the charge dependence has been assumed (86, 87, 105) to be linear with coverage according to the formula

$$q_M = q_{\theta=0}(1 - \theta) + q_{\theta=1}\theta \text{ (at constant potential } E) \quad \text{(Eq. 61)}$$

or

$$q_M = q_{\theta=0}(1 - \theta) + C_{\theta=1}(E_r - E_N)\theta \quad \text{(Eq. 62)}$$

In terms of the measured capacity, the above equation can be written as

$$C = \frac{\partial q}{\partial E_r} = \theta C_{\theta=1} + (1 - \theta)C_{\theta=0} + (q_{\theta=1} - q_{\theta=0})\frac{\partial \theta}{\partial E_r} \quad \text{(Eq. 63)}$$

when $\partial\theta/\partial E_r$ is assumed to be negligible; *i.e.*, in the vicinity of e.c.m., the measured capacity is equal to the capacity of two condensers connected in parallel, one a water-filled condenser and the other organic, *i.e.*

$$C = \theta C_{\theta=1} + (1 - \theta)C_{\theta=0} \quad \text{(Eq. 64)}$$

Now for the calculation of θ from the capacity values, $C_{\theta=1}$ should be known. In the absence of a method for obtaining the $C_{\theta=1}$ independently, an extrapolation procedure has been adopted. This consists in plotting

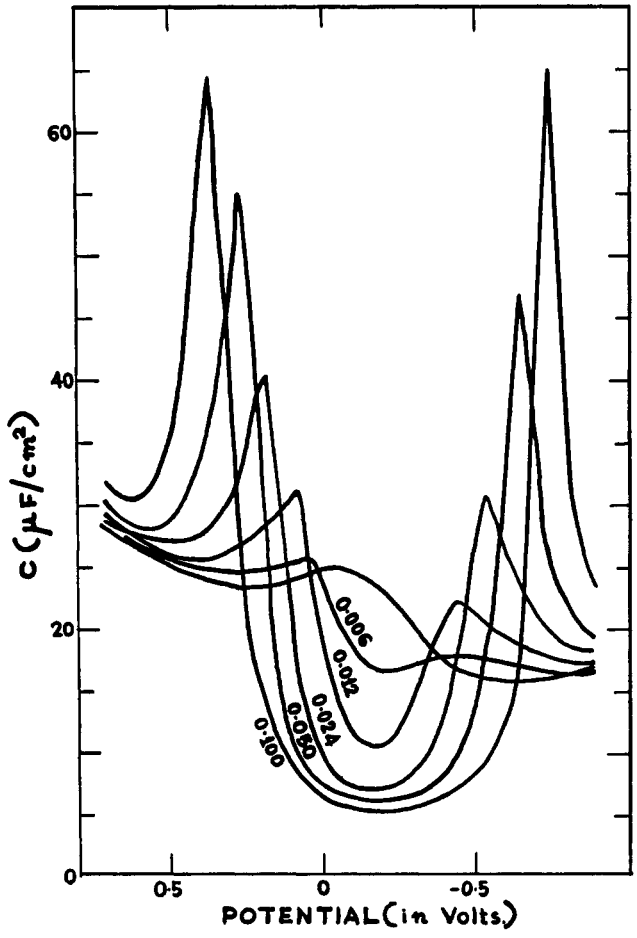

Figure 35.—Differential capacity curves extrapolated to zero frequency for various concentrations of n-amyl alcohol in 1 M $NaClO_4$ and 0.001 M $HClO_4$ (reproduced from ref. 59).

1/minimum capacity *vs.* 1/bulk concentration and finding the capacity value at infinite bulk concentration assuming the curve to be linear. But from an inspection of the capacity curves (see Figure 35), it can be seen that the minimum capacity is linear with concentration in dilute solutions and tends to become constant at higher concentrations. Hence the above method of getting $C_{\theta=1}$ is not correct and has no physical significance. But if the value of the minimum capacity obtained at high concentrations is taken as $C_{\theta=1}$ and used in Eq. 61 or 64, θ values in agreement with the thermodynamic data have been obtained (31). However, the values of θ, obtained from Eq. 61 or 64, are reliable only in the neighborhood of e.c.m.

But for calculating θ over the complete range of potentials, Eq. 63 has to be used. For this purpose, the last term $(\partial\theta/\partial E_r)$ can be evaluated from the thermodynamic identity

$$\left(\frac{\partial \ln a_{org}}{\partial \theta}\right)\left(\frac{\partial \theta}{\partial E_r}\right) = \left(\frac{\partial \ln a_{org}}{\partial E_r}\right)_\Gamma = -\frac{1}{RT\Gamma_m}\left(\frac{\partial q_M}{\partial \theta}\right)_{E_r} \quad \text{(Eq. 65)}$$

By substituting $\partial \ln a_{org}/\partial\theta$ from Frumkin's isotherm (86)

$$Bc_{org} = \frac{\theta}{1-\theta}\exp(-2a\theta) \qquad \text{(Eq. 66)}$$

and $\partial q_M/\partial\theta$ from Eq. 61, in Eq. 65, one can write Eq. 63 in the form

$$C = C_{\theta=0}(1-\theta) + C_{\theta=0}\,\theta + \frac{[q_{\theta=0} + C_{\theta=1}(E_N - E_r)]^2 h}{RT\Gamma_m} \qquad \text{(Eq. 67)}$$

where

$$h = \frac{\theta(1-\theta)}{1-2a\theta(1-\theta)} \qquad \text{(Eq. 68)}$$

This equation, though satisfactory for some compounds, breaks down when applied to compounds like *n*-valeric acid in 0.1 *N* $HClO_4$ (48, 155). Hence variation of a with E is assumed (45, 46). Therefore, Eq. 67 will read as

$$C = C_{\theta=0}(1-\theta) + C_{\theta=1}\theta + \left[q_{\theta=0} + C_{\theta=1}(E_N^\circ - E_r) - 2RT\Gamma_m\theta\frac{\partial a}{\partial E_r}\right]^2 h \qquad \text{(Eq. 69)}$$

where $E_N^\circ = E_N$ if $da/dE_r = 0$.

In the above equation, all quantities vary with potential except $C_{\theta=1}$. It can be solved for θ, provided da/dE_r or a is known. a can be evaluated from the experimental data as follows. The concentration dependence of the adsorption peaks has been shown (45) to be given by

$$\frac{\Delta E_p}{2}\left(\frac{\partial \log c_{org}}{\partial E^{max}}\right) \cong \log\frac{1+r_p}{1-r_p} - \frac{a}{2.3}r_p \qquad \text{(Eq. 70)}$$

where

$$r_{p^{1/2}} = \sqrt{\frac{2-a}{4-a}},\ r_{p^{3/4}} = \sqrt{\frac{2-a}{8-a}},\ r_p = \frac{h_p}{h_p^{max}}$$

h_p being the height of the peak.

Thus from the a values found at the adsorption–desorption peaks and at the potential of maximum adsorption by Eq. 64 and 66, the dependence of a on E_r is evaluated. The a values for most of the aliphatic organic compounds have been found (47, 105) to be $\geqslant 1.0$. The term da/dE_r can be calculated from the a *vs.* E_r curve and is found (45, 47, 48, 105) to be linear with E_r for aliphatic organic compounds

$$a = a_0 + KE_r \qquad \text{(Eq. 71)}$$

where a_0 is the intercept of a *vs.* E_r curve. Now knowing all the parameters in the Eq. 69, θ values have been calculated from the differential capacity curves for aliphatic organic compounds.

From the base capacity curve, with the aid of $C_{\theta=1}$, and the values of da/dE_r and θ obtained earlier, the experimental capacity curves in the presence of organic compounds have been reconstructed (45, 47, 48, 105). This shows the internal consistency of the method. However, in the case of aromatic compounds, it is not possible to calculate (47, 50) the θ values from Eq. 69.

It should be noted that the a parameter varies from one substance to another and for the same substance in different supporting electrolytes. Further the above treatment neither explains the a variations nor gives any method of independently obtaining a from molecular parameters and thus obscures the physical picture of the double layer making the a parameter a "catch all."

b. Devanathan's Model Method (58–60)

This method is based on a proposed model for the structure of the double layer in the presence of organic substances.

When an organic substance is added, the differential capacity varies because of two effects: (i) due to the contribution to the measured potential from the dipole moment of the organic molecule and (ii) due to the lowering in the effective dielectric constant of the compact layer.

Since it is known that the components of ionic charge are not altered much in the presence of organic molecules, the q_d/K_{m-2} term can be expressed as

$$\phi_M + \Delta\phi_{ion} + \Delta\phi_{org} - \phi_2 = q_d/K_{m-2} \qquad \text{(Eq. 72)}$$

Assuming that the ion and its image form a dipole, $\Delta\phi_{ion}$ can be written as

$$\Delta\phi_{ion} = \frac{4\pi r_i e_0 n_i}{\epsilon} = \frac{q_1}{K_{m-1}} \qquad \text{(Eq. 73)}$$

The potential due to the dipoles is assumed to be equal to

$$\Delta\phi_{org} = \frac{2\pi\mu_d\Gamma_{org}}{\epsilon} = \frac{e_0\Gamma_{org}}{K_{org}} \qquad \text{(Eq. 74)}$$

when there is no change in dielectric constant of the compact layer, substituting Eq. 73 and 74 in Eq. 72, and by suitable modifications, it can be shown that the measured capacity is equal to

$$\frac{1}{C} = \frac{1}{C_b} + \frac{e_0}{K_{org}}\frac{d\Gamma_{org}}{dq_M} \qquad \text{(Eq. 75)}$$

Hence

$$\frac{d\Gamma_{org}}{dq_M} = \left(\frac{1}{C} - \frac{1}{C_b}\right)\frac{K_{org}}{e_0} \qquad \text{(Eq. 76)}$$

The above equation can also be derived, in a much simpler way, as follows. The potential of the metal due to ionic and χ contributions can be written, in general, as

$$\phi_M = \phi + \chi \qquad \text{(Eq. 77)}$$

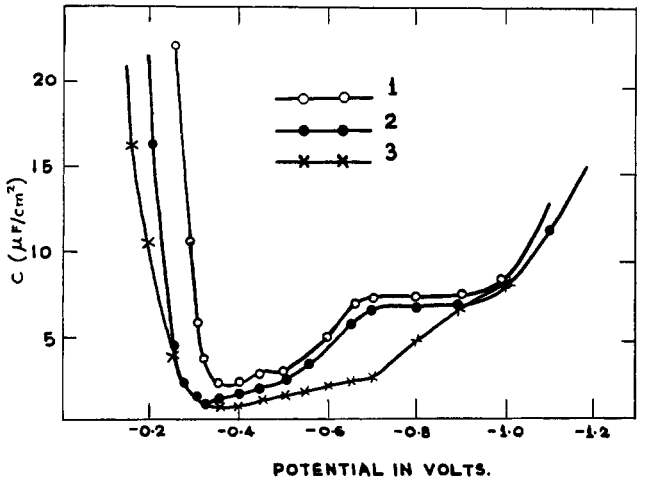

Figure 36.—Differential capacity curves on mercury. 1, 1 N KCl saturated with octyl alcohol; 2, 0.1 N KCl saturated with octyl alcohol; 3, 0.01 N KCl saturated with octyl alcohol (reproduced from ref. 221).

where ϕ is the potential drop in the absence of adsorbed species at a particular value of q_M. In the presence of the adsorbate, *e.g.*, thiourea, the dipole reduces the initial field by χ which is assumed to be $2\pi\Gamma_{org}\mu_d/\epsilon$ and hence

$$\phi_M = \phi - \frac{2\pi\mu_d\Gamma_{org}}{\epsilon} = \phi - \frac{e_0\Gamma_{org}}{K_{org}} \qquad \text{(Eq. 78)}$$

Differentiating Eq. 78, one finds

$$\frac{d\phi_M}{dq_M} = \frac{1}{C} = \frac{1}{C_b} - \frac{e_0}{K_{org}}\frac{d\Gamma_{org}}{dq_M} \qquad \text{(Eq. 79)}$$

which is the same as Eq. 75.

Thus from the differential capacity curves, Γ_{org} has been obtained and found to be in agreement with thermodynamic values for the adsorption of thiourea where the capacity increases, because at constant q_M, the field is reduced by the dipole in adsorbing with the S end of the C=S group toward the metal.

This procedure is absolute in that from the capacity data alone, the Γ_{org} is obtained by substituting values for e_0/K_{org} obtained by independent data, unlike the method of Damaskin, and is very sensitive to the constants chosen. The excellent agreement with the thermodynamic data shows that the magnitude of the contribution to the measured potential is correctly given by Eq. 74. However, it should be pointed out that formulas for χ_{dipole} presently available represent idealizations rarely obtained in practice. This aspect is dealt with in greater detail in a later section.

In the case of aliphatic organic compounds, Eq. 75 or 76 cannot be applied to evaluate the Γ_{org} because most of the aliphatic organic compounds are adsorbed with their paraffinic group, which has no dipole moment toward the metal, and hence there is no contribution to the measured potential. As the adsorption of a hydrocarbon group displaces approximately two water molecules, each of dipole moment 1.87 D., the K_{org} has to be calculated on the basis of displaced water molecules. On this basis, the capacity lowering is the consequence of the presence of the hydrocarbon group, which has a dielectric constant of 1.6 in the inner layer. Consequently, the minimum capacity can be calculated, provided the compact layer thickness is constant, from the ratio of dielectric constants and is approximately 5–6 μf./cm.^{2} at the e.c.m. Hence the dielectric constant which is now composed of contributions from water and the organic molecules can be written in analogy with the formula for the dielectric constant of mixtures as

$$\epsilon' = \epsilon_0\Theta + \epsilon_w(1 - \Theta) \qquad \text{(Eq. 80)}$$

Equation 75 can be modified, to take into account changes due only to dielectric constant variation at constant q_M, to read

$$\frac{1 - \alpha\Theta}{C} = \frac{1}{C_b} - \frac{e_0}{K_{org}}\frac{d\Gamma_{org}}{dq_M} \qquad \text{(Eq. 81)}$$

where

$$\alpha = \frac{\epsilon_w - \epsilon_0}{\epsilon_w} \qquad \text{(Eq. 82)}$$

This equation has been solved by successive approximations for Θ from the capacity curves in the presence of amyl alcohol and found to be in good agreement with the thermodynamic values.

With the aid of Eq. 81, the shape of the differential capacity curves can be understood. When Θ is very small, the capacity curve in the presence and absence of the organic species is the same. As Θ increases, $d\Theta/dq_M$ increases rapidly and so the capacity increases. But this rise in capacity is immediately counteracted by the lowering of the dielectric constant as more organic molecules enter the compact layer, and this results in the decrease of the capacity, thereby creating the adsorption–desorption peaks. As the coverage increases, $d\Theta/dq_M$ becomes small and the capacity is below the base curve. If, in the initial stages of adsorption, $d\Theta/dq_M$ is small, then no marked peaks should be observed, as found (306) in the case of dioxane in potassium halide solutions.

The main postulate made in the above treatment, *i.e.*, at constant q_M, "The components of ionic charge are unaltered by the adsorbate," is its own limitation. Hence, Eq. 81 cannot be used when the compact layer thickness increases to a distance equal to the length of organic molecules from the metal as a consequence of expulsion of the water molecules due to the formation of water-free coherent film (124). Such a behavior is marked only when there is strong van der Waals' interactions as in the case of long-chain organic compounds. So, under these conditions, the minimum

capacity could be further lowered as is observed with hexyl and octyl alcohols (221) (see Figure 36). However for small molecules, the compact layer thickness in the absence of water-free coherent film is governed only by the water molecules.

In contrast, the $C_{\theta=1}$ value which is an important factor in Frumkin and Damaskin's theory is based on the assumption that the thickness of the double layer in the presence of organic compounds is greater than in the absence of organic compounds. But the factors which determine $C_{\theta=1}$, *viz.*, the dielectric constant and the length of the organic chain, have not been separately evaluated and correlated with molecular dimensions.

B. POTENTIAL DUE TO PERMANENT DIPOLES AT THE METAL–SOLUTION INTERFACE

Whether the expression to be used for calculating the χ_{dipole} is $4\pi N_d\mu_d/\epsilon$ or $2\pi N_d\mu_d/\epsilon$ has been a subject of controversy for a long time among surface chemists and recently among electrochemists (58, 105, 215). The potential due to dipoles under vacuum, on a continuous model, from classical electrostatics, is $4\pi \cdot N_d\mu_d/\epsilon$. But on the basis of a discrete model for infinite surfaces *in vacuo*, Gomer (125) has shown that the potential rises on either side of the dipole array slowly with distance (see Figure 37) and approaches a 4π formula. However, for a finite array of dipoles under vacuum at sufficiently greater distance, several times the dimensions of the sheet, the potential decays back to zero (1, 153) as given by the classical formulas.

When the dipoles are adsorbed on a metal, by considering the interaction between dipole and its image, it can be shown that the potential is equal to $4\pi N_d\mu_d/\epsilon$. But in the presence of an electrolyte, the potential is affected (61) due to two factors: (a) due to the ions in the solution and (b) due to the high dielectric constant of water. Consequently χ_{dipole} is less than $4\pi \cdot N_d\mu_d/\epsilon$ and is difficult to evaluate by means of an explicit formula.

A simplification (61) can be brought out if one assumes that the electrolyte solution beyond the outer Helmholtz plane is equivalent to a metal. Only then one can apply the Helmholtz formula for that part of the dipole which is within the first water layer and not the dipole moment of whole molecule to calculate χ_{dipole}. However, this is open to the objection that the same medium is regarded as a conductor when discussing potentials due to dipoles and as a dielectric when discussing the potential due to ions as in diffuse layer theory.

It should, however, be pointed that many workers (259, 283), unaware of the complexity of the situation, have used idealized expressions in which the dielectric constant is a disposable parameter. Thus the proponents of the 4π formula have used a value of ~14

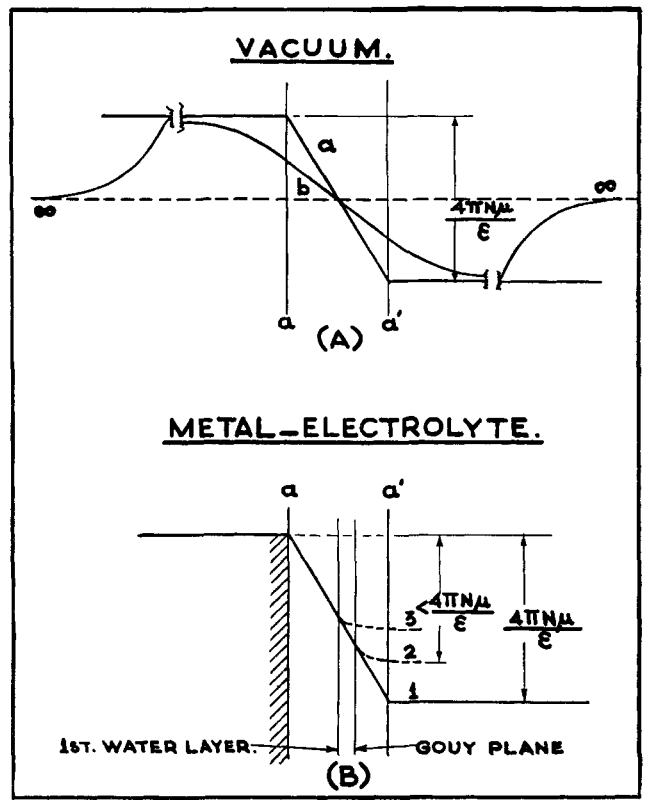

Figure 37.—Schematic representation of the potential due to dipoles. (A) Dipole *in vacuo:* a, potential drop based on the classical model; b, based on a discrete model. (B): 1, dipole in contact with a metal (on the classical model); 2 and 3, dipoles on a metal in electrolyte solutions.

and those supporting the 2π formula a value of 7, thereby obtaining a good agreement with experiment.

Now that the dielectric constant of water is known to be between 6 and 7 (57, 239, 275, 287, 305), the use of a 4π formula with the full moment leads to erroneous values of χ_{dipole}. In the case of the 2π formula which has been applied for thiourea, the agreement (58, 308) is fortuitous because, for thiourea, the product of 2π times the full moment is nearly equal to 4π times the moment of the C=S group which is within the first water layer. In the case of water molecules, the degree of discreteness as defined by the ratio r/δ is so large that the potential at any point along the axis of the molecule gets little or no contribution from neighboring molecules. Under these conditions, the molecule is equivalent to a dipolar disk of molecular dimensions. For such a system, the potential decays in distances of molecular dimensions, even in case of a vacuum, and hence the contribution to the measured potential whether there is solution or not is $2\pi N_d\mu_d/\epsilon$.

C. THEORY OF THE ADSORPTION OF NEUTRAL MOLECULES

Adsorption is essentially a result (20, 34, 35) of competition for sites, at the interface, between the water molecules and the organic species. Since, at the point of zero charge, no electric field effects exist, the intrinsic

adsorption characteristics can be evaluated for the following four systems.

Hydrocarbon Molecules.—The low solubility of hydrocarbons in aqueous solution is due to weak hydrophobic hydration. Hence the adsorption at the Hg–solution interface is caused by squeezing types of forces (34, 35, 140, 240), which eject the molecule from the bulk to the surface, and not as a result of specific interaction between the metal and the organic species. Therefore the adsorption at the mercury–solution interface should be similar to that at the air–water interface, as is normally observed.

Hydrocarbons with Polar Groups.—The presence of a polar group attached to a hydrocarbon chain increases its solubility because of the interaction of the polar groups with water molecules. This reduces the energy of the squeezing type of forces with the result that the hydrocarbons with polar groups are adsorbed to a lesser extent than hydrocarbons. The polar group also confers a fixed orientation to the molecule which is adsorbed with the polar group in the water. As the length of the hydrocarbon chain increases, the influence of the polar group decreases. Consequently, the longer the chain length, the less is the solubility and the greater the adsorbability.

When the chain length is sufficiently large, the van der Waals' forces between the adjacent hydrocarbon chains are sufficient to expel the intervening water molecules, forming condensed water-free films.

Molecules with Specifically Interacting Atoms.—The above two systems refer to the adsorption which is a result of weak adsorbate–solvent interactions and not due to any adsorbate–adsorbent interactions. The latter type of forces between the metal and the organic molecule can be seen clearly when one considers the adsorption of urea and thiourea at the air–water and the Hg–solution interface. At the air–water interface, both are negatively adsorbed as shown (88) by an increase in the interfacial tension. But at the Hg–solution interface, thiourea is more strongly adsorbed than urea. This is due to the strong chemisorptive or covalent forces between the metal (Hg) and the sulfur of thiourea. These interactions can be lessened if the molecule contains a hydrophobic group, *e.g.*, N-methylthiourea, because now adsorption is an outcome of the competition between the hydrophobic group and the sulfur end of the molecule.

Aromatic Molecules.—There is yet another type of electrostatic interaction between the metal and the organic molecule arising from π electrons (10, 11, 15, 16, 36, 47, 50, 118, 119, 121, 123) of the unsaturated organic compounds, *e.g.*, benzene, phenol, pyridine, etc. But this is dominant only on the anodic side of the e.c.m.

The above conclusions can also be deduced from a thermodynamic standpoint (22). This consists in considering the usual thermodynamic cycles for the adsorption of water and the organic substances, for separately evaluating the standard free energies of adsorption of water and organic substance from the solution, starting from the vapor state. Since, adsorption from aqueous solution is a competitive process between the water and organic molecules, the free energy of adsorption (ΔG_a) is equal to the difference in the standard free energies of adsorption of water and organic substance and can be written as

$$\Delta G_s \text{ (water)} = \Delta G_p \text{ (water)} + \Delta G_v \text{ (water)} \quad \text{(Eq. 83)}$$

$$\Delta G_s \text{ (organic)} = -\Delta G_d \text{ (organic)} - \Delta G_p \text{ (organic)} + \Delta G_v \text{ (organic)} \quad \text{(Eq. 84)}$$

Therefore

$$\Delta G_a = \Delta G_s \text{ (organic)} - n\Delta G_s \text{ (water)} \quad \text{(Eq. 85)}$$

The subscript s refers to the free energy of adsorption from solution; p to the term $-RT \ln P_0$ where P_0 is the vapor pressure at temperature T; v to the free energy of adsorption from vapor phase at 1 atm.; and d to the free energy of dilution which can be expressed for organic substance as $RT \ln c_{org}/c_s$, c_s being the saturation concentration of the organic substance. n is the number of water molecules displaced by the organic substance.

$$\Delta G_a = -RT \ln \frac{c_s}{55.4} - RT \ln \frac{P_0 \text{ (organic)}}{P_0^n \text{ (water)}} + \Delta G_v \text{ (organic)} + n\Delta G_v \text{ (water)} \quad \text{(Eq. 86)}$$

Thus adsorption is a function of the adsorbate–solvent forces (first two terms in Eq. 86) and also adsorbate–adsorbent forces (the last two terms in Eq. 86).

Now the effect of the electrical field can be discussed for the above four systems. Molecules respond to the electric field owing to their polarizability. Since the dielectric constant, which is a measure of polarizability, is 6 for water as compared to $\sim$1.8 for hydrocarbons, the introduction of an electric field will tend to favor the adsorption of water molecules thereby decreasing the coverage of organic molecules, irrespective of the direction of the field. Therefore the organic molecules are desorbed on either side of the e.c.m. The polar groups attached to hydrocarbons are normally situated far beyond the outer Helmholtz plane and are subjected (64) to only the influence of the weak Gouy field. Hence the desorption of these substances is slow as compared to hydrocarbons with no polar groups. This behavior is noticed with butyl compounds with various substituent groups (see Figure 38).

When the dipole of the molecule, *e.g.*, C=S of the thiourea molecule or S of dibutyl sulfide, is oriented towards the metal in only one particular direction because of specific forces and is in the compact layer,

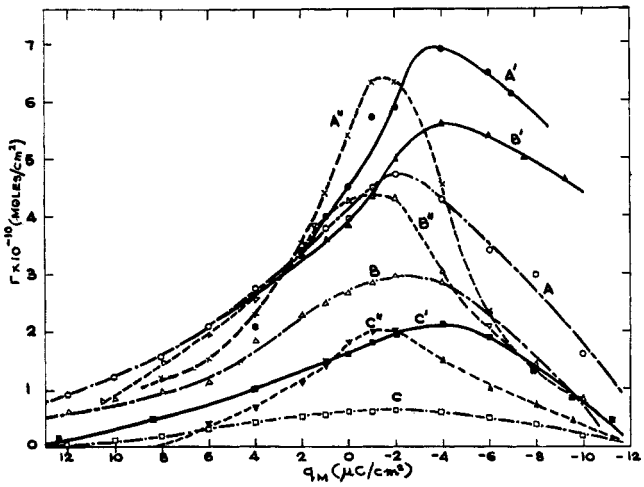

Figure 38.—Surface excess curves plotted as a function of q_M. A, A′, and A″ refer to 0.1 N solutions of butanol, valeronitrile, and valeric acid, respectively; B, B′, and B″ refer to 0.05 N solutions of butanol, valeronitrile, and valeric acid, respectively; C, C′, and C″ refer to 0.01 N solutions of butanol, valeronitrile, and valeric acid, respectively (plotted from the data of Blomgren, *et al.* (16)).

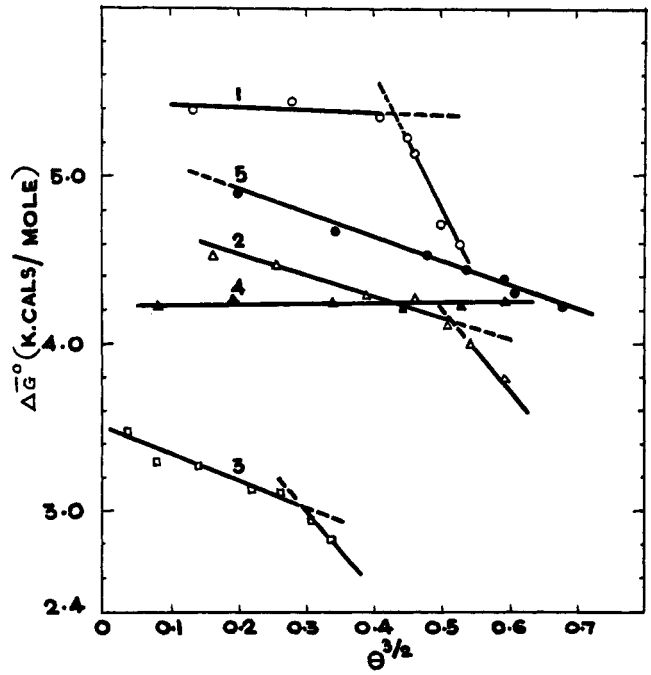

Figure 39.—$\Delta\bar{G}^\circ$ (kcal./mole) plotted as a function of $\theta^{3/2}$. 1, 2-chloropyridine in N KCl at −600 mv.; 2, 1,2,3,6-tetrahydropyridine in N KCl at −400 mv.; 3, pyridine in N KCl at −400 mv.; 4, 2-aminopyridine in N KCl at −600 mv.; 5, aniline in N KCl at −600 mv. (plotted from the data of Conway and Barradas (11, 36)).

then the field favors the adsorption on one side (anodic side in this case) and desorption on the cathodic side.

In the case of compounds with π electrons, the field once again favors the adsorption, but apparently only on the anodic side. This aspect is discussed in a later section.

D. ISOTHERMS FOR ORGANIC ADSORPTION

The most widely used isotherm (20, 59, 100, 198, 209, 283) is that of Langmuir, although other isotherms like Frumkin's (86, 105, 155, 156, 239), modified Helfand, Frisch, and Lebowitz's (263), Virial (58, 259), and modified Volmer (154, 175), which are basically Langmuir's with minor modifications, have been employed. However, the changes in the free energy of adsorption are not radically different if evaluated by isotherms other than Langmuir's. Thus in case of thiourea, it has been shown (70) that the changes in the free energies of adsorption obtained from Virial and Langmuir isotherms are the same within the limits of computational error.

A slightly different approach (11, 15, 16, 36) that has been adopted recently is to consider that the Langmuir isotherm is the correct ideal form for low coverages and to introduce a surface activity coefficient factor to look after the deviations from ideality at high coverages. Thus when the lateral interactions are accounted for in this way, Langmuir's isotherm reads as

$$\ln\left[\frac{\theta}{1-\theta}\cdot\frac{55.5}{c_{org}}\right] - \ln f_\theta = -\frac{\bar{\Delta}G^\circ}{RT} \qquad \text{(Eq. 87)}$$

where f_θ, the surface activity coefficient at a coverage of θ, is a measure of the nonideal free energy of interaction $(G')_\theta$ of the adsorbate dipole and is equal to

$$f_\theta = \exp\left(\frac{(G')_\theta}{RT}\right) \qquad \text{(Eq. 88)}$$

The nonideal free energy can now be expressed as

$$G' = \frac{1}{2}N^*n^*\phi_{11} \qquad \text{(Eq. 89)}$$

where N^* refers to 1 mole of the adsorbed molecules and n^* the coordination number of the adsorbate species. The ϕ_{11} term is due to (i) dipole and dipole interaction energy between the neutral molecules at the interface and (ii) van der Waals-London interaction term. ϕ_{11} is evaluated from the known constants according to the formula

$$\phi_{11} = \frac{\mu_d{}^2\theta^{3/2}}{\epsilon_s\pi^{3/2}R_0{}^3} - \frac{1190Zh\theta^3}{\epsilon_{0,w}\pi^3R_0{}^{3/2}} \qquad \text{(Eq. 90)}$$

where ϵ_s is the dielectric constant of surface layer, $\epsilon_{0,w}$ the optical dielectric constant of water, R_0 the radius of organic adsorbate, Z the number of electrons in the outermost shell of the molecule, and h Planck's constant. The first term in Eq. 90, for organic ions is the Coulombic interaction between the neighboring ions, *i.e.*, $e_0{}^2/\epsilon_sR_0$. Hence the corresponding equation for ions (15) is

$$\phi_{11} = \frac{Ne_0{}^2\theta^{1/2}}{\epsilon_s\pi^{1/2}R_0} - \frac{1190Zh\theta^3}{\epsilon_{0,w}\pi^3R_0{}^{3/2}} \qquad \text{(Eq. 91)}$$

Neglecting the θ^3 term, since it is significant only when $\theta > 0.6$, and assuming μ_d in the surface layer to be

twice its normal value, according to Eq. 87-90, the electrochemical free energy of adsorption $\overline{\Delta G}^\circ$ should decrease linearly with $\theta^{1/2}$. Plots of $\overline{\Delta G}^\circ$ *vs.* $\theta^{1/2}$ show two linear segments which have been interpreted as due to the change in the orientation of the organic species with θ. This approach has been used to infer (11, 36) changing orientation in the case of heterocyclic compounds like tetrahydropyridine and pyridine in 1 *N* KCl, and constant orientation in the case of aniline and 2-aminopyridine in 1 *N* KCl solutions (see Figure 39).

It should be pointed out that the above method is applied to the systems at constant E. It is difficult to say to what extent this behavior is a consequence of the use of constant E scale. It appears necessary to re-examine these conclusions using constant q_M plots.

Instead of obtaining the free energies and interpreting them in terms of molecular parameters, Parsons (258, 262, 263) has chosen the isotherm *a priori*, assumes a pre-set dependence for the variation of the free energy with charge, and then works back the shape of the capacitance curve. This method even though correct in principle does not throw much light on the fine structure of the double layer in the presence of organic molecules. Further, the physical basis for the assumed dependence is not explicitly stated except that any variation can be mathematically expressed in the form of a power series.

Hitherto it has been the practice of most of the workers to employ the potential scale to depict the characteristics of adsorption. It has been correctly pointed out (20, 263, 264) that the potential difference at an interface is a complex quantity, being the sum of contributions from ions in inner layer, ions from outer layer, oriented dipoles, and diffuse layer, and does not represent a clear picture of the physical situation in regard to interactions in the electrical double layer. But the charge on the metal is a thermodynamically definable and obtainable quantity and enables the computation of the field due to the charge residing on the metal. Thus, for example, a comparison of adsorbabilities at air–water and Hg–solution interfaces, is impossible on a potential scale. But on a charge scale, it is obviously the $q_M = 0$ value that has to be compared with the corresponding values at air–water interface, which is all the time at the point of zero charge only. Thus it appears reasonable to use the charge scale while discussing adsorption.

E. QUANTITATIVE THEORIES OF THE EFFECT OF THE ELECTRIC FIELD ON ADSORPTION

1. *Frumkin–Butler Theory*

Frumkin proposed the first theory (86, 87, 105) in which the energy of adsorption (ω) was taken into account by considering two effects: (i) the energy to replace the water molecules and the lengthening of the double layer and (ii) the energy to form a dipole array at the electrode. The formula for the work of adsorption is

$$\omega = {}^1/_2(C_{\theta=0} - C_{\theta=1})E_r^2 + C_{\theta=1}E_N E_r \quad \text{(Eq. 92)}$$

As discussed already, this model, which is valid only under extreme conditions, leans heavily on the experimental data and further it makes use of macroscopic properties of double layer and is semiempirical.

Butler (34) developed a molecular kinetic approach to the adsorption process based on the competition theory. The energy changes due to adsorption, according to him, are (a) due to alteration in the dielectric constant in the compact region which has been accounted in terms of the differences in the polarizability of the organic molecule (α_o) and water molecule (α_w) and (b) due to difference in the dipole moments of water (μ_w) and the adsorbed molecule (μ_o). The expression for the change in the free energy of adsorption, hence, is

$$d(\overline{\Delta G}_a) = [{}^1/_2(\alpha_w - \alpha_o)X^2 + (\mu_w - \mu_o)X]\delta V \quad \text{(Eq. 93)}$$

where X is the field strength expressed as the applied potential difference and δV the volume element of the surface layer. From the above expression, the calculated changes in interfacial tension caused by adsorption are found to be in agreement with experiment. But in order to calculate the polarizability from the expression

$$\alpha_w = \frac{D - 1}{4\pi} \quad \text{(Eq. 94)}$$

bulk dielectric constant values have been used. Since the ϵ in the compact region is much lower than in the bulk due to dielectric saturation effects at high field strengths, correct choice of molecular parameters is necessary for the successful application of the above expression.

2. *Bockris, Devanathan, and Muller's Theory*

The above theories do not specify any model for the structure of water at the interface. As shown earlier, the basic mechanism of adsorption is one of competition between water and organic molecule for sites at the interface, and hence a correct molecular model for water at the interface is an essential prerequisite for evaluating its interaction with the field.

An attempt in this direction has been made by Bockris, Devanathan, and Muller (20). They postulated the interface to be occupied by two types of water molecules, one standing up and the other standing down, independent of each other (Watts-Tobin's model (233, 307)), and examined the problem from the point of (a) χ_{dipole} and (b) organic adsorption. The need for

considering χ_{dipole} arises from the fact that any explanation based on water turning over with the electric field to promote desorption of organic compounds will also predict a large χ_{dipole} and hence a low C_{dipole} for the base electrolyte. As a matter of fact, experimental data (see references in 71 and 109; 196) seem to suggest that χ_{dipole} is constant with potential and also is negligibly small (~60 to 70 mv.).

For the above model, the χ_{dipole} has been deduced as

$$\chi_{dipole} = \frac{2\pi\mu_w N_T}{\epsilon_w} \tanh \frac{\mu_w X}{kT} \qquad \text{(Eq. 95)}$$

Hence the contribution of χ_{dipole} to the measured capacitance is

$$\frac{d\chi_{dipole}}{dq_M} = \frac{1}{C_{dipole}} = \frac{8\pi^2\mu_w^2 N_T}{\epsilon_w^2 kT} \operatorname{sech}^2 \frac{\mu_w X}{kT} \qquad \text{(Eq. 96)}$$

where C_{dipole} is the capacity due to adsorbed dipoles. Since the capacity of the electrical double layer is mainly governed by ions and not the solvent molecules, the C_{dipole} should be high. Because water molecules reduce the applied field by proper orientation, the measured capacity can be expressed as

$$\frac{1}{C} = \frac{1}{C_{\text{double layer}}} - \frac{1}{C_{dipole}} \qquad \text{(Eq. 97)}$$

Equation 96 gives a value of 14 μf. at $q_M = 0$ for C_{dipole} which is too small. By assuming that the variation of free energy of adsorption of aliphatic compounds is governed only by the $\mu_w x$ term for water dipoles, Bockris, *et al.* (20), found that the organic compounds are desorbed more rapidly than shown by the experiment.

Hence they invoked lateral interaction between the neighboring dipoles to reduce the applied field still further and thereby slowing down the turning over of the water molecules. Thus the expression for χ_{dipole} is

$$\chi_{dipole} = 2\pi\mu_w N_T \tanh\left[\frac{\mu_w X}{kT} - R^* \frac{C^*E^*}{kT}\right] \qquad \text{(Eq. 98)}$$

where

$$R^* = \tanh\left[\frac{\mu_w X}{kT} - R^* \frac{E^*C^*}{kT}\right] = \frac{N\uparrow - N\downarrow}{N_T} \qquad \text{(Eq. 99)}$$

Consequently C_{dipole} is

$$\frac{1}{C_{dipole}} = \frac{8\pi^2\mu_w^2 N_T}{\epsilon_w^2 kT}\left[\frac{(1 - R^{*2})}{1 + \frac{E^*C^*}{kT}(1 - R^{*2})}\right] \qquad \text{(Eq. 100)}$$

Assuming a value of 8 for C^* the coordination number, expressing E^*, the dipole–dipole interaction energy, as equal to $\mu_w^2/\epsilon_w kT r_0^3$ where r_0 is the distance between adjacent dipoles, and giving a value of 6 for ϵ_w, they found that the adsorbed water dipoles do not contribute much to the measured potential, the value of C_{dipole} being ~120 μf. at $q_M = 0$.

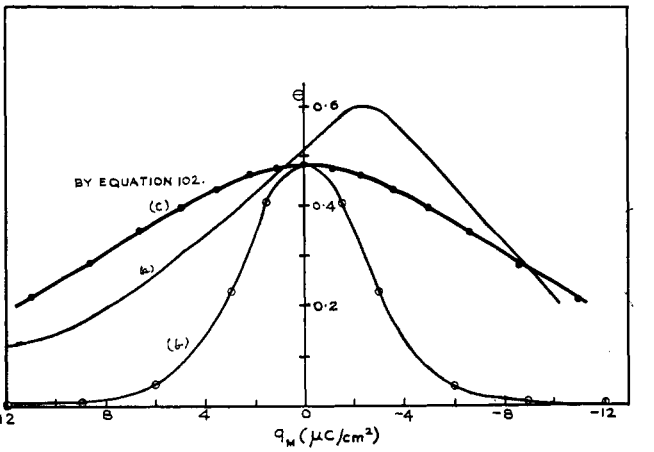

Figure 40.—Comparison of the experimental adsorption curve (a) for 0.1 *N* butanol; with the theoretical curves (b) without taking into account lateral interactions, and (c) taking into account the lateral interactions (Eq. 102) (plotted from the data of Bockris, *et al.* (20)).

From this model, the variation of free energy of adsorption has been expressed as

$$d(\overline{\Delta G}_a) = nR^*\left[\frac{\mu_w X}{kT} - R^* \frac{C^*E^*}{kT}\right] \qquad \text{(Eq. 101)}$$

Here n refers to the number of water molecules displaced by a single organic molecule.

Assuming a Langmuir isotherm, they calculated the Θ values from the equation

$$\frac{\Theta}{1 - \Theta} = \frac{c_{org}}{55.4} \exp\left(\frac{-\overline{\Delta G}_a^\circ}{kT}\right) \times \exp\left\{nR^*\left[\frac{\mu_w X}{kT} - R^* \frac{E^*C^*}{kT}\right]\right\} \qquad \text{(Eq. 102)}$$

(where $\overline{\Delta G}_a^\circ$ is the non-Coulombic free energy of adsorption) and found these to be in agreement with experiment (see Figure 40) for a 0.1 *N* butanol solution for appropriately selected values of E^* and C^*. However, the rate of desorption is critically dependent on E^* and C^*, and there is no basis suggested for the selection of these constants. Further, the values of E^* and C^* vary as the coverage changes, and this variation has been ignored. Any method for incorporating these dependencies will make Eq. 102 cumbersome for purposes of calculation. Besides, it is difficult to imagine the easy turning over of the water molecules, especially in view of the large heat of adsorption (17.6 kcal.) of water (177) on mercury. However, Bockris, *et al.*, have stressed the need to consider the orientation of dipoles and emphasized the competitive basis for the adsorption of organic compounds.

3. Absolute Calculation of the Electrostatic Free Energy of Adsorption

An alternate orientation suggested (71) recently for the water molecules at a metal–solution interface is that they are adsorbed at an angle of 80° normal to

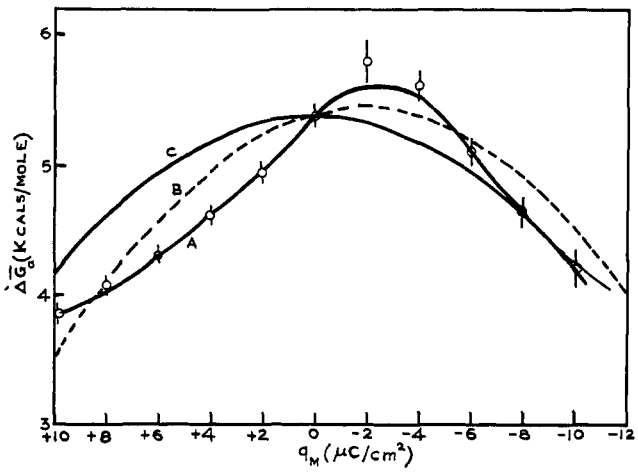

Figure 41.—Variation of the electrostatic part of the free energy of adsorption of amyl alcohol with q_M. A, experimental curve; B, by Eq. 103, taking into account the μ_w term; C, by Eq. 103, omitting the μ_w term.

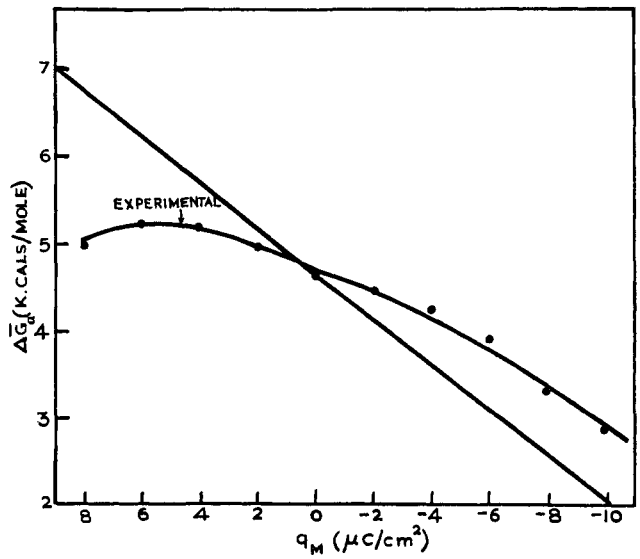

Figure 42.—Variation of the electrostatic part of the free energy of adsorption of thiourea with q_M. The full line is the theoretically calculated curve according to Eq. 103.

the interface, *i.e.*, water molecules are virtually lying flat. This model is based on a critical survey of the existing literature on the nature and magnitude of potential due to water dipoles and gives a constant value of ~63 mv. for χ_{dipole}, thus making the water molecules field insensitive.

Aliphatic Organic Compounds.—Now the changes in the electrostatic part of the free energies of adsorption ($\Delta(\overline{\Delta G}_a)$) of organic molecules can be quantitatively evaluated by considering the changes in the primary water layer alone. Thus from an extension of Butler–Frumkin concepts, it has been shown (71) for simple aliphatic molecules that $\Delta(\overline{\Delta G}_a)$ can be written in the form

$$\Delta(\overline{\Delta G}_a) = 2\pi t q_M^2\left(\frac{A_o}{\epsilon_o'} - \frac{A_o}{\epsilon_w}\right) + 4\pi q_M\left(\frac{\mu_o}{\epsilon_o'} - \frac{n\mu_w}{\epsilon_w}\right) \quad \text{(Eq. 103)}$$

where t is the thickness of the water molecules, A_o the area of the organic molecule, ϵ_w the dielectric constant of water which is 6, and ϵ_o' the dielectric constant of the organic group within first water layer. Since only the paraffinic group of the hydrocarbons is inside the compact layer, μ_o is zero, and, neglecting μ_w, Eq. 103 predicts the same symmetrical pattern for all the aliphatic compounds, whereas the experimental data reveal the adsorption maximum to be at $q_M = -2$ μc./cm.^{2}. A shift of this magnitude has been obtained by substituting the omitted μ_w term in Eq. 103 (see Figure 41). However, there is some disagreement on the anodic and cathodic side (see Figure 38). This is the consequence of ignoring the coverage of anions on the anodic side and not taking into account the interaction of the Gouy field with the dipole on the cathodic side.

Adsorption of Thiourea.—Thus, it is possible to calculate absolutely the changes in free energy with charge. This procedure can be extended to the adsorption of molecules like thiourea. For thiourea, the area term is negligible since $\epsilon_o' \simeq \epsilon_w$, and hence only the $\mu_o x$ term represents the free energy variations. When such a calculation is compared with experiment (see Figure 42), the agreement on the cathodic side is found to be good, but on the anodic side the theoretical curve shows always an increase in $\overline{\Delta G}_a$ while the experiment points to near constancy of $\overline{\Delta G}_a$. This reveals that the adsorption of thiourea is not purely electrostatic, but is operative through covalent binding between Hg and S. Hence the difference can be understood in terms of the decreasing concentration of electrons on the metal with increasing positive q_M, as a result of which the extent of covalent binding decreases. The similarity of electrocapillary curves and capacity curves of thiourea with halide ions had prompted the suggestion (75, 215) that thiourea behaves like the anion S^{2-}. If this be the case, the free energy of adsorption after accounting for electrostatic contribution should be independent of q_M. But the above results suggest that the adsorption of thiourea is governed by covalent bonding.

The above theory has been applied to HCHO and other compounds and is discussed in detail elsewhere (71).

Aromatic Compounds.—Aromatic and unsaturated organic compounds, in addition to the above effects, exhibit attraction toward Hg due to π bonding. The effect of π electrons has been demonstrated (111, 118, 119, 121, 123) from a comparative study of the conjugated unsaturated hydrocarbons and their hydrogenated derivatives. These studies showed that

the unsaturation enhances adsorption on the anodic side when compared with the saturated compounds. This effect increases with an increasing number of π bonds. The intrinsic free energies of adsorption (16) for butyl, phenyl, and naphthyl compounds are -6.4, -8.9, and -12.4 kcal./mole, respectively, and point to the increase of adsorbability due to the presence of π bonds.

These effects can be quantitatively (71) formulated by considering the polarizability of the π electrons. Kemball (176) has shown that each π electron can be regarded as having a polarizability of 4.4×10^{-25} cc. Hence the π-bond contribution (α_π) towards the free energy from the six π electrons is $8\pi^2 q_M^2 \alpha_\pi / \epsilon^2 kT$. Here ϵ is the dielectric constant of vacuum. Since aromatic compounds are adsorbed flat, the π electrons interact with the metal directly. The π contribution to the free energy of adsorption has to be included only on the anodic side, consistent with the known chemistry of the π complexes.

Thus it has been possible to calculate the electrostatic free energy of adsorption for the adsorption of phenol taking the area from Catalin models and assuming that the hydroxyl group moment is parallel to the mercury surface and fixed in this position due to its interaction with water molecules. Such a calculation is found to be in reasonable agreement with the experimental values (see Figure 43).

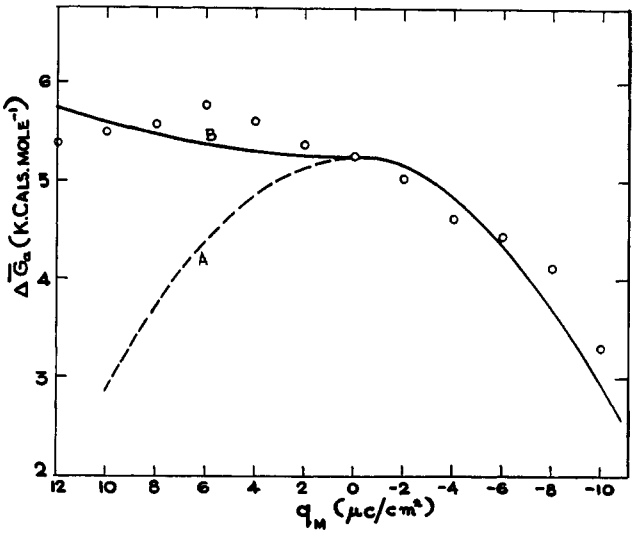

Figure 43.—Variation of the electrostatic part of the free energy of adsorption of phenol with q_M. The open circles indicate the experimental values. A, by Eq. 103 omitting the second term; B, by Eq. 103 omitting the second term and then accounting for π electrons on the anodic side only.

A result of the above polarizability term is that it predicts the absence of desorption on the anodic side for aromatic compounds. However, there is experimental evidence (21, 74, 150) that, at extreme anodic polarizations, aromatic compounds without any ionic group do get desorbed. This may be the consequence of a salting-out effect following an increase in the population of anions. Alternatively it is possible that π-electron polarizability may apply only at low field strengths and may be much smaller at high anodic fields. However, the above calculation for aromatic compounds is only the first attempt at a quantitative formulation for what was until now only qualitatively discussed.

F. ADSORPTION OF ORGANIC IONS AT THE MERCURY–SOLUTION INTERFACE

Earlier, it was shown that the adsorption in the case of neutral organic compounds is governed by the solubility which is a result of the competition between polar groups for positions in the aqueous phase and the hydrophobic groups for sites at the interface.

1. Anions

When the polar group is replaced by an ionic group, then the tendency is for the ionic groups to be adsorbed at the interface forming part of the total charge at the interface. Thus when the hydrophobic group is small, the orientation is governed by the ionic groups which are adsorbed on the metal. This will not produce any lowering of dielectric constant since the hydrocarbon group will be pushed into the aqueous phase, *e.g.*, di- and tricarboxylic acids like oxalic and glutaric acid, etc. (240), in the presence of the supporting electrolyte. Hence the capacity increases with increasing coverage.

In the case of adsorption of small ions like iodide, even though a maximum charge of $\sim$160 μc. can be expected to be packed on 1 cm.^{2} of Hg surface, only a charge of 40 μc. is observed. This is due to the lateral interaction between two ions, and thus each ion behaves as if it has an area of $\sim$40 Å.^{2}. If the ion size itself is greater than 40–50 Å.^{2}, then one should expect a unit coverage of the anions. This is observed with the benzene-*m*-disulfonate ion (254) which has an area of 60–70 Å.^{2}/unit charge and hence a unit coverage corresponds to only $\sim$30 μc./cm.^{2}. If the surface excess reaches a saturation value, then the dq_1/dq term becomes small (see Eq. 29), and hence the capacity should come down either to the supporting electrolyte curve or to 17 μf./cm.^{2} when there is no supporting electrolyte. This behavior is observed with ionized polymethacrylic acid (238, 240, 241) and sodium benzene-*m*-disulfonate. In the latter case, the SO_3^- group is toward the metal and the benzene ring is parallel but away from the metal. With ionized polymethacrylic acid, the adsorption commences very near the e.c.m. and saturation coverage is reached within $\sim$250 mv. Consequently, the differential capacity curve exhibits a very sharp adsorption peak in the vicinity of e.c.m.

If the hydrocarbon group is very large, the hydrophobic forces outweigh the electrostatic forces and the

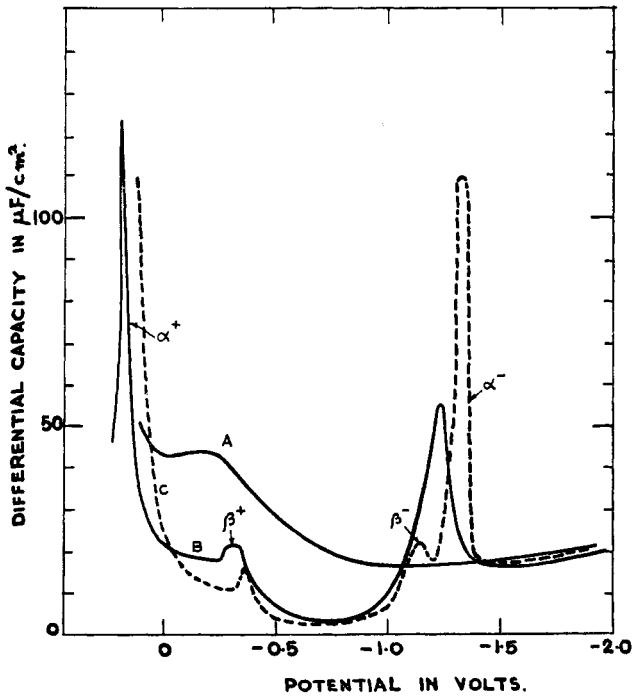

Figure 44.—Differential capacity curves, for mercury, of sodium decyl sulfate. A, 4.0 N Na_2SO_4 alone; B, 0.02 N sodium decyl sulfate alone; C, 0.02 N sodium decyl sulfate in 4.0 N Na_2SO_4 solutions (plotted from the data of Eda (76)).

usual orientation will prevail. This behavior is observed with alkylsulfonic acids and alkylcarboxylic acids (53, 76–78). The potential variation of adsorption $(\partial\Gamma^-/\partial E)_c$ is very rapid in these cases. The differential capacity curves of alkyl sulfates (76, 78) exhibit peculiarities when studied as pure salts and as an added compound. In the absence of a supporting electrolyte, the capacity curves (see Figure 44) show two peaks marked β^+ and α^-. β^+ occurs round about the e.c.m. on the anodic side and was named the rotation peak because of the change in the orientation of the adsorbed species. This is seen even in the presence of a supporting electrolyte and becomes dominant with increasing chain length and concentration. The α peak is the desorption peak, but is resolved into two peaks, β^- and α^-, in the presence of a supporting electrolyte. The β^- peak is independent of concentration and frequency unlike the desorption peak α^-, but is a function of temperature and disappears with increasing temperature. This has been interpreted as first due to the desorption of a gaseous film and then the condensed film. The β^- and α^- peaks normally are merged and can be separated by varying the concentration of the cation of the base electrolyte. The increasing ability of these cations to split the two peaks follows the lyotropic series for cations. This suggests a relationship between hydration of ions and their screening power or ion-pairing power against the SO_4^- group in the adsorption layer. The above behavior is also observed with higher fatty acids. In both cases, the capacity curves have been interpreted in terms of formation and destruction of micelles (53), but it is very difficult to conceive of micelle formation—a three-dimensional effect—at the interface unless two-dimensional micelle formation is invoked. No evidence in favor of such a hypothesis is available. A plausible interpretation is that, since the concentration of these ions is higher at the interface than in the bulk, as soon as a critical concentration is reached, the micelles which are formed are thrown into the bulk. To compensate for the sudden depletion, ions adsorb quickly and hence this process might result in a peak. But a systematic study is necessary for further analysis of these systems.

2. *Cations*

The capacity of the electrical double layer is determined by the distance of closest approach of charge-determining species (c.d.s.). If the c.d.s. is an anion, then in the absence of formation of compact films, the distance of closest approach is the radius of the anion itself. But when coherent monolayers are formed, the inner Helmholtz plane is pushed to a distance equal to the length of the molecule.

When the c.d.s. is the cation, then the distance of closest approach is its radius. Thus for tetraalkylammonium salts (51, 63, 84, 244), the capacity minimum is a function of the radius of the cation and also its dielectric constant, since the paraffinic groups are now in the first layer. These cations, too, appear to form compact films as shown (51) by a small hump in the capacitance curves.

Aromatic cations (10, 11, 15, 36, 97, 120, 122) like anilinium, dimethylanilinium, pyridinium, etc., adsorb on the cathodic and on the anodic side of the e.c.m. as well. The adsorption on the anodic side has been attributed to the π-electronic interaction with Hg.

The Esin–Markov coefficients for anilinium, aminopyridinium, pyridinium, and piperidinium ions have been found, from $dE^{\pm}/RT \ln a^{\pm}$ and dq_1/dq_M plots (10) to be -0.24, -0.14, -0.22, and -0.60, respectively. These values are much smaller than the ones observed for inorganic halides and also organic anions. The probable reason for these lower values is that these systems are complicated by the lowering of the dielectric constant, alteration in the compact layer thickness, and the effect of permanent dipoles and π electrons. These conclusions are obtained from electrocapillary studies. But information on the corresponding capacitance curves is not available for these systems.

Sulfoxides, sulfoxonium ions, and decylamines (249, 250, 252) in moderate concentrations of HCl and H_2SO_4 (0.1 N HCl, 1 N H_2SO_4) behave normally in that only one species is adsorbed. In concentrated solutions of supporting electrolytes (6 N HCl, 12 N H_2SO_4), humps in the capacitance troughs are observed. This is not

observed with dibenzyl sulfoxide or dihexyl sulfoxide. These humps are frequency independent and are interpreted as due to transition of the adsorbate ion from the outer Helmholtz plane to the inner Helmholtz plane. However, these systems require further analysis.

It should be pointed that the studies so far made on the adsorption of organic ions are only of a preliminary type. In order to understand their complex behavior, systematic studies of the electrocapillary and differential capacitance curves should be made as only one type of measurement will not give the basic information needed for interpretation.

G. ROLE OF WATER AT THE INTERFACE

1. Relaxation of Water Molecules

The electrical analog of the ideally polarizable electrode system is a condenser and a resistance connected in parallel. The resistance and the capacitance of the double layer should normally be frequency independent. But some workers (19, 79, 157) have found variations in the resistance and capacitance with the a.c. frequency and attributed the changes to the finite relaxation times (242) of water at the interface. However, recent exhaustive studies (43, 126, 147, 220, 222) have established that all such variations are spurious and are due to improper electrode design; they are not reflections of the properties of the electrical double layer. Hence the resistance and the capacitance variations appear to be a consequence of the nonuniformity of the a.c. voltage distribution on the mercury drop (132, 141), creeping of liquid film into the capillary (147), and the bridge circuit (43, 44). Thus the capacity is found to be constant over a frequency range of 10–50,000 c.p.s. in 1 *N* KCl (220) to 10,000 c.p.s. in 0.01 *N* KCl solutions. Recent work of Lorenz (208) with the T-bridge has established the constancy of capacity up to 1 Mc.p.s. The resistance is also found to be constant up to ~9000 c.p.s. (147).

The above studies point to the complete absence (147) of relaxation times in the range 10^{-8} to 5×10^{-2} sec. Further, if the relaxation time of the water molecule is as low as 10^{-2} sec., then charge–discharge transients would have shown some indication. But until now no such influences due to water molecules have been noticed, and if noticed, one has to be cautious in interpreting them especially because of the influences of improper electrode designs. The above evidence is in favor of the theory (71) that the water molecules are adsorbed flat and insensitive to field.

2. Hyperpolarizability of Water Molecules (71)

It is interesting to find the reason why water molecules displace organic molecules so easily at high field strengths. The reason is obvious if one compares the dielectric constant of water at high field strengths (value of 6) with that of the organic molecules (value of ~1.79). Whereas the ϵ_w of 6 for water is due to the nuclear and electron polarizations, the value of 1.79 for ϵ_o is only due to the electron polarization. Using the square of the refractive index as a measure of the optical dielectric constant, the dielectric constant of water free of any electronic contribution is 4.21. This can be ascribed to the contribution from protons of the water molecule and hence is a measure of the hyperpolarizability of water molecules. It is this property of the water molecule that is responsible for the desorption of organic compounds.

On this basis, any other substance with ϵ greater than 6 in the microwave region should displace water even at high field strength with ease. The bulk dielectric constants of formamide, N-methylformamide, and butylacetamide are known to be higher than water. But they all attain dielectric saturation even at low field strengths. Thus it has been shown (49) that even though the D for N-methylformamide in the bulk is 132, it reaches a value of ~80 at the Gouy plane itself and attains a much lower value than for water at the interface, whereas for water the D up to the Gouy plane is ~80 and comes down to 7.2 in the inner layer. This shows that the hyperpolarizability of the water molecule is unparalleled by any other molecule because of the unique structure of water, especially its small size and its two protons.

V. ADSORPTION OF IONS AT THE MERCURY–SOLUTION INTERFACE IN NONAQUEOUS SOLVENTS

It was pointed out earlier that the q_M at which all the anions desorb is -12 to -13 μc./cm.^{2} in aqueous solutions. Since the studies on mercury are confined only to a q_M of $+20$ to -20 μc./cm.^{2}, the range available for specific adsorption of cations is small (from -13 to -20 μc./cm.^{2}, *i.e.*, only 7 μc.). In nonaqueous media (134) (see Figure 45), the corresponding charge on the metal for complete desorption of anions is -4 to -6 μc./cm.^{2}. Thus in nonaqueous media, the span available for the specific adsorption of cations is more than in aqueous solutions. On the other hand, the anodic branch is very small and rarely exceeds $+4$ to $+6$ μc./cm.^{2}.

Now it is necessary to know the solvation forces in nonaqueous media. The essential physical properties required (60) for a good ionizing solvent are: (a) small molecular dimensions with a nearly symmetric disposition of the dipole, which enables the solvent to cluster round cations and anions with equal facility; (b) large dipole moment, which means large ion–dipole interaction energy and also large bulk dielectric constant.

The above requirements are satisfied by the water molecules with the result that it is a solvent *par excellence*. Other solvents like methanol, formamide, N-

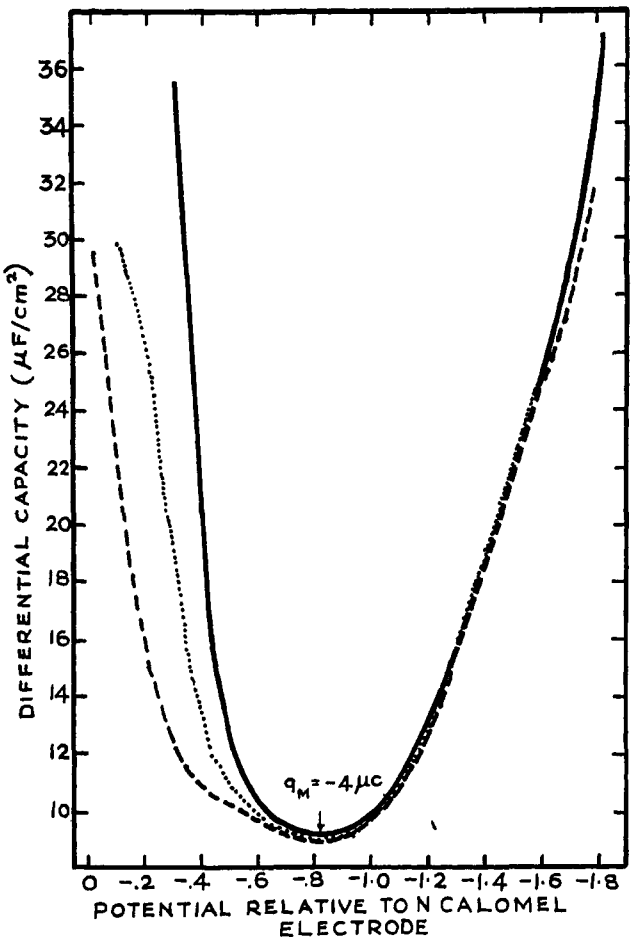

Figure 45.—Differential capacity data on mercury of 0.1 *N* solutions in methanol at 25°. Solid line, NH_4Cl; dotted line, NH_4NO_3; dashed line, NH_4F (reproduced from ref. 134 with the permission of the editors).

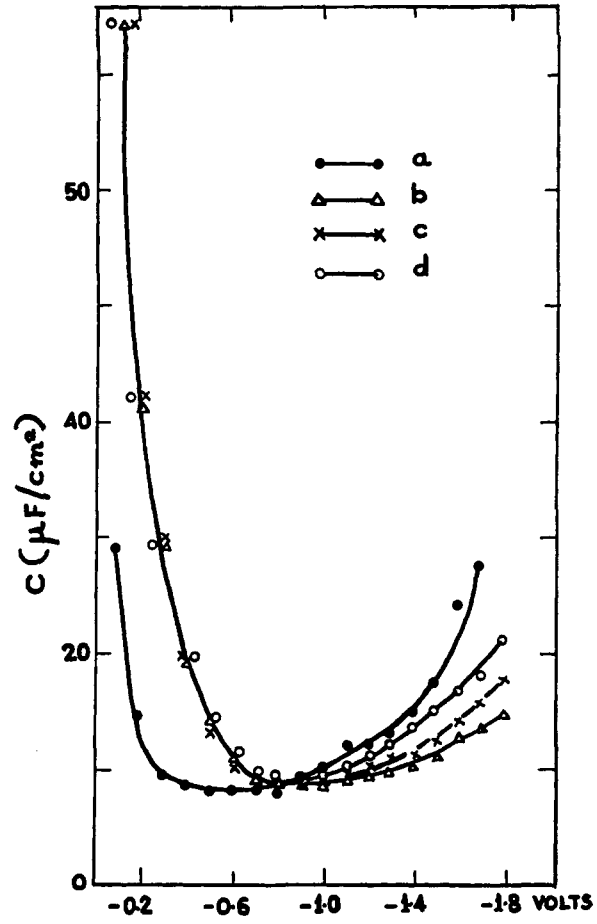

Figure 46. Differential capacity of mercury in methanol solutions. a, 0.1 *N* KF; b, 0.1 *N* LiCl; c, 0.1 *N* NaCl; d, 0.05 *N* KCl (reproduced from ref. 226).

methylformamide, hydrogen cyanide, etc., because of their asymmetric disposition of the dipole, can solvate predominantly only one ionic species. Owing to the condition of electroneutrality, the solubility of the salt is restricted by the solubility of the ionic species which is solvated least. Since solubility is small in non-aqueous solutions, the adsorbability of both ions is likely to be greater. Owing to the large span available for cationic adsorption, substantial specific adsorption effects may be anticipated. However, for anions, the limited range is a consequence of an extremely rapid specific adsorption.

The general Eq. 29 points to two salient features in the differential capacity curves. (i) When specific adsorption is absent ($dq_1/dq = 0$), the capacity should be equal to the solvent capacity which can be calculated from molecular parameters, *i.e.*, ϵ and t. (ii) When specific adsorption is present ($dq_1/dq > 0$), the capacity should increase. From this standpoint, the capacity curves in organic solvents and inorganic solvents can be discussed.

A. ORGANIC SOLVENTS
(BULK DIELECTRIC CONSTANT < 80)

Thus in the case of methanol (134, 223–229, 234, 235), butanol (181, 182), and acetonitrile (230) the minimum capacity is 9–10 μf./cm.². But for ethanol (186, 227, 230) and dimethylformamide (230) the corresponding value is 6–7 μf./cm.². This pattern can be understood from the following model which serves for a semiquantitative calculation of the solvent capacity K_S. If it is assumed that the solvent molecules are adsorbed with the oxygen end on the mercury surface and lie flat, then with the aid of Catalin models, it is seen that the distance of closest approach of an ion is approximately 4 Å. (for an ion of radius 1 Å.). In the absence of any known values of dielectric constant measured in the microwave region, we may assume that the ϵ of methanol in the compact layer is the average of that of the water molecule (6) and of the methyl group (1.7), *i.e.*, 3.8, because the area occupied by the OH and CH_3 groups is roughly the same. For ethanol, the area occupied by the hydrocarbon group is roughly twice the area of CH_3 group, and hence the average dielectric constant can be taken as 3.0. These models also show that propyl-, butyl-, and di-

methylformamide molecules are contacting mercury over an area roughly equal to that of the methanol molecule, the other section of the molecules being projected into the solution phase. In the case of ethanol and dimethylformamide, the area occupied is more or less equal to the area of the ethanol molecule.

Now using the classical electrostatic formula, with the above dielectric constants and the same distance of closest approach, the solvent capacity is approximately 9–10 μf./cm.^{2} for methanol and 6–7 μf./cm.^{2} for ethanol, as observed.

In the case of butanol, the solvent capacity is indeed seen clearly by its constancy from 0.5 to 1.7 v. at 9–10 μf./cm.^{2}.

The rise on either side of the -4 μc. or -0.8 v. is due to the specific adsorption of ions (see Figure 46). The gradations in adsorbability of cations and anions follow the same pattern as observed in aqueous solutions, but the adsorption is stronger in view of the low solubility of the salts or smaller solvation number than in aqueous media. Further, the adsorbability increases with increasing charge of the cation (223).

A study of the electrocapillary behavior (56, 266) and the differential capacity curves (234, 235) of HCl in methanol has shown that the anions are adsorbed on the cathodic side of the electrocapillary maximum also. This may be due to the fact that undissociated HCl molecules which may be present in substantial amounts in nonaqueous solutions may adsorb on account of the large dipole moment. A point of interest to be noted here is that the mole fraction of organic substance to water at the mercury–solution interface at the electrocapillary maximum is the same as that at the air–solution interface for a series of mixtures of water with methanol (56, 266) and ethanol (217). No capacitance humps are observed in the above solvents.

B. ORGANIC SOLVENTS (BULK DIELECTRIC CONSTANT > 80)

The general shape of the curves for formamide (230) and N-methylformamide (49, 54) is similar to the ones mentioned earlier except that broad humps are observed (see Figure 47) (-4 to -16 μc. for KCl in N-methylformamide (49). These humps occur (i) on the cathodic side of the electrocapillary maximum, (ii) do not disappear with increase in temperature but only decrease in height, and (iii) disappear when water is added. A comparison of these humps with the components of charge does not show these to be due to saturation adsorption of either cation or anion (see section III-I). Consequently, this must be a reflection of the reorientation of the solvent molecules. This hypothesis appears plausible in view of the solvent capacity variations.

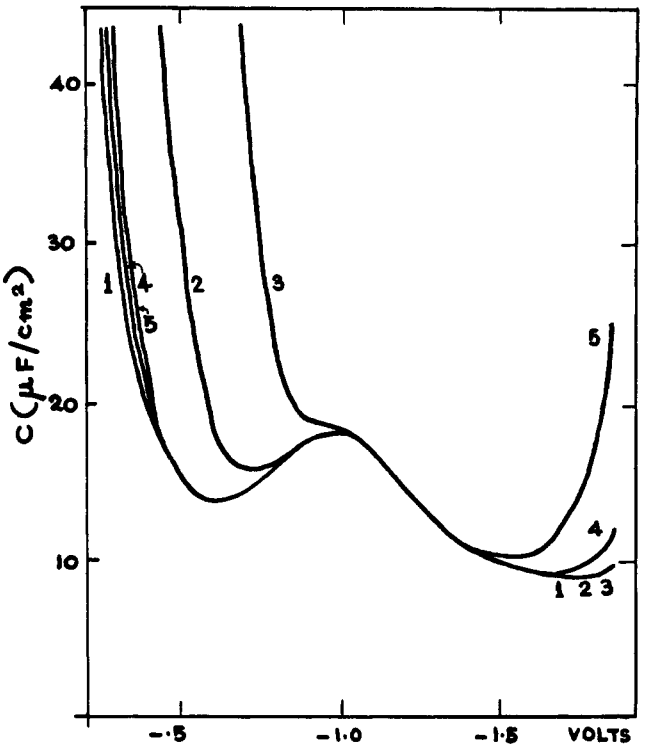

Figure 47.—Differential capacity of mercury in 0.1 *N* halide solutions in N-methylformamide. 1, KCl; 2, KBr; 3, KI; 4, RbCl; 5, CsCl (reproduced from ref. 54).

C. INORGANIC SOLVENTS

The only solvent in which the electrocapillary behavior of organic molecules and halide ions has been investigated is liquid NH_3 (236, 237). The anodic branch of the electrocapillary curve is very small perhaps due to the electron-donating ability of the NH_3 molecule which leads to a faradaic process. The adsorbability of halide ions and also tetraalkyl ions is found to be similar to their behavior in aqueous solutions. The minimum capacity (11 μf./cm.^{2}) calculated from electrocapillary curves is lower than in aqueous solutions. Since the dimensions of the NH_3 molecule cannot be very different from that of water, it appears that the microwave dielectric constant of NH_3 molecules is around 4.

The electrocapillary curves of the aromatic organic compounds in liquid NH_3 do not show a shift of the point of zero charge as in alcoholic solutions (118, 119, 121, 123, 187). Thus the π-electron interaction observed in the later media are presumably absent in liquid NH_3.

Renewal of interest in nonaqueous solutions dates back only to about 10 years. The work reported is usually confined to a study of either the differential capacity or the electrocapillary curves at single concentrations. It must be stressed here that both electrocapillary and differential capacity curves have to be studied in a systematic way for further progress.

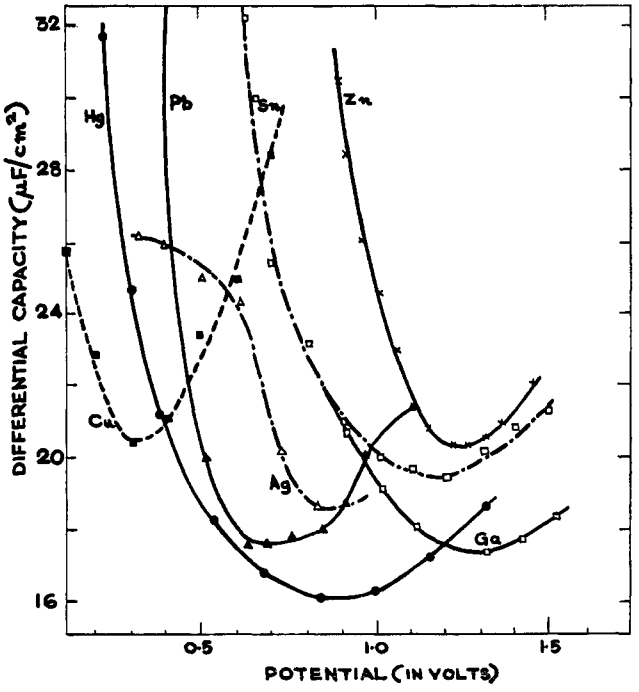

Figure 48.—Differential capacity curves on various metals in aqueous media. Hg, Ga, and Zn single crystal in 0.1 *N* KCl against n.h.e. (293); Ag in 1 *N* Na_2SO_4 *vs.* n.h.e. (165, 202); Pb in 0.1 *N* H_2SO_4 *vs.* n.h.e. (165, 202); Sn in 0.1 *N* $KClO_4$ solution *vs.* n.c.e. (276), and Cu in 1 *N* Na_2SO_4 *vs.* s.c.e. (219) (plotted from the data given in parentheses).

VI. Adsorption on Solid Metals in Aqueous Media

A. Electrocapillary Properties

Since the interfacial tension between solid metal and the solution is not directly measurable, the physical properties which should reflect the interfacial tension may be made use of for obtaining (see 91, 96, 101, 105, 255) the analog of the electrocapillary curves. Such properties are contact angle, hardness, and friction. The contact angle is a direct measure of γ, whereas there is no explicit relationship between γ and the frictional coefficient or hardness. These methods are described in detail elsewhere (see, for references, 91, 96, 101, 255). By far the best method for obtaining qualitative information on adsorption is the study of friction. Recently, this method has been improved (288) for electrocapillary studies on Cu and stainless steel in the presence of organic molecules. However, the main obstacle in interpreting these data quantitatively is the lack of an explicit relationship between the interfacial tension and the friction measured. The contact angle method requires the knowledge of the interfacial tension between gas–liquid and gas–solid to obtain γ and has not been quantitatively used to evaluate the Gibbs surface excesses.

B. Differential Capacity Studies

Progress in the differential capacity measurements by the a.c. bridge methods or pulse methods (32, 219, 273, 274, 278) is retarded mainly by the irreproducibility of smooth electrode surfaces because surface roughness introduces (96, 293) frequency dispersion of capacity. In this connection, it is of interest to note that the frequency dispersion of capacity in the range 1–10 kc.p.s. with zinc single crystals (293) is very small, about 5–8%, whereas with polycrystalline zinc, it is much more and is attributed to the surface heterogeneity and microscopic cracks. Another difficulty is the preparation of oxygen-free solutions, since the presence of O_2 interferes with the required nonfaradaic capacity. This can be overcome only if the high purification technique, *viz.*, distillation and preparation of solutions *in situ* in a current of hydrogen or argon, is adopted. The presence of oxide films on the surface and also adsorbed hydrogen introduce uncertainties in the measurements of the differential capacity. Hence it is necessary, in the case of solid metals, to first prove that what is measured is the true double layer capacity at the metal–solution interface under ideally polarizable conditions. However, the differential capacity curves of Pb (23, 24, 165, 185, 202, 203), Zn (165, 202, 203, 293), Tl, Cd (23, 24), Ag (165, 202, 203), Sn (276), Ga (107, 137, 140), and Cu (219) in contact with inert electrolytes are very similar to those with mercury. But the minimum capacity varies from metal to metal and is in the range 16–22 μf./cm.^{2} (see Figure 48).

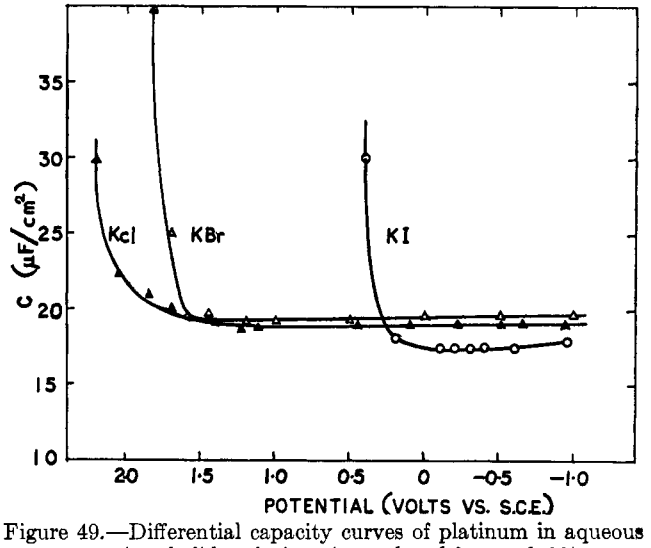

Figure 49.—Differential capacity curves of platinum in aqueous potassium halide solutions (reproduced from ref. 66).

The most exhaustively studied metal is platinum (see reviews 96, 98; and 9, 13, 28–30, 219, 274, 279, 282, 285), but the data are conflicting. This is a consequence of the stable oxide on platinum which interferes with the measurements. But recently a method has been developed in this laboratory (66) in obtaining reproducible, oxide-free, platinum surfaces by treatment with potassium iodide solutions and washing with deoxygenated water prior to the capacity

measurements. These data on platinum show that the base capacity is 20 μf./cm.^{2} (see Figure 49). (Breiter (29) also obtained constant capacity with 10^{-5} N HI and 10^{-4} N HBr in 1 N $HClO_4$ solutions at ~20–25 μf./cm.^{2} from 0.3 to 1.3 v. on the anodic side but interpreted it as due to I^{3-} ions which are larger in size compared to I^- ions.) Thus it appears that, for most of the metals, the minimum capacity in aqueous solutions is around 16 to 20 μf./cm.^{2}. These small variations can be attributed to the surface roughness of the solid electrodes. But the minimum capacities of mercury and gallium (140) in contact with 0.1 N halide solutions are 16.0 and 17.5 μf./cm.^{2}, respectively. This points to the specific influence of the nature of the metal in determining the base capacity in addition to the solvent capacity.

The specific adsorbability of the halide ions is the same as obtained for mercury in the case of many solid metals except platinum. In the case of platinum, the constant capacity of 20 μf./cm.^{2} is unaltered with KCl, KBr, and KI and also with HBr and HI. This result confirms the theory that specific adsorption is primarily covalent, and, since platinum cannot readily form covalent complexes with halide ions, the capacity curves do not show any variations, thus revealing only the solvent capacity. But some results obtained from kinetic studies (see, for references, reviews 96 and 98; 13) and radioactive studies (6–8, 172–174) on platinum indicate that the halide ions are adsorbed very strongly on platinum. It is quite conceivable that in all the above cases, the effects are due to the adsorption of halide ions in their neutral state and not due to electrostatic adsorption of ions, similar to what is observed on mercury or gallium. However, the differential capacity curves have not been thoroughly analyzed (see section III) to obtain the components of charge because of difficulties in the determination of the coordinates of electrocapillary maximum (e.c.m.) or the point of zero charge or Lippmann's potential.

C. DETERMINATION OF POINT OF ZERO CHARGE ON SOLID METALS

The point of zero charge (z.c.p.) is dependent on the nature of the metal and the solution as well. It is an important reference point for every solution and is desirable to have methods of locating this point whatever the nature of the solution. The following are the broad physical principles used in the methods available at present (for original references see reviews 4, 90, 91, 96, 101).

1. Expanding Surface Method

The relationship between the current (i) and the rate of variation of electrode area (dA/dt) is

$$i = q_M \frac{dA}{dt} \qquad \text{(Eq. 104)}$$

It follows from Eq. 104, that, when dA/dt is finite, i will be zero (under ideally polarizable conditions) only when q_M is zero. Hence the problem is one of obtaining reproducible dA/dt. In the case of dropping mercury electrodes, it is automatic (142, 164, 271), whereas in the case of solid electrodes, dA/dt can be accomplished by dipping an electrode (163), by scratching the electrode surface (3), or by suddenly bringing the solution in contact with the metal. Thus by any one of the above methods, from the current direction, the z.c.p. can be spotted. This assumes that the current in the circuit is entirely due to double layer charging. So careful purification of the solution to free it from O_2 is necessary because the faradaic current due to O_2 reduction masks the true electrocapillary maximum (72).

2. Interfacial Tension Method

The analogs of γ are the frictional coefficient and the contact angle. The former should exhibit a maximum and the latter a minimum at the electrocapillary maximum. The accuracy of the value of electrocapillary maximum obtained using these methods is very poor and is probably ± 0.1 v.

3. Properties of Diffuse Layer

Since the diffuse charge is minimum at the electrocapillary maximum (note the Γ^+ variations in Figure 3) in the absence of specific adsorption, properties which are dependent on diffuse charge can be utilized to spot the electrocapillary maximum. Such properties are capacity and force required to contact two wires (303) of the same metal. Both the methods exhibit minima at the e.c.m. The most extensively used property to locate the e.c.m. is the capacity minimum in dilute solutions. A serious limitation in this method is that specific adsorption should be absent. But this condition does not hold with most electrolytes.

A different procedure making use of the diffuse layer properties has been recently (149) proposed to evaluate the electrocapillary maximum from the organic surface excesses obtained by the radiotracer method, in the presence of a dilute and a concentrated solution of the supporting electrolyte. The main assumptions are (a) the absence of shift of z.c.p. in the presence of organic adsorption (this assumption holds at low coverages for compounds with no permanent dipole moment); (b) constancy of z.c.p. with changing base electrolyte concentration (this assumption means that only a base electrolyte which shows no specific adsorption can be used).

Thus the measured potential E may be written as

$$E = E_{z.c.p} + \psi_{m-2} + \phi_2 \qquad \text{(Eq. 105)}$$

TABLE II

POTENTIAL OF ZERO CHARGE FOR SOME METALS IN AQUEOUS SOLUTIONS

Sample no.	Metal	Point of zero charge vs. n.h.e., v.	Medium	Ref.[l]
1	Hg	-0.19^a	0.01 N NaF	131
2	Ga	-0.61^a	1 N $NaClO_4$ + 0.1 N $HClO_4$	114
3	Tl amalgam 41.5%	-0.65^a	1 N Na_2SO_4	106
4	Cd amalgam 4.8%	-0.466^c	1 N KCl	102
5	In amalgam 58%	-0.65^a	1 N Na_2SO_4 + 0.01 N H_2SO_4	272
6	Pt	0.18^h	0.005 N Cs_2SO_4; pH 2.7	8
		0.2^e	0.001 N KCl	303
		0.3^j	0.1 N H_2SO_4	25
		-0.4 ± 0.05^g	0.1 N KCl; pH 12	3
7	Ag	-0.7 ± 0.05^b	0.001 N Na_2SO_4	202
		-0.80 ± 0.05^g	0.1 N KCl; pH 7	3
8	Cu	0.05^k	0.1 N NaOH	298
		0.07^f	0.01 N KCl	163
		-0.35^g	0.1 N KCl; pH 7	3
9	Au	0.3^i	$NaClO_4$ + 0.001 N $HClO_4$	149
		-0.09^g	0.1 N KCl; pH 7	3
10	Pb	-0.64 to -0.67^b	0.001 N K_2SO_4 + 0.001 N H_2SO_4	23, 24, 165, 202, 203, 276
		-0.62^d	0.1 N NaCl	301
		-0.56^d	1 N Na_2SO_4	301
		-0.55^d	1 N NaOH	301
11	Sn	-0.46^b	0.001 N $KClO_4$	276
		-0.38^f	0.01 N KCl	163
12	Tl	-0.82^b	0.001 N KCl	205
		-0.69^d	1 N Na_2SO_4	301
13	Cd	-0.90^b	0.001 N KCl	23, 24
14	Fe	-0.37^b	0.001 N H_2SO_4	5
		-0.34^e	0.003 N HCl	303
		-0.65^b	0.1 N H_2SO_4	12
15	Zn	-0.62^d	1 N Na_2SO_4	301
16	Ni	$+0.19^f$	0.001 N KCl	163
17	Al	-0.52^f	0.01 N KCl	163

Superscripts in column 3 refer to the method used for determining the z.c.p.: [a] From electrocapillary data. [b] Capacity minimum. [c] Null solutions (102). [d] Hardness (301). [e] Crossed wires (303). [f] Dipping (163). [g] Scratch method (3). [h] Adsorption of ions (8). [i] Adsorption of organic substances (149). [j] Friction. [k] Contact angle. [l] The sources for the values z.c.p. are given in the last column.

From simple electrostatics, ψ_{m-2} can be expressed in the absence of specific adsorption of ions as

$$\psi_{m-2} = \frac{q_d 4\pi x_2}{\epsilon} \qquad \text{(Eq. 106)}$$

Since ψ_{m-2} does not vary with the supporting electrolyte concentration for the same maximum Θ, and ϕ_2 can be neglected when the ionic concentration is high, E at high (E_h) and low (E_l) supporting electrolyte concentrations is given by

$$E_h = E_{z.c.p} + \psi_{m-2} \qquad \text{(Eq. 107)}$$

$$E_l = E_{z.c.p} + \psi_{m-2} + \phi_2 \qquad \text{(Eq. 108)}$$

Thus from the potentials at the same maximum adsorption at two ionic concentrations, ϕ_2 for the dilute solution can be found and hence ψ_{m-2} from Eq. 106, where q_d is calculated from the diffuse layer theory. Once ψ_{m-2} is known, $E_{z.c.p}$ can be calculated.

This approach has been used to obtain the electrocapillary maximum on Au in perchlorate solutions containing C^{14} naphthalene. The value of the electrocapillary maximum obtained depends on the correct evaluation of the magnitude of ψ_{m-2}. This means that correct values of q_d, ϵ, and x_2 must be used.

It is likely that x_2 is unchanged. However, the value of ϵ would be appreciably altered on the introduction of organic substances such as naphthalene into the compact layer. This has not been taken into account in the above treatment. Thus the method is restricted in its applications even at low coverages.

4. Properties of the Components of Charge

A unique feature in the components curve for the Γ^+ and Γ^- (see Figure 3) is that only at the electrocapillary maximum the values of Γ^+ and Γ^- are equal. So from a determination of the adsorbed ionic quantities as a function of potential, the point of zero charge can be found (see Figure 50). This principle has been used (7, 8, 172–174) to determine the z.c.p. on platinum from the surface excesses of ions obtained by the radiotracer techniques and is by far the best available method.

However, it is to be noted that the experiments have been performed by taking the metal out of the solution and then wiping the liquid film prior to the radio-

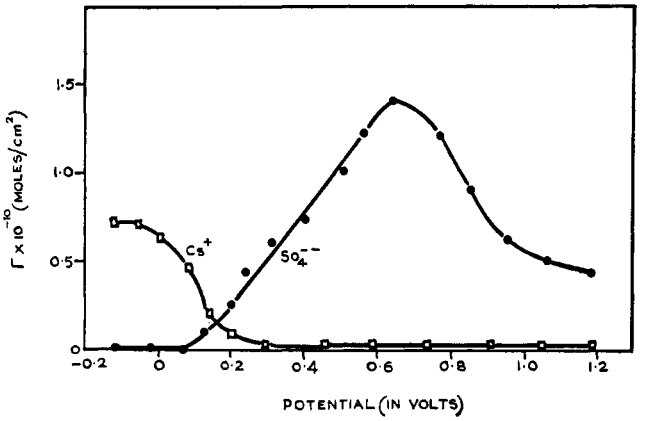

Figure 50.—Surface excess of Cs^+ and SO_4^{2-} ions determined by the radioactive methods from 0.01 N Cs_2SO_4 + 0.01 N H_2SO_4 (reproduced from ref. 173).

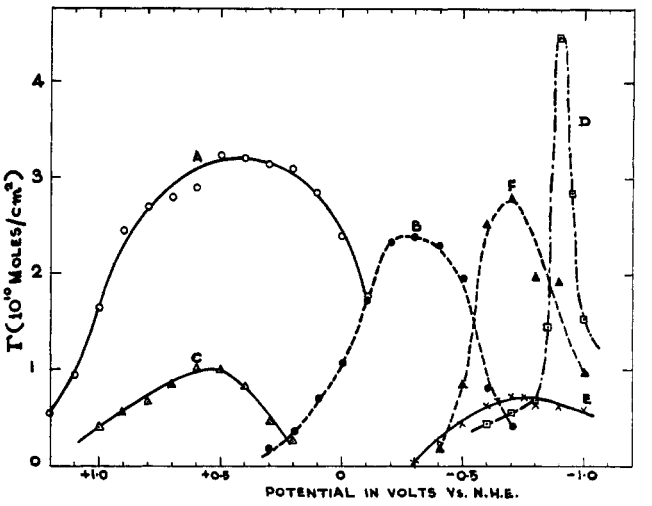

Figure 51.—Surface excess of naphthalene on various metals as a function of potential. A, platinum in 0.9 N $NaClO_4$ + 1 N $HClO_4$ containing 10^{-4} M naphthalene; B, platinum in 0.9 N $NaClO_4$ + 0.1 N NaOH containing 10^{-4} M naphthalene; C, gold in 0.5 M H_2SO_4 containing 10^{-4} M naphthalene; D, copper in 1 N $NaClO_4$ containing 10^{-4} M naphthalene; E, nickel in 1 N $NaClO_4$ containing 7.5×10^{-5} M naphthalene; F, iron in 0.9 N $NaClO_4$ + 0.1 N NaOH containing 10^{-4} M naphthalene (plotted from the data of Bockris, *et al.* (21), and Green, *et al.* (150)).

activity measurements. The surface excesses evaluated by the above method agree with measurements carried out with internally polarized electrodes using potential buffers. This coincidence shows that the adsorption of ions like iodide is not electrostatic on platinum, since during washing the samples with water it is impossible to imagine electrostatic adsorption equilibrium prevailing at the interface. The adsorption that is observed could perhaps be due to the neutralized ions entrained along with electrolyte solution in the grain boundaries. It appears necessary to carry out an *in situ* determination of ionic adsorption by radiotracer techniques in preference to the above method.

The available data on electrocapillary maxima are summarized in Table II.

D. ORGANIC ADSORPTION

Only by direct methods outlined earlier, has it been possible to obtain Gibbs' surface excess in the case of solid electrodes (10, 21, 22, 37, 39, 150, 151, 308). Differential capacity data can be useful only in deducing (12, 26, 27, 165, 178–180, 188, 210–212, 253, 284) the adsorption of organic substances qualitatively. This difficulty arises as a result of lack of knowledge of z.c.p. which is vital for quantitative interpretation. However, approximate values have been obtained (26, 27) using Frumkin's equation (see Eq. 64).

Differential capacity data show that the adsorption of organic compounds on solid metals is similar to that observed on mercury, except for the following minor differences. (i) The adsorption–desorption peaks are smaller (204) on solids than on liquid metals. Further complete desorption of organic compounds is not observed (178). (ii) From a study of the adsorption of naphthalene (21) on various metals, it is found that the range available for adsorption (on the potential scale) differs from metal to metal (see Figure 51). This behavior is observed even with amalgams (270). Another fact to be taken notice of is that on gold (150) the adsorption of aliphatic compounds could not be detected. (For the radioactive method to be successful, there should be a considerable difference between the surface to bulk concentration. It is preferable to have low bulk concentrations of the organic substances so that the background radiation does not interfere with the radiation from the adsorbed species. Hence it is likely that moderate or high coverage can be obtained only with large bulk concentration for aliphatic compounds, and large bulk concentrations give substantial background radiation with the result that the measurement of the difference in counts becomes difficult. If, however, dilute solutions are used, the coverage itself is small and therefore not detectable. Thus it appears that this anomalous result is a consequence of the technique rather than the weak adsorbability which has been attributed to the strong interaction between H_2O and Au.) These differences can arise only as a result of the possible differences in the heat of adsorption of water on different metals. For example, the double layer region or the nonfaradaic region for mercury is mostly on the cathodic side, whereas on platinum it is on the anodic side. Thus the stability of water which varies from metal to metal governs the range for adsorption since adsorption is essentially a competitive process with water in aqueous media.

However, *n*-decylamine adsorbs (22) over a wide range of potentials on Ni, Pt, Fe, and also Cu (see Figure 52). Thus the narrow range of adsorption of naphthalene on copper appears to be anomalous and cannot be explained in terms of stronger adsorption of water.

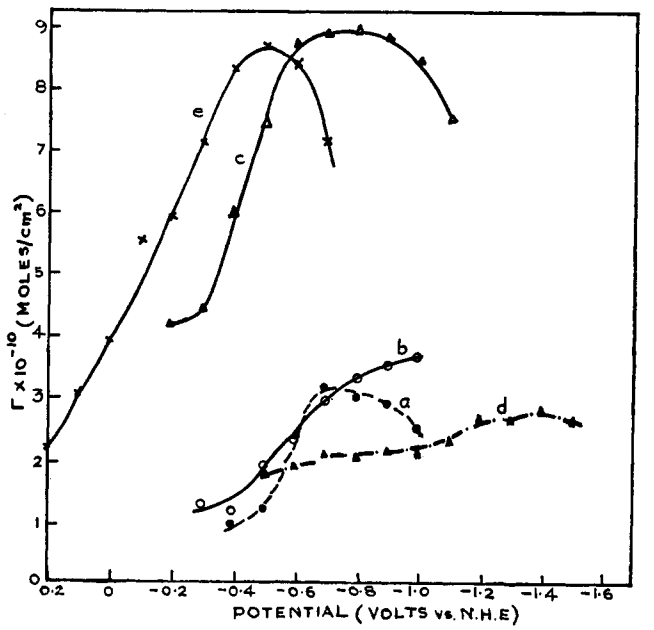

Figure 52.—Adsorption of *n*-decylamine on various metals. a, b, and c are for Ni, Fe, and Cu in 0.9 *N* $NaClO_4$ (pH 12) containing 5×10^{-5} *M* *n*-decylamine; d, Pb in 1 *N* $NaClO_4$ (pH 12) containing 6×10^{-5} *M* *n*-decylamine; e, Pt in 0.9 *N* $NaClO_4$ (pH 12) containing 6×10^{-5} *M* *n*-decylamine (plotted from the data of Bockris, *et al.* (22)).

The adsorption data (150) for benzene and cyclohexene show the importance of π bonding as observed on mercury. Further the shift of the adsorption maximum for naphthalene adsorption on various metals suggests (21) the formation of a bond between the metal and the π orbitals with a moment whose negative end is towards the solution. Further, these π complexes appear to be formed only with Ni, Fe, and Pt and not with Au and Cu.

E. ISOTHERMS FOR ORGANIC ADSORPTION

Pursuing the "water competition" model, the adsorption process has been represented (21, 22, 150) according to the chemical equilibrium

$$\text{organic (solution)} + n\text{H}_2\text{O (adsorbed)} \rightleftharpoons \text{organic (adsorbed)} + n(\text{H}_2\text{O}) \text{ (solution)}$$

The free energy of the reaction and hence the isotherm is

$$\frac{\theta}{(1-\theta)^n} \frac{\{\theta + n(1-\theta)\}^{n-1}}{n^n} = \frac{c_{org}}{55.4} \exp\left(\frac{-\overline{\Delta G}^\circ}{RT}\right) \qquad \text{(Eq. 109)}$$

Equation 109 reduces to the Langmuir form when $n = 1$. With the aid of Eq. 109, the $\overline{\Delta G}^\circ$ values have been evaluated for the adsorption of naphthalene, *n*-decylamine on various metals, and the variations in the free energy of adsorption in the case of aromatic hydrocarbons on Au. The above calculations have been carried out at constant potential.

An attempt (21, 22, 150) has been made to assess the influence of the metal on the adsorption process by considering (a) the variations in ΔG_a° (obtained by extrapolation of $\overline{\Delta G}^\circ$ to zero coverage) at the potential of maximum adsorption and (b) the variations in the intrinsic binding energy ΔE^c (*i.e.*, non-Coulombic or chemical interaction energy) at the potential of maximum adsorption which can be obtained from the equation

$$\Delta E^c = -2\mu_\omega X \qquad \text{(Eq. 110)}$$

Variations in ΔG_a°.—These values (see Table III) have been found to be constant for various metals and suggest the role of only physical forces, such as dispersion forces between the adsorbed molecule and the metal surface.

TABLE III

SOME CHARACTERISTICS OF ADSORPTION OF ORGANIC COMPOUNDS ON SOLID METALS AT THE POTENTIAL OF MAXIMUM ADSORPTION (FROM THE DATA GIVEN IN 21 AND 22)

Meta	ΔG_a° for the adsorption of *n*-decylamine, kcal./mole (ref. 22)	ΔE^c for the adsorption of naphthalene on various metals, kcal./mole (ref. 21)
Ni	−6.8	2
Fe	−6.6	1.2
Cu	−7.3	4.2
Pb	−6.2	...
Pt	−7.4	0.6
Hg	...	0.7

A calculation of the dispersion interaction (u_{disp}) using the relationship

$$u_{disp} = \frac{\pi \bar{N} \eta}{6\tau^3} \qquad \text{(Eq. 111)}$$

where $\bar{N}$ is the number of metal atoms/cc., τ the distance of the closest approach of the adsorbed molecule, *viz.*, water, and η a constant, has shown that u_{disp} for various metals is also constant and almost same as ΔG_a°.

Variations of ΔE^c.—Starting from the "up and down water model," these changes (see Table III) have been attributed to the image interaction energy (E_{image}) of the two types of water molecules and also to the Δu_{disp} of water in two orientations with the metal, since E_{image} alone cannot account for the observed variations. But Δu_{disp}, too, does not account for the observed ΔE^c values satisfactorily. The difference has been attributed to the neglect of the influence of the surface dipole of the metal on E_{image} and Δu_{disp} of water. The above behavior can be understood on the basis of the model previously discussed (see section IV-E-3); *i.e.*, decylamine is adsorbed with the hydrocarbon end on the metal. The interaction of the latter with the hydrocarbon is negligible. The free energy of adsorption is therefore governed primarily by the squeezing-type forces, and hence for this substance and the same solvent,

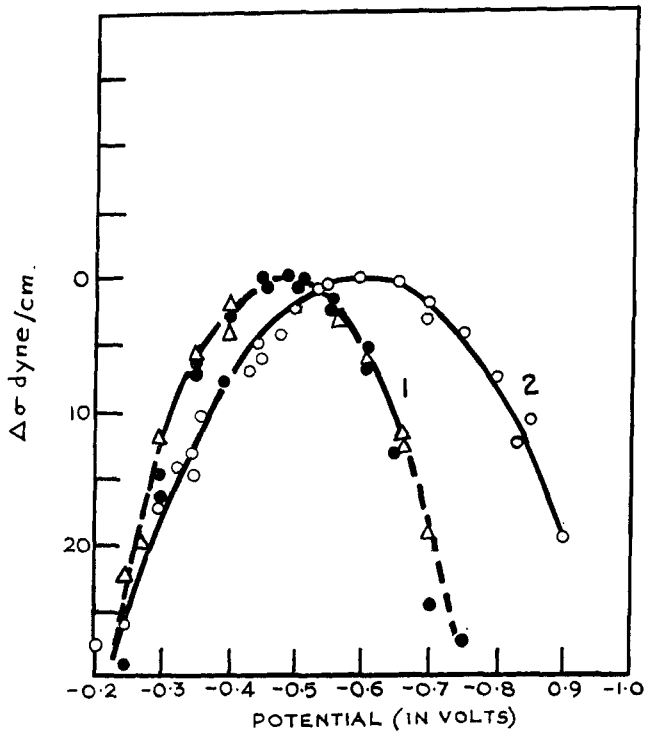

Figure 53.—Electrocapillary curves of Pb. 1, in NaCl; and 2, in KCl melts at 820°. Points refer to experimental values and the curve to the twice-integrated values from capacity curves (reproduced from ref. 297).

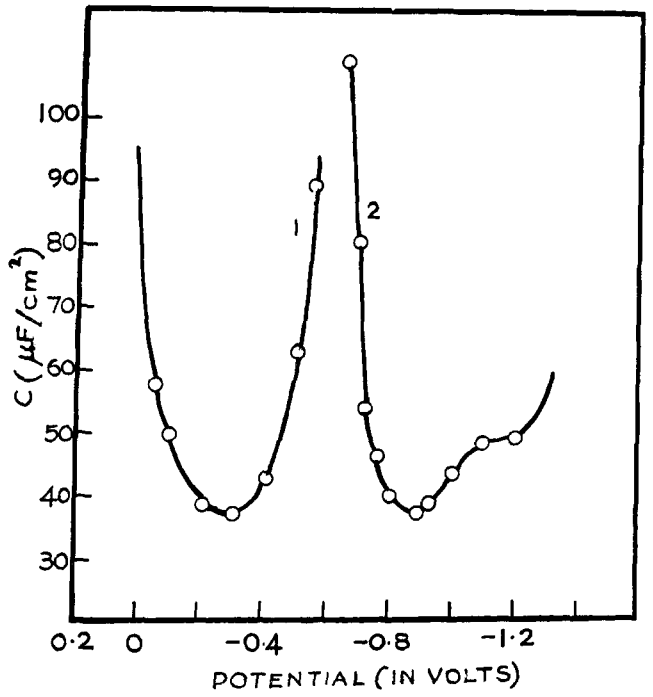

Figure 54.—Differential capacity curves. 1, molten Bi in KCl–NaCl mixtures at 700° (20 kHz.); and 2, molten Tl in KCl–NaCl mixtures at 700° (200 kHz.) (reproduced from ref. 296).

namely water, the free energy of adsorption should be the same as is observed.

An examination of free energy data for naphthalene also shows little variation with the nature of the metal, and this may be taken as an indication of the lack of specificity in the interaction of aromatic hydrocarbon with the metal.

Interpretation of the ΔE^c term must, however, await more reliable data on the z.c.p.'s of various metals in these systems.

VII. Electrical Double Layer in Molten Salts

A. Solid Metals

Capacity measurements have been carried out by a.c. bridge methods (158, 197, 199, 201), by relaxation methods (200), and by measuring (159) the faradaic capacity and extrapolating to infinite frequency. The capacity data are frequency dependent to a very great extent. This has been ascribed to various reasons like the presence of traces of water and impurities. However, the studies so far on this subject are not reliable enough to draw any conclusions on the double layer capacity on various metals.

B. Liquid Metals

Even though systematic electrocapillary work in molten systems had started as early as 1936 (168), attempts at elucidation of the structure by differential capacity studies (33, 294–297, 299) are of very recent origin. The major contribution to this field, except on Hg (277), is from the Soviet electrochemists who have kept an active interest in this subject. The experimental aspects have been described in detail elsewhere (see references in 297).

The measured capacity has been established to be the true double layer capacity by integrating the capacity curves twice and obtaining concordance (see Figure 53) with independently measured electrocapillary data (see Eq. 10).

The capacity data obtained on as many as 16 or 17 metals in alkali halide melts show that for most of the metals the capacity curve is parabolic with a pronounced minimum (20–75 μf./cm.²) at the z.c.p. and steep rise on either side of the electrocapillary maximum. But for Ag, Tl, and Sn, there is a flat region in the capacity curve on the cathodic side, the anodic side being the same as observed for the above metals (see Figure 54). The cause of this step is not well understood.

The following are the experimentally observed trends for the capacity minimum (C_{min}). (a) C_{min} occurs at the point of zero charge and is not significantly dependent on the nature of the metal. (b) For the same cation, at constant temperature, the C_{min} (i) increases with increasing radius of the anion (see Figure 55) and (ii) increases rapidly when a bigger ion is replacing a smaller ion and is at a low concentration. When the concentration reaches a particular value, the C_{min} is constant and is independent of the concentration (see

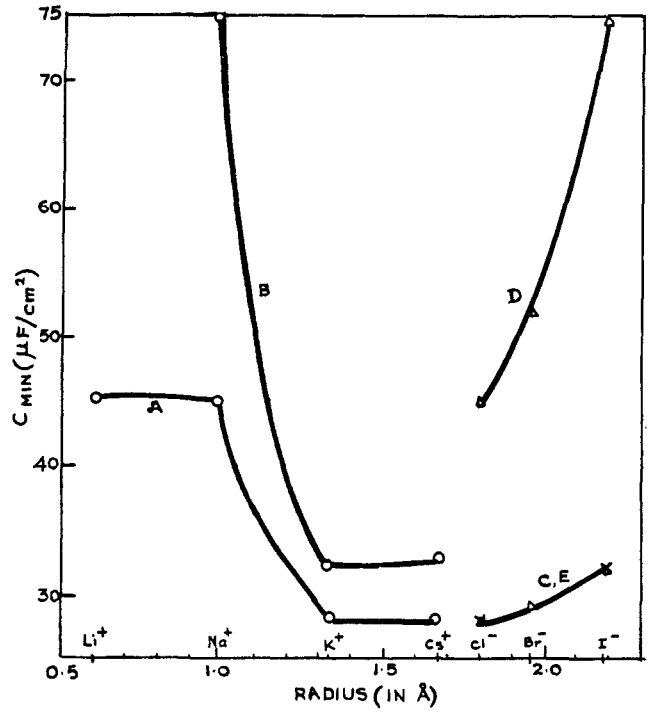

Figure 55.—Variation of C_{min} of Pb at 800° (in the case of NaCl the temperature is 820°) with the radius of the cation keeping the anion constant; A, chloride; B, iodide. Variation of C_{min} of Pb at 800° (for NaCl the temperature is 820°) with the radius of the anion keeping the cation constant: C, potassium; D, sodium; and E, cesium (from the data of Ukshe, *et al.* (297)).

Figure 56). (c) For the same anion at constant temperature, the C_{min} remains constant up to a cationic radius of ~1 Å. and rapidly decreases with increasing radius of the cation. When once the radius increases above ~1.30 Å., C_{min} is again virtually constant with cationic radius (see Figure 55). (d) The C_{min} increases

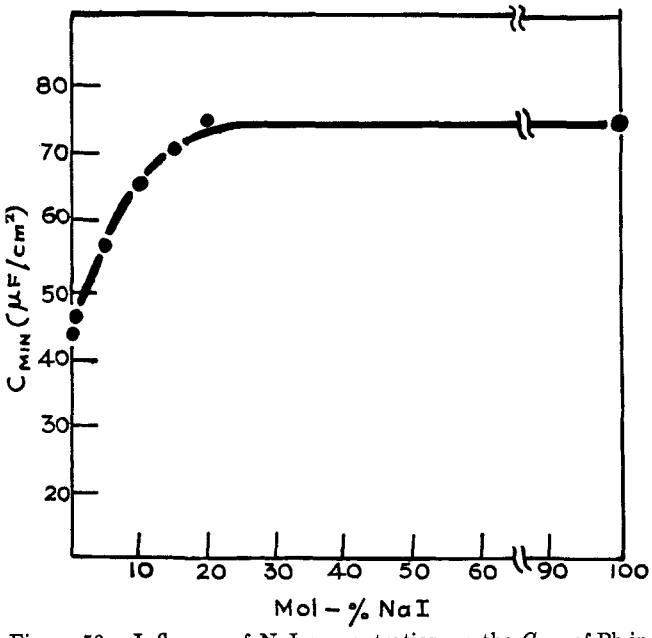

Figure 56.—Influence of NaI concentration on the C_{min} of Pb in NaCl at 820° (reproduced from ref. 297).

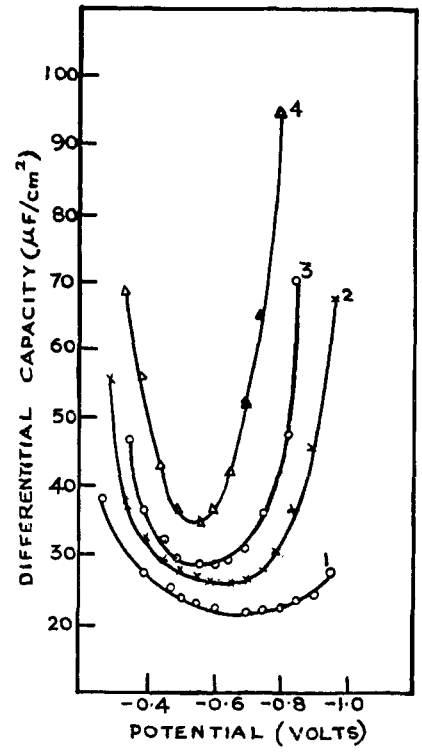

Figure 57.—Differential capacity curves of Pb in KCl–LiCl (1:1) melt. 1, 450°; 2, 600°; 3, 700°; and 4, 800° (reproduced from ref. 297).

with increasing temperature (see Figure 57). (e) The temperature coefficient (per 100°) of the minimum capacity is large for small crystal volumes and small for larger crystal lattices. Thus for NaCl and LiCl, the $dC_{min}/dT/100°$ is 11.0, and for KI and CsCl it is 3.3. For intermediate volumes, for example, KCl–NaCl or KCl–LiCl, it is 5.0.

These features, *viz.*, the capacity minimum and the steep rise, can be understood qualitatively if one first looks at (i) what is hydration in molten salts and (ii) what is the nature of specific adsorption.

1. Minimum Capacity

Since there is no solvent in molten salts as the ions themselves form the solvent, it is reasonable to expect anionic solvation in terms of cations surrounding anions and cationic solvation in terms of anions surrounding cations, giving rise to short-range order, characteristic of such systems. Specific adsorption in aqueous solutions has been defined as dehydration in the direction of the metal. But this concept is untenable in molten salts since there is no solvent. Hence both ions approach the metal thereby determining the minimum capacity depending on their size. But there is yet another factor to be considered, *i.e.*, the electron envelope from the metal which, as a prelude to electron emission, protrudes from the metal surface as the temperature is increased. This effectively reduces the distance between the metal and the locus of the centers of the ions and hence increases the capac-

ity. Further it provides a clue to the increasing capacity with temperature. Thus it is necessary to view the double layer from a structural angle. This is because a calculation of C_{min} from diffuse layer theory shows that C_{min} should decrease with increasing temperature, but actually the reverse is true. Hence any attempt to explain these data from a diffuse layer theory is bound to be futile since the formation of a diffuse layer itself is a consequence of an equilibrium between thermal and electrical forces and thermal forces dominate at higher temperature to promote the diffuseness at higher temperature. Further, one cannot calculate the capacity from the Helmholtz formula using for the thickness the actual radius of one ion only, as in aqueous solutions. One has to take into account the distance between the locus of centers of the nearest ion and the advancing electron envelope of the metal and then calculate the capacity as a parallel combination of two capacitances due to anion and cation.

Recently (73) a quantitative attempt has been made in terms of a distribution function of ions in the diffuse layer taking into account short-range interaction and its perturbation due to the electric field. This approach which leads to an oscillatory distribution of charges in the diffuse layer has been proposed by some other workers (81, 218, 297, and 291 for ionic systems) also. The expression for capacity is

$$C_{min} = \frac{\chi_d^2 \lambda d^2}{8\pi^4} \qquad \text{(Eq. 112)}$$

where d is the distance of first maximum of the oscillatory distribution of charges, λ its wave length, and χ_d the Debye–Hückel length. This equation predicts that C is inversely proportional to $1/T$ whereas experimentally $C \propto T$. This is explained (73) as due to the neglect of the increase of λ. However, no expression for λ as a function of temperature has been deduced and any estimate of it shows it to be not sufficiently sensitive to temperature. The explanation must therefore be regarded as *ad hoc*.

2. Steep Rise

This rise has been attributed (297) to adsorption resulting in a rearrangement of ions in the double layer and the consequent electrostriction of the adsorbed ions. An alternate way of understanding is by invoking adsorption pseudo-capacity prior to discharge or dissolution. This, of course, gives very high capacities, as observed, and also is very reasonable because of the very short potential range available for the electrode to be ideally polarizable. It may be noted that a wide range of ideal polarizability can be obtained only at low temperatures. As temperature is increased, the steep portions on either side approach each other resulting in a diminuition in the range of polarizability (see Figure 57).

C. ELECTROCAPILLARY STUDIES OF ALLOYS AND AMALGAMS (IN MOLTEN AND AQUEOUS MEDIA)

Most of the investigations have been carried out to study the dependence of the electrocapillary maximum on the composition of the metallic phase. The systems studied are Tl–Sb (302), Cd–Bi (192), Sn–Au (167), Sn–Zn (169, 170) (in chloride and iodide melts), Sn amalgam (166), Bi amalgam (166), Tl amalgam (106, 170), Cd amalgam (102), Bi–Te (167), Sn–Cd (194), Te–Tl (191), and Cd–Sn (243). The electrocapillary curves are determined either in molten systems or in aqueous solutions for a few cases. The observed facts are (i) Antonov's law for interfacial tensions is not obeyed. (ii) In some systems like Sn–Au, Sn–Zn, Sn–Hg, Bi–Te, Bi–Hg, in chloride melts, there is a minimum in the surface tension *vs.* composition of the alloy curves. This is not present in iodide melts, indicating the importance of specific adsorption. (iii) The variation of surface tension with melt composition (*in vacuo*) parallels the variation of interfacial tension of the melt–alloy. (iv) The surface concentration of the added metal, for example, Tl in Tl–Hg, is a linear function of the bulk concentration up to 20%. In Sn–Cd system, the surface concentration of Cd is less than in the bulk. (v) The main purpose behind these investigations appears to be to verify Frumkin's theory that the electrocapillary maximum is a function of the composition of the surface layer. Thus in Cd–Bi, Sn–Cd, and Te–Tl, the electrocapillary maximum is found to be a linear function of the added metal, but this is not true for Hg–Tl and Sn–Bi systems. It is also to be noted that in the Te–Tl system, the surface excess determination showed that the Tl layer is uni- or dimolecular.

VIII. NATURE AND SIGNIFICANCE OF THE POTENTIAL OF THE ELECTROCAPILLARY MAXIMUM

It is known from electrostatic considerations that when two metals are in direct contact or through a series of intervening electronic conductors, the measured potential difference is equal to the inner or Galvani potential difference. This assumes the absence of any specific interaction at the interfaces. The equilibrium in this case is achieved by an instantaneous transfer, across the interface, of electrons. But since the charge transferred is of the order of micro-microcoulombs, the two metals can still be regarded for practical purposes as uncharged.

When two metals (A and B) are separated by an electrolyte under ideally polarizable conditions for the two interfaces, it is not possible to obtain equilibrium between the two metals and the potential will be indeterminate. However, the exchange currents due to traces of extraneous substances, which exist even in highly purified solutions, provide the necessary

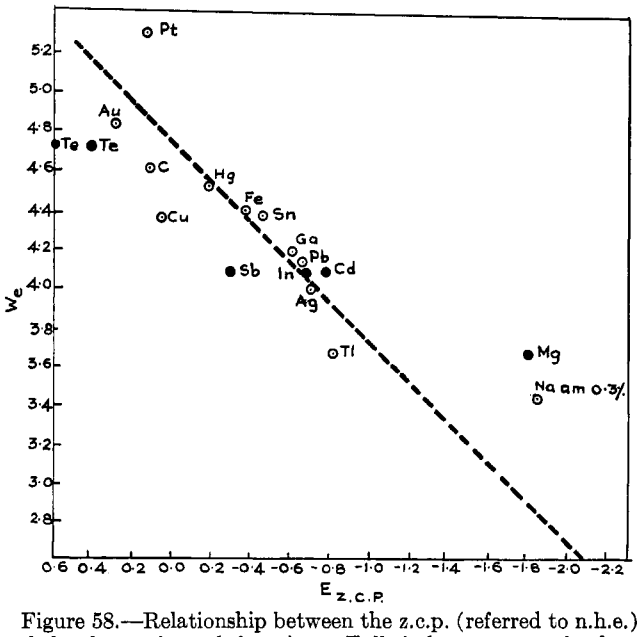

Figure 58.—Relationship between the z.c.p. (referred to n.h.e.) and the electronic work function. Full circles represent the data obtained in molten salts and recalculated on the n.h.e. scale assuming that the differences of z.c.p. values in molten salts and aqueous solutions are identical (reproduced from ref. 101).

micro-microcoulombs at each interface for the attainment of equilibrium.

Thus the measured potential difference can be written as

$$\phi_A - \phi_B = (\psi_A - \psi_B) + (\chi_A - \chi_B) \quad \text{(Eq. 113)}$$

and is equal to the Volta potential difference if $(\chi_A - \chi_B)$ is either small or constant, *i.e.*

$$\phi_A - \phi_B = \psi_A - \psi_B \quad \text{(Eq. 114)}$$

Since $(\psi_A - \psi_B)$ is a measure of the difference in the electronic work functions of the two metals, it is obvious that the difference of z.c.p. of different metals, when measured with respect to a constant reference electrode or an electrode at its z.c.p., should be equal to the differences in the electronic work function (W_e) of the two metals, *i.e.*

$$\phi_A - \phi_B = W_e^A - W_e^B \quad \text{(Eq. 115)}$$

The experimental findings to support Eq. 115 and Eq. 114 are (i) it is found (190–195) that in molten alloy systems, the z.c.p. differences of molten alloys referred to the z.c.p. of Pb are more or less the same as the measured Volta potential differences *in vacuo* (see Table IV). (ii) (a) The electrocapillary maximum differences of Tl–Hg in aqueous solution and molten salts agree (170) with each other. (b) The values of electrocapillary maximum of metals in aqueous solutions and molten salts are virtually the same (101, 171, 292) but for a minor difference of 60–70 mv. when referred to the z.c.p. of Pb (see Table V). (iii) The

TABLE IV

VOLTA POTENTIAL DIFFERENCES AND ZERO CHARGE POINT (193, 195)

Metal	Alloy	Volta potential between the metal and alloy	Difference of z.c.p.'s between the metal and the alloy in KCl + NaCl
Sn	Sn–Te (0.15%)	−0.15	−0.18
Sn	Sn–Tl (23.8%)	0.17	0.24
Sn	Sn–Cd (53%)	0.25	0.27
Bi	Bi–Te (3.6%)	−0.30	−0.25
Bi	Bi–Te (9%)	−0.35	−0.33
Tl	Tl–Te (50.5%)	−0.65	−0.67

TABLE V

POTENTIAL OF Z.C.P. OF VARIOUS METALS REFERRED TO THE Z.C.P. OF Pb IN AQUEOUS AND MOLTEN MEDIA (101)

Metal	Aqueous media	Molten salts
Te	1.25	1.06
Hg	0.46	0.52
Bi	0.29	0.23
Sn	0.19	0.31
Ga	0.04	0.13
Ag	−0.05	0.01
Tl	−0.17	−0.15
Cd	−0.25	−0.12

z.c.p.'s of various metals in aqueous media and melts vary linearly (101) (with a slope of 1) with electronic work function (see Figure 58) when fitted to the equation

$$E_{z.c.p} = W_e - 4.72 \quad \text{(Eq. 116)}$$

This idea was proposed first by Frumkin (88, 101, 106) and supported by others (280, 300). However, the data for both the potential of e.c.m. and the thermionic work function is unreliable with solid metals as both these quantities are extremely sensitive to the presence of traces of impurities. A proper verification can therefore be carried out with liquid metals and amalgams for which both the quantities can be determined accurately. Such a verification has been given by Frumkin (101).

Fact (i) is understandable because of the absence of χ_{dipole} in molten salts. The 60–70-mv. difference observed in (ii) can be attributed to the χ_{dipole} in aqueous solutions and is consistent with the suggested (70, 71) model for water dipoles at the mercury–solution interface. A suggestion that should be made here is that χ_{dipole} for solvents other than water can be obtained by comparison of the electrocapillary maximum in that solvent with the corresponding data in molten salts.

The above discussion refers to the electrocapillary maxima in ideally polarizable systems. Hence whether the electrode is externally polarized or internally polarized (in reversible systems), the potential of point of zero charge should be same. This has been proved (91, 101, 102, 166) by the studies on thallium amalgams and Cd amalgams which show that the z.c.p. value determined under ideally polarizable and non-

polarizable conditions (null solution method) is the same. Thus the notion that the Billiter potential is the electrocapillary maximum or z.c.p. for reversible electrodes (245–248, 280) is misconceived. Had it been the z.c.p. of reversible systems, then it must have been a measure of the work function of the metal. But the value of Billiter potential (+0.475 v. on the hydrogen scale) is remarkably constant with various metals. Since these experiments have been performed without observing any precautions regarding deaeration of the solution or the surface of the metal, the independency of Billiter potential with the nature of the metal suggests that it must be due to some common oxidation–reduction process involving O_2. However, the exact process which is responsible for this value of the potential remains, at present, obscure.

ACKNOWLEDGMENTS.—We wish to thank the following authors for their kind permission to reproduce the figures: Dr. P. L. De Bruyn (Figure 19); Dr. R. Parsons (Figures 26, 28–31, and 33); Dr. V. I. Melik-Gaikazyan (Figure 36); Dr. S. Minc (Figure 46); Dr. B. B. Damaskin (Figure 47); Dr. V. E. Kasarinov (Figure 50); and Dr. E. A. Ukshe (Figure 53, 54, 56, and 57). We wish to express our gratitude to Prof. J. O'M. Bockris of the University of Pennsylvania, for keeping us informed of the developments in his laboratory, and to Professor A. N. Frumkin, Institute of Electrochemistry, Moscow, for advance copies of some papers pertaining to this work and for kind permission to reproduce Figure 58 and Table V. Our thanks are due to Mr. V. K. Venkatesan for discussions and translation of some Russian articles, Mr. P. V. Vasudeva Rao for translation of some German articles, and Mr. S. Lakshmanan for his assistance in the course of this work.

IX. GLOSSARY OF SYMBOLS

a = attraction coefficient between the adsorbed molecules in Frumkin's isotherm

a_+ (a_-) = activity of cations (anions) in the solution

a_{org} = activity of the organic compound in the solution

a_s = activity of the salt in the solution

B = constant of adsorption equilibrium in Frumkin's isotherm

C = differential capacity (measured) of the electrical double layer

C_+ = part of the total differential capacity which is due to cations only and is equal to $Z_+\mathfrak{F}(d\Gamma^+/dE)_{\mu_s}$

C_d = differential capacity of the diffuse layer

C_H = differential capacity of the compact layer or Helmholtz layer or inner layer

$C_{\theta=0}$ = differential capacity when $\theta = 0$

$C_{\theta=1}$ = differential capacity when $\theta = 1$

C_b = differential capacity of the base electrolyte, *i.e.*, in the absence of added organic compounds

C_{dipole} = capacitative contribution of water dipoles to the measured capacity

$C_{double\ layer}$ = capacity of the electrical double layer due to ions only

c = molar concentration of ions in the solution

c_{org} = molar concentration of the neutral organic species

D = bulk dielectric constant of water

E = potential difference at an ideally polarizable interface as read on the potentiometer

E^+ (E^-) = potential difference at an ideally polarizable interface when the reference electrode is reversible to cations (anions) of the salt solution

$E_{e.c.m}$ ($E_{z.c.p}$) = potential of the electrocapillary maximum (e.c.m.) or zero charge point (z.c.p.)

E_{ref} = potential of the ideally polarizable electrode measured with respect to a constant reference electrode

E^b = potential of ideally polarizable electrode in the absence of organic compounds in the solution

E_r = potential of the ideally polarizable electrode with reference to the point of zero charge in the absence of organic compounds in the solution

E_N = shift of the potential of zero charge when the coverage changes from $\theta = 0$ to $\theta = 1$

E^{max} = potential of the adsorption–desorption peaks

E_p = the width of the adsorption–desorption peaks in terms of the potential E_r

e_0 = elementary electronic charge

$\mathfrak{F}$ = Faraday's constant

ΔG = nonelectrostatic free energy of adsorption

$\overline{\Delta G}_a$ = electrostatic part of the free energy of adsorption

$\overline{\Delta G}^\circ$ = standard electrochemical free energy of adsorption at concentration c_{org} and at a particular value of θ

K_{m-1} = integral capacity of the region between the metal and the inner Helmholtz plane

K_{1-2} = integral capacity of the region between the inner Helmholtz plane and the outer Helmholtz plane

K_s = integral capacity due to the solvent

k_0 = dielectric constant when the dipoles cannot rotate (according to Mott and Watts-Tobin)

K_{org} = integral capacity of organic species ($= \epsilon/2\pi l$)

k = Boltzmann's constant

l = length of the organic molecule

N = Avagadro's number

N_d = number of dipoles on 1 cm.^{2} of the surface

N_T = total number of water dipoles, *i.e.*, ($N\uparrow + N\downarrow$) at the interface

$N\uparrow$ = number of water molecules standing up at the interface

$N\downarrow$ = number of water molecules standing down at the interface

n_i = number of specifically adsorbed ions on 1 cm.^{2} of the surface

n_0 = number of ions/cc. in the bulk of the solution

M = Madelung constant

q^β or q = charge density on the solution side of the electrical double layer

q_M = surface charge density on the metal

q_1 = quantity of the specifically adsorbed charge (*i.e.*, the charge in the inner Helmhotz plane)

q_d = charge density due to the charges in the diffuse layer or Gouy plane

$q_{\theta=0}$ = surface charge density of the metal when $\theta = 0$ at E_r

$q_{\theta=1}$ = surface charge density of the metal when $\theta = 1$ at E_r

$q_{M,inflection}$ = the charge on the metal at which an inflexion in the q_1 *vs.* q_M curves is observed

$q_{M,hump}$ = charge on the metal at which the hump in capacity curves is noticed

R = gas constant

r = distance between the neighboring ions in the specifically adsorbed plane
r_i = radius of the ith ion
S_s = surface excess of entropy
T = absolute temperature
w_e^A (w_e^B) = electronic work function of the metal A (B)
X = field strength in the compact layer, which is equal to $4\pi q_M/\epsilon$
$x_{salt(x_{HO_2})}$ = mole fraction of the salt (water) in the solution
x_1 = distance between the metal and the inner Helmholtz plane
x_2 = distance between the metal and the outer Helmholtz plane
Z_+ (Z_-) = valence of the cation (anion) including sign
z = absolute value of the valence of an ion
α = the metallic phase of an ideally polarizable electrode
β = nonmetallic phase of an ideally polarizable electrode
β' = distance between the metal and the inner Helmholtz plane (according to Grahame)
Γ_i = Gibbs' surface excess of the ith component in the system. A superscript when used refers to the phase in which the component is present and a subscript, to the species concerned
Γ^+ (Γ^-) = Gibbs' surface excess of cations (anions)
Γ_{org} = surface excess of the organic molecules
Γ_m = surface excess of organic molecules when the bulk concentration of organic substance is infinite
γ = interfacial tension
γ' = distance between the inner Helmholtz plane and the outer Helmholtz plane (according to Grahame)
$\gamma_{e.c.m}$ = interfacial tension at the potential of electrocapillary maximum
γ^b = interfacial tension of the base electrolyte, *i.e.*, in the absence of organic compounds
δ = distance between the inner Helmholtz plane and its reflection in the bulk with reference to the outer Helmholtz plane
δ_i = diameter of the ion
ϵ = effective dielectric constant in the compact layer
ϵ' = effective dielectric constant in the Helmholtz layer in the presence of organic molecules
ϵ_{org} = dielectric constant of organic molecule in the inner region
ϵ_ω = dielectric constant of the water molecule in the inner region
Θ = fraction of the surface covered by the organic molecules
$\bar{\mu}_i$ = electrochemical potential of the ith component in the system. A superscript when used refers to the phase and a subscript, to the component in the bulk
μ_i = chemical potential of the ith component in the system
μ = chemical potential of the neutral organic species
μ_a = chemical potential of the salt
μ_w = dipole moment of the water molecule
μ_d = dipole moment of the dipole
μ_- (μ_+) = chemical potential of the anion (cation)
ν^+ (ν^-) = number of cations (anions) formed by dissociation of one molecule of the electrolyte
ξ^b = ξ of the base electrolyte, *i.e.*, in the absence of organic compounds (see Eq. 11)
ϕ^β = inner potential of the phase β
ϕ^α (ϕ_A) (ϕ_B) = inner potential of the phase α (*i.e.*, metal or A or B)
ϕ_m = potential of the metal surface with respect to the interior of the solution taken as zero
ϕ_1 = potential of the inner Helmholtz plane with respect to the interior of the solution taken as zero
ϕ_2 = potential of the Gouy plane with respect to the interior of the solution taken as zero
$\Delta\phi_{ion}$ = contribution to the measured potential from the specifically adsorbed ions
$\Delta\phi_{org}$ = contribution to the measured potential from the adsorbed organic species
χ = potential difference due to surface dipoles (subscript in the text refers to the species, except A or B, for which the surface potential is between surface A or B and vacuum)
ψ^u = experimentally observed potential drop across the Helmholtz layer after correcting for the potential of e.c.m. of an unadsorbed electrolyte and ϕ_2
ψ_{m-2} = potential drop across the compact layer
ψ_A = Volta potential of the metal A
ψ_B = Volta potential of the metal B

XI. REFERENCES

(1) Abraham, M., and Becker, R., "Classical Theory of Electromagnetism," Hafner Publishing Co., New York, N. Y., 1951, p. 28.
(2) Anderson, T. N., and Bockris, J. O'M., *Electrochim. Acta*, **9**, 347 (1964).
(3) Anderson, T. N., Perkins, R. S., and Eyring, H., *J. Am. Chem. Soc.*, **86**, 4496 (1964).
(4) Antropov, L. I., *J. Indian Chem. Soc.*, **35**, 309 (1958).
(5) Ayazyan, E. O., *Dokl. Akad. Nauk SSSR*, **100**, 473 (1955); *Chem. Abstr.*, **49**, 11532 (1955).
(6) Balashova, N. A., *Z. physik. Chem.* (Leipzig), **207**, 340 (1957).
(7) Balashova, N. A., *Electrochim. Acta*, **7**, 559 (1962).
(8) Balashova, N. A., and Merkulova, N., "Soviet Electrochemistry," Vol. 1, Consultants Bureau, New York, N. Y., 1961, p. 23.
(9) Banta, M. C., and Hackerman, N., *J. Electrochem. Soc.*, **111**, 114 (1964).
(10) Barradas, R. G., Ph.D. Thesis, University of Ottawa, 1960.
(11) Barradas, R. G., and Conway, B. E., *Electrochim. Acta*, **5**, 349 (1961).
(12) Beloglazov, S. M., *Uch. Zap. Permsk. Gos. Univ.*, **19**, 43 (1961); *Chem. Abstr.*, **58**, 7605 (1963).
(13) Birintseva, T. P., and Kabanov, B. N., *Zh. Fiz. Khim.*, **33**, 844 (1959).
(14) Blomgren, E., and Bockris, J. O'M., *Nature*, **186**, 305 (1960).
(15) Blomgren, E., and Bockris, J. O'M., *J. Phys. Chem.*, **63**, 1475 (1959).
(16) Blomgren, E., Bockris, J. O'M., and Jesch, C., *J. Phys. Chem.*, **65**, 2000 (1961).
(17) Bockris, J. O'M., *Quart. Rev.* (London), **3**, 173 (1949).
(18) Bockris, J. O'M., personal communication, 1964.
(19) Bockris, J. O'M., and Conway, B. E., *J. Chem. Phys.*, **28**, 707 (1958).
(20) Bockris, J. O'M., Devanathan, M. A. V., and Muller, K., *Proc. Roy. Soc.* (London), **A274**, 55 (1963).
(21) Bockris, J. O'M., Green, M., and Swinkels, D. A. J., *J. Electrochem. Soc.*, **111**, 743 (1964).
(22) Bockris, J. O'M., and Swinkels, D. A. J., *J. Electrochem. Soc.*, **111**, 736 (1964).

(23) Borisova, T. I., and Ershler, B. V., *Zh. Fiz. Khim.*, **24**, 337 (1950).
(24) Borisova, T. I., Ershler, B. V., and Frumkin, A. N., *Zh. Fiz. Khim.*, **22**, 925 (1948).
(25) Bowden, F. P., and Young, L., *Nature*, **3**, 235 (1950).
(26) Breiter, M. W., *Electrochim. Acta*, **7**, 533 (1962).
(27) Breiter, M. W., *J. Electrochem. Soc.*, **109**, 42 (1962).
(28) Breiter, M. W., General Electric Research Laboratory, Report No. 63-RL-(3310M), April 1963.
(29) Breiter, M. W., *Electrochim. Acta*, **8**, 925 (1963).
(30) Breiter, M. W., *J. Electroanal. Chem.*, **8**, 230 (1964).
(31) Breiter, M. W., and Delahay, P., *J. Am. Chem. Soc.*, **81**, 2938 (1959).
(32) Brodd, R. J., and Hackerman, N., *J. Electrochem. Soc.*, **104**, 704 (1957).
(33) Bukun, N. G., and Ukshe, E. A., *Zh. Fiz. Khim.*, **37**, 1401 (1963).
(34) Butler, J. A. V., *Proc. Roy. Soc.* (London), **A122**, 399 (1929).
(35) Butler, J. A. V., "Electrocapillarity," Chemical Publishing Co., Inc., New York, N. Y., 1940.
(36) Conway, B. E., and Barradas, R. G., *Electrochim. Acta*, **5**, 319 (1961).
(37) Conway, B. E., and Barradas, R. G., "Transactions of the Symposium on Electrode Processes," E. Yeager, Ed., John Wiley and Sons, Inc., New York, N. Y., 1961, p. 299.
(38) Conway, B. E., Bockris, J. O'M., and Ammar, I. A., *Trans. Faraday Soc.*, **47**, 756 (1951).
(39) Conway, B. E., Barradas, R. G., and Zawidski, T., *J. Phys. Chem.*, **62**, 676 (1958).
(40) Craxford, S. R., *Trans. Faraday Soc.*, **36**, 85 (1940).
(41) Craxford, S. R., Gatty, O., and McKay, H. A. C., *Phil. Mag.*, **22**, 359 (1936).
(42) Craxford, S. R., Gatty, O., and Philpot, J. St. L., *Phil. Mag.*, **14**, 849 (1933); **17**, 54 (1934); **19**, 965 (1935).
(43) Damaskin, B. B., *Zh. Fiz. Khim.*, **32**, 2199 (1958).
(44) Damaskin, B. B., *Russ. Chem. Rev.*, **30**, 78 (1961).
(45) Damaskin, B. B., *Dokl. Akad. Nauk SSSR*, **144**, 1073 (1962).
(46) Damaskin, B. B., *Zh. Fiz. Khim.*, **37**, 2483 (1963).
(47) Damaskin, B. B., *Electrochim. Acta*, **9**, 231 (1964).
(48) Damaskin, B. B., and Grigorjev, N. B., *Dokl. Akad. Nauk SSSR*, **147**, 135 (1962).
(49) Damaskin, B. B., and Ivanova, R. V., *Zh. Fiz. Khim.*, **38**, 176 (1964).
(50) Damaskin, B. B., Menshutkina, I. P., Gerovich, V. M., and Kaganovich, R. I., *Zh. Fiz. Khim.*, **38**, 1797 (1964).
(51) Damaskin, B. B., and Nikolaeva-Fedorovich, N. V., *Zh. Fiz. Khim.*, **35**, 1279 (1961).
(52) Damaskin, B. B., Nikolaeva-Fedorovich, N. V., and Frumkin, A. N., *Dokl. Akad. Nauk SSSR*, **121**, 129 (1958).
(53) Damaskin, B. B., Nikolaeva-Fedorovich, N. V., and Ivanova, R. V., *Zh. Fiz. Khim.*, **34**, 894 (1960).
(54) Damaskin, B. B., and Povarov, Yu. M., *Dokl. Akad. Nauk SSSR*, **140**, 394 (1961).
(55) Delahay, P., *Ann. Rev. Phys. Chem.*, **8**, 229 (1957).
(56) Devanathan, M. A. V., Ph.D. Thesis, London, 1951.
(57) Devanathan, M. A. V., *Trans. Faraday Soc.*, **50**, 373 (1954).
(58) Devanathan, M. A. V., *Proc. Roy. Soc.* (London), **A264**, 133 (1961).
(59) Devanathan, M. A. V., *Proc. Roy. Soc.* (London), **A267**, 256 (1962).
(60) Devanathan, M. A. V., "Introduction to Modern Electrochemistry," in press.
(61) Devanathan, M. A. V., in preparation.
(62) Devanathan, M. A. V., and Canagaratna, S. G., *Electrochim. Acta*, **8**, 77 (1963).
(63) Devanathan, M. A. V., and Fernando, M. J., *Trans. Faraday Soc.*, **58**, 368 (1962).
(64) Devanathan, M. A. V., Muller, K., and Bockris, J. O'M., paper presented at the Los Angeles Meeting of the Electrochemistry Society, May 1962.
(65) Devanathan, M. A. V., and Peries, P., *Trans. Faraday Soc.*, **50**, 1236 (1954).
(66) Devanathan, M. A. V., and Ramakrishnaiah, K., in preparation.
(67) Devanathan, M. A. V., and Tilak, B. V. K. S. R. A., paper presented at the Symposium on Chemical and Nonchemical Interactions, Gorakhpur, 1965.
(68) Devanathan, M. A. V., and Tilak, B. V. K. S. R. A., in preparation.
(69) Devanathan, M. A. V., and Tilak, B. V. K. S. R. A., in preparation.
(70) Devanathan, M. A. V., and Tilak, B. V. K. S. R. A., unpublished results.
(71) Devanathan, M. A. V., and Tilak, B. V. K. S. R. A., in preparation.
(72) Devanathan, M. A. V., and Tilak, B. V. K. S. R. A., unpublished results.
(73) Dogonadse, R. R., and Chismadzhev, U. A., *Dokl. Akad. Nauk SSSR*, **157**, 944 (1964).
(74) Dojlido, J., and Behr, B., *Roczniki Chem.*, **37**, 1043 (1963).
(75) Doss, K. S. G., Rangarajan, S. K., and Narayan, R., in preparation.
(76) Eda, K., *J. Chem. Soc. Japan*, **80**, 343, 347, 349, 461, 708 (1959).
(77) Eda, K., *J. Chem. Soc. Japan*, **81**, 689, 875, 879 (1960).
(78) Eda, K., and Tamamushi, B., *Proc. Intern. Congr. Surface Activity, 3rd, Cologne, 1960*, Vol. 2, p. 291.
(79) Epelboin, I., and Viet, L., *J. chim. phys.*, **60**, 857 (1963).
(80) Ershler, B. V., *Zh. Fiz. Khim.*, **20**, 679 (1956).
(81) Esin, O. A., *Zh. Fiz. Khim.*, **30**, 3 (1956).
(82) Esin, O. A., and Markov, B. F., *Acta Physicochem. URSS*, **10**, 353 (1939).
(83) Esin, O. A., and Shikov, V. M., *Zh. Fiz. Khim.*, **17**, 236 (1943).
(84) Fernando, M. J., M.S. Thesis, University of Ceylon, 1960.
(85) Freyberger, W. L., and De Bruyn, P. L., *J. Phys. Chem.*, **61**, 586 (1957).
(86) Frumkin, A. N., *Z. physik. Chem.* (Leipzig), **116**, 466 (1925).
(87) Frumkin, A. N., *Z. physik.*, **35**, 792 (1926).
(88) Frumkin, A. N., *Colloid Symp. Ann.*, **7**, 89 (1930).
(89) Frumkin, A. N., *Usp. Khim.*, **4**, 938 (1935).
(90) Frumkin, A. N., *Vestn. Mosk. Univ., Ser. II: Khim.*, **9**, 37 (1952).
(91) Frumkin, A. N., *Z. Electrochem.*, **59**, 807 (1955).
(92) Frumkin, A. N., *Zh. Fiz. Khim.*, **30**, 2066 (1956).
(93) Frumkin, A. N., *Proc. Intern. Congr. Surface Activity, 2nd, London, 1957*, Vol. 3, p. 58.
(94) Frumkin, A. N., "Surface Phenomena in Chemistry and Biology," Pergamon Press, London, 1958, p. 189.
(95) Frumkin, A. N., "Transactions of the Symposium on Electrode Processes," E. Yeager, Ed., John Wiley and Sons, Inc., New York, N. Y., 1961, p. 1.
(96) Frumkin, A. N., *J. Electrochem. Soc.*, **107**, 461 (1960).
(97) Frumkin, A. N., *Electrochim. Acta*, **5**, 265 (1961).
(98) Frumkin, A. N., "Advances in Electrochemistry and Electrochemical Engineering," Vol. 3, P. Delahay, Ed., Interscience Publishers, New York, N. Y., 1963, Chapter 5.
(99) Frumkin, A. N., *Electrochim. Acta*, **9**, 465 (1964).
(100) Frumkin, A. N., *J. Electroanal. Chem.*, **7**, 152 (1964).

(101) Frumkin, A. N., *Kem. Tidsskr.*, in press.
(102) Frumkin, A. N., and Cirves, F. J., *J. Phys. Chem.*, **34**, 74 (1930).
(103) Frumkin, A. N., Damaskin, B. B., and Nikolaeva-Fedorovich, N. V., *Dokl. Akad. Nauk SSSR*, **115**, 751 (1957).
(104) Frumkin, A. N., and Damaskin, B. B., *J. Electroanal. Chem.*, **3**, 36 (1962).
(105) Frumkin, A. N., and Damaskin, B. B., "Modern Aspects of Electrochemistry," Vol. 3, J. O'M. Bockris, Ed., Butterworths, London, 1964.
(106) Frumkin, A. N., and Gorodetskaya, A., *Z. physik. Chem.* (Leipzig), **136A**, 451 (1928).
(107) Frumkin, A. N., Grigoriev, I. V., and Bagotskaya, I. A., *Dokl. Akad. Nauk SSSR*, **157**, 957 (1964).
(108) Frumkin, A. N., and Iofa, Z. A., *Zh. Fiz. Khim.*, **13**, 931 (1939).
(109) Frumkin, A. N., Iofa, Z. A., and Gerovich, M. A., *Zh. Fiz. Khim.*, **30**, 1455 (1956).
(110) Frumkin, A. N., Ivanov, R. V., and Damaskin, B. B., *Dokl. Akad. Nauk SSSR*, **157**, 1202 (1964).
(111) Frumkin, A. N., and Kaganovich, R. I., *Dokl. Akad. Nauk SSSR*, **141**, 670 (1961).
(112) Frumkin, A. N., and Nikolaeva-Fedorovich, N. V., "Progress in Polarography," Vol. 1, Interscience Publishers, New York, N. Y., 1962, p. 223, and references cited therein.
(113) Frumkin, A. N., and Polianovskaya, N. S., *Zh. Fiz. Khim.*, **32**, 157 (1958).
(114) Frumkin, A. N., Polianovskaya, N. S., and Grigoriev, N. V., *Dokl. Akad. Nauk SSSR*, **157**, 1455 (1964).
(115) Frumkin, A. N., and Titievskaya, A., *Zh. Fiz. Khim.*, **31**, 485 (1957).
(116) Gerischer, H., "Advances in Electrochemistry and Electrochemical Engineering," Vol. I, P. Delahay, Ed., Interscience Publishers, New York, N. Y., 1961, Chapter 4.
(117) Gerischer, H., *Ann. Rev. Phys. Chem.*, **12**, 227 (1961).
(118) Gerovich, M. A., *Dokl. Akad. Nauk SSSR*, **86**, 543 (1954).
(119) Gerovich, M. A., *Dokl. Akad. Nauk SSSR*, **105**, 1278 (1955).
(120) Gerovich, M. A., "Soviet Electrochemistry," Vol. 1, Consultants Bureau, New York, N. Y., 1961, p. 34.
(121) Gerovich, M. A., and Olman, O. G., *Zh. Fiz. Khim.*, **28**, 19 (1954).
(122) Gerovich, M. A., and Polyanovskaya, N. S., *Nauchn. Dokl. Vysshei Shkoly, Khim i Khim Tekhnol.*, **4**, 651 (1958).
(123) Gerovich, M. A., and Rybal'Chenko, G. F., *Zh. Fiz. Khim.*, **32**, 109 (1958).
(124) Gierst, L., Bermane, D., and Corbusier, P., *Ric. Sci. Suppl.*, 4, (1959).
(125) Gomer, R., *J. Chem. Phys.*, **21**, 1869 (1953).
(126) Grahame, D. C., *J. Am. Chem. Soc.*, **68**, 301 (1946).
(127) Grahame, D. C., *Chem. Rev.*, **41**, 441 (1947).
(128) Grahame, D. C., *Compt. Rend. CITCE*, **3**, 330 (1951).
(129) Grahame, D. C., *J. Electrochem. Soc.*, **98**, 343 (1951).
(130) Grahame, D. C., *J. Chem. Phys.*, **21**, 1054 (1953).
(131) Grahame, D. C., *J. Am. Chem. Soc.*, **76**, 4819 (1954).
(132) Grahame, D. C., *Ann. Rev. Phys. Chem.*, **6**, 337 (1955).
(133) Grahame, D. C., *J. Chem. Phys.*, **23**, 1725 (1955).
(134) Grahame, D. C., *Z. Elektrochem.*, **59**, 740 (1955).
(135) Grahame, D. C., *J. Am. Chem. Soc.*, **79**, 2093 (1957).
(136) Grahame, D. C., Technical Report to the Office of Naval Research, No. 5, Aug. 1, 1957.
(137) Grahame, D. C., *Anal. Chem.*, **30**, 1736 (1958).
(138) Grahame, D. C., *J. Am. Chem. Soc.*, **80**, 4201 (1958).
(139) Grahame, D. C., *Z. Elektrochem.*, **62**, 264 (1958).
(140) Grahame, D. C., "Soviet Electrochemistry," Vol. 1, Consultants Bureau, New York, N. Y., 1961, p. 5.
(141) Grahame, D. C., "Soviet Electrochemistry," Vol. 1, Consultants Bureau, New York, N. Y., 1961, p. 31.
(142) Grahame, D. C., Larsen, R. P., and Poth, M. A., *J. Am. Chem. Soc.*, **71**, 2978 (1949).
(143) Grahame, D. C., and Parsons, R., *J. Am. Chem. Soc.*, **83**, 1291 (1961).
(144) Grahame, D. C., Poth, M. A., and Cummings, J. I., *J. Am. Chem. Soc.*, **74**, 4422 (1952).
(145) Grahame, D. C., and Soderberg, B. A., *J. Chem. Phys.*, **22**, 449 (1954).
(146) Grahame, D. C., and Whitney, R. B., *J. Am. Chem. Soc.*, **64**, 1548 (1942).
(147) Grantham, D. H., Ph.D. Thesis, Iowa State College of Science and Technology, Ames, Iowa, 1962.
(148) Green, M., "Modern Aspects of Electrochemistry," Vol. 2, J. O'M. Bockris, Ed., Butterworths, London, 1960, p. 343.
(149) Green, M., and Dahms, H., *J. Electrochem. Soc.*, **110**, 466 (1963).
(150) Green, M., and Dahms, H., *J. Electrochem. Soc.*, **110**, 1075 (1963).
(151) Green, M., Swinkels, D. A. J., and Bockris, J. O'M., *Rev. Sci. Instr.*, **33**, 18 (1962).
(152) Gurenkov, B. S., *Zh. Fiz. Khim.*, **30**, 1830 (1956).
(153) Gurney, R. W., "Ionic Processes in Solution," Dover Publications, Inc., New York, N. Y., 1962.
(154) Hansen, R. S., Kelsh, D. J., and Grantham, D. H., *J. Phys. Chem.*, **67**, 2316 (1963).
(155) Hansen, R. S., Minturn, R. E., and Hickson, D. A., *J. Phys. Chem.*, **60**, 1185 (1956).
(156) Hansen, R. S., Minturn, R. E., and Hickson, D. A., *J. Phys. Chem.*, **61**, 953 (1957).
(157) Hickson, D. A., Ph.D. Thesis, Iowa State College, Ames, Iowa, 1958.
(158) Hill, D. L., Hills, G. J., Young, L., and Bockris, J. O'M., *J. Electroanal. Chem.*, **1**, 79 (1959).
(159) Hills, G. J., and Johnson, K. E., *J. Electrochem. Soc.*, **108**, 1013 (1961).
(160) Iofa, Z. A., and Frumkin, A. N., *Acta Physicochem. URSS*, **10**, 473 (1939).
(161) Iofa, Z. A., Ustinskii, B., and Eiman, F., *Zh. Fiz. Khim.*, **13**, 934 (1939).
(162) Iwasaki, I., and De Bruyn, P. L., *J. Phys. Chem.*, **62**, 594 (1958).
(163) Jakuszewski, B., and Kozlowski, Z., *Roczniki Chem.*, **36**, 1873 (1962).
(164) Jenkins, D. A., and Newcombe, R. J., *Electrochim. Acta*, **7**, 685 (1962).
(165) Kabanova, B., Kiseleva, I., and Leikis, D., *Dokl. Akad. Nauk SSSR*, **99**, 805 (1954).
(166) Karpachev, S. V., Kochergin, V. P., and Iordan, E. F., *Zh. Fiz. Khim.*, **22**, 521 (1948).
(167) Karpachev, S., and Rodigina, E., *Zh. Fiz. Khim.*, **23**, 953 (1949).
(168) Karpachev, S., and Stromberg, A., *Z. physik. Chem.* (Leipzig), **A176**, 182 (1936).
(169) Karpachev, S., and Stromberg, A., *Zh. Fiz. Khim.*, **10**, 739 (1937).
(170) Karpachev, S., and Stromberg, A., *Acta Physicochem., URSS*, **12**, 523 (1940).
(171) Karpachev, S., and Stromberg, A., *Acta Physicochem. URSS*, **16**, 331 (1942).
(172) Kasarinov, V. E., *Z. physik. Chem.* (Leipzig), **A226**, 167 (1964).
(173) Kasarinov, V. E., paper presented at the Fifth Seminar on Electrochemistry, C.E.C.R.I., Karaikudi, India, 1965.

(174) Kasarinov, V. E., and Balashova, N. A., *Dokl. Akad. Nauk SSSR*, **157**, 1174 (1964).
(175) Kelsh, D. J., Ph.D. Thesis, Iowa State University, Ames, Iowa, 1962.
(176) Kemball, C., *Proc. Roy. Soc.* (London), **A187**, 53, 73 (1946).
(177) Kemball, C., *Proc. Roy. Soc.* (London), **A190**, 117 (1947).
(178) Kheiftz, V. L., and Krasikov, B. S., *Dokl. Akad. Nauk SSSR*, **94**, 101 (1954).
(179) Kheiftz, V. L., and Krasikov, B. S., *Zh. Fiz. Khim.*, **31**, 1227 (1957).
(180) Kheiftz, V. L., Krasikov, B. S., Sysoeva, V. V., and Guseva, I. V., *Vestn. Leningr. Univ., Ser. Fiz. i Khim.*, No. 1, 127 (1957); *Chem. Abstr.*, **51**, 16043 (1957).
(181) Kirkov, P. A., *Zh. Fiz. Khim.*, **34**, 2375 (1960).
(182) Kirkov, P. A., Konstantinova-Taskovska, D., Cumbelic-Gigova, N., and Vilarova-Babamova, A., *Glasnik Hem. Drushtva, Beograd*, **21**, 129 (1956); *Chem. Abstr.*, **52**, 16082 (1958).
(183) Koenig, F. O., *J. Phys. Chem.*, **38**, 339 (1934).
(184) Koenig, F. O., Wohlers, H. C., and Bandini, D., paper presented at the 14th Comité International de Thermodynamique et de Cińebique Electrochimiques Meeting, Moscow, 1963.
(185) Kolotyrkin, J., and Bune, N., *Zh. Fiz. Khim.*, **29**, 435 (1955).
(186) Korchinskii, G. A., *Zh. Fiz. Khim.*, **34**, 2759 (1960).
(187) Korchinskii, G. A., *Ukr. Khim. Zh.*, **28**, 473 (1962); *Chem. Abstr.*, **57**, 15832 (1962).
(188) Kraskiov, B. S., and Pevnitskaya, M. V., *Vestn. Leningrad Univ., Ser. Fiz. i Khim.*, No. 2, 133 (1958); *Chem. Abstr.*, **52**, 18028 (1958).
(189) Krylov, V. S., *Electrochim. Acta*, **9**, 1247 (1964).
(190) Kuznetsov, V. A., paper presented at the 14th Comité International de Thermodynamique et de Cinébique Electrochimiques Meeting, Moscow, 1963.
(191) Kuznetsov, V. A., Aksenov, V. I., and Klevtsova, M. P., *Dokl. Akad. Nauk SSSR*, **128**, 763 (1959).
(192) Kuznetsov, V. A., D'yakova, T. D., and Mal'tseva, V. P., *Zh. Fiz. Khim.*, **33**, 1551 (1959).
(193) Kuznetsov, V. A., Klevtsova, M. P., Zagaynova, L. S., Vaintraub, L. S., and Korobova, T. A., *Zh. Fiz. Khim.*, **34**, 1345 (1960).
(194) Kuznetsov, V. A., Kochergin, V. P., Tischchenko, N. V., and Pozdnyscheva, E. G., *Dokl. Akad. Nauk SSSR*, **92**, 1197 (1953).
(195) Kuznetsov, V. A., and Zagaynova, L. S., *Dokl. Akad. Nauk SSSR*, **138**, 156 (1961).
(196) Law, J. T., Ph.D. Thesis, London, 1951.
(197) Laitinen, H. A., and Gaur, H. C., *J. Electrochem. Soc.*, **104**, 730 (1957).
(198) Laitinen, H. A., and Mosier, B., *J. Am. Chem. Soc.*, **80**, 2363 (1958).
(199) Laitinen, H. A., and Osteryoung, R. A., *J. Electrochem. Soc.*, **102**, 598 (1955).
(200) Laitinen, H. A., and Roe, D. K., *Collection Czech. Chem. Commun.*, **25**, 3065 (1960).
(201) Laitinen, H. A., Tischer, R. P., and Roe, D. K., *J. Electrochem. Soc.*, **107**, 546 (1960).
(202) Leikis, F., *Dokl. Akad. Nauk SSSR*, **135**, 1429 (1960).
(203) Leikis, D., and Kabanov, B. N., *Tr. Inst. Fiz. Khim. Akad. Nauk SSSR*, **No. 6**, *Novye Metody Fiz.-Khim. Issled.*, **No. 2**, 5 (1957); *Chem. Abstr.*, **53**, 918 (1959).
(204) Leikis, D., and Sevastyanov, E. S., *Dokl. Akad. Nauk SSSR*, **144**, 1320 (1962).
(205) Leikis, D., and Venstrom, E. K., *Dokl. Akad. Nauk SSSR*, **112**, 97 (1957).
(206) Levich, V. G., Kiryanov, V. A., and Krylov, V. S., *Dokl. Akad. Nauk SSSR*, **135**, 1425 (1960).
(207) Levine, S., Bell, G. M., and Calvert, D., *Can. J. Chem.*, **40**, 518 (1962).
(208) Lorenz, W., *Z. physik. Chem.* (Frankfurt), **26**, 424 (1960).
(209) Lorenz, W., Mockel, F., and Muller, W., *Z. physik. Chem.* (Frankfurt), **25**, 145 (1960).
(210) Losev, V., *Dokl. Akad. Nauk SSSR*, **88**, 499 (1953); *Chem. Abstr.*, **50**, 9179 (1956).
(211) Losev, V., and Kabanov, B. N., *Izv. Akad. Nauk SSSR, Otd. Khim. Nauk*, 414 (1957); *Chem. Abstr.*, **51**, 14446 (1957).
(212) Loshkarev, M., Khristov, A., and Kryukova, A., *Zh. Fiz. Khim.*, **23**, 221 (1949).
(213) MacDonald, J. R., *J. Chem. Phys.*, **22**, 1857 (1954).
(214) MacDonald, J. R., and Barlow, C. A., Jr., *J. Chem. Phys.*, **36**, 3062 (1962).
(215) MacDonald, J. R., and Barlow, C. A., Jr., *J. Chem. Phys.*, **39**, 412 (1963).
(216) Mackor, E. L., *Rev. trav. chim.*, **70**, 763 (1951).
(217) Maizlish, R. S., Tverdovskii, I. P., and Frumkin, A. N., *Zh. Fiz. Khim.*, **28**, 87 (1954).
(218) Martynov, G. A., and Deryaguin, B., *Dokl. Akad. Nauk SSSR*, **152**, 140 (1963).
(219) McMullen, J. J., and Hackerman, N., *J. Electrochem. Soc.*, **106**, 341 (1959).
(220) Melik-Gaikazyan, V. I., *Zh. Fiz. Khim.*, **26**, 560 (1952).
(221) Melik-Gaikazyan, V. I., *Zh. Fiz. Khim.*, **26**, 1184 (1952).
(222) Melik-Gaikazyan, V. I., and Dolin, P. I., *Dokl. Akad. Nauk SSSR*, **64**, 409 (1949).
(223) Minc, S., and Brzostowska, M., *Roczniki Chem.*, **34**, 1109 (1960).
(224) Minc, S., and Brzostowska, M., *Roczniki Chem.*, **36**, 1909 (1962).
(225) Minc, S., and Jastrzebska, J., *Roczniki Chem.*, **31**, 1339 (1957).
(226) Minc, S., and Jastrzebska, J., *Dokl. Akad. Nauk SSSR*, **120**, 114 (1958).
(227) Minc, S., and Jastrzebska, J., *J. Electrochem. Soc.*, **107**, 135 (1960).
(228) Minc, S., and Jastrzebska, J., *Roczniki Chem.*, **36**, 1901 (1962).
(229) Minc, S., and Jastrzebska, J., *Roczniki Chem.*, **37**, 507 (1963).
(230) Minc, S., Jastrzebska, J., and Brzostowska, M., *J. Electrochem. Soc.*, **108**, 1160 (1961).
(231) Mohilner, D., *J. Phys. Chem.*, **66**, 724 (1962).
(232) Mott, N. F., Parsons, R., and Watts-Tobin, R. J., *Phil. Mag.*, **7**, 483 (1962).
(233) Mott, N. F., and Watts-Tobin, R. J., *Electrochim. Acta*, **4**, 79 (1961).
(234) Moussa, A. A., Sammour, H. M., and Ghaly, H. A., *Egypt. J. Chem.*, **1**, 165 (1958).
(235) Moussa, A. A., Sammour, H. M., and Ghaly, H. A., *J. Chem. Soc.*, 1269 (1958).
(236) Murtazaev, A. M., *Acta Physicochem. URSS*, **12**, 225 (1940).
(237) Murtazaev, A., and Igamberdyev, I., *Zh. Fiz. Khim.*, **14**, 217 (1940); *Chem. Abstr.*, **36**, 3724 (1942).
(238) Miller, I. R., *Proc. Intern. Congr. Surface Activity, 2nd, London, 1957*, Vol. 3, p. 53.
(239) Miller, I. R., *Electrochim. Acta*, **9**, 1453 (1964).
(240) Miller, I. R., and Grahame, D. C., *J. Am. Chem. Soc.*, **79**, 3006 (1957).
(241) Miller, I. R., and Grahame, D. C., *J. Colloid Sci.*, **16**, 23. (1961).

(242) Narayan, R., Venkatesan, V. K., and Doss, K. S. G., *J. Sci. Ind. Res.* (India), **20B**, 450 (1961).
(243) Naryshkin, I. I., *Trans. Leningrad. Polytech. Inst.*, **188**, 106 (1957).
(244) Nikolaeva-Fedorovich, N. V., Damaskin, B. B., and Petrii, O. A., *Collection Czech. Chem. Commun.*, **25**, 2982 (1960).
(245) Oel, H. J., and Strehlow, H., *Z. physik. Chem.* (Frankfurt), **1**, 241 (1954).
(246) Oel, H. J., and Strehlow, H., *Z. Elektrochem.*, **58**, 665 (1954).
(247) Oel, H. J., and Strehlow, H., *Z. physik. Chem.* (Frankfurt), **4**, 89 (1955).
(248) Oel, H. J., and Strehlow, H., *Z. Elektrochem.*, **59**, 818 (1955).
(249) Ostrowski, Z., Brune, H. A., and Fischer, H., *Electrochim. Acta*, **9**, 175 (1964).
(250) Ostrowski, Z., and Fischer, H., *Electrochim. Acta*, **8**, 1, 37 (1963).
(251) Overbeek, J. Th. G., "Colloid Science 1," H. R. Kruyt, Ed., Elsevier Publishing Corp., Inc., Amsterdam, 1952, Chapter 4.
(252) Palczewska, W., and Wroblowa, H., *Bull. Acad. Polon. Sci., Ser. Chim., Geol. Georgraph.*, **6**, 191 (1958).
(253) Pamfilov, A. V., and Kuzub, V. S., *Ukr. Khim. Zh.*, **28**, 528 (1962); *Chem. Abstr.*, **58**, 229 (1963).
(254) Parry, J. M., and Parsons, R., *Trans. Faraday Soc.*, **59**, 241 (1963).
(255) Parsons, R., "Modern Aspects of Electrochemistry," Vol. I, J. O'M. Bockris, Ed., Academic Press Inc., New York, N. Y., and Butterworths, London, 1954, Chapter 3.
(256) Parsons, R., *Trans. Faraday Soc.*, **51**, 1518 (1955).
(257) Parsons, R., *Proc. Intern. Congr. Surface Activity, 2nd, London, 1957*, Vol. 3, p. 38.
(258) Parsons, R., *Trans. Faraday Soc.*, **55**, 999 (1959).
(259) Parsons, R., *Proc. Roy. Soc.* (London), **A261**, 79 (1961).
(260) Parsons, R., "Advances in Electrochemistry and Electrochemical Engineering," Vol. I, P. Delahay, Ed., Interscience Publishers, New York, N. Y., 1961, Chapter 1.
(261) Parsons, R., "Soviet Electrochemistry," Vol. 1, Consultants Bureau, New York, N. Y., 1961, p. 18.
(262) Parsons, R., *J. Electroanal. Chem.*, **5**, 397 (1963).
(263) Parsons, R., *J. Electroanal. Chem.*, **7**, 136 (1964).
(264) Parsons, R., *J. Electroanal. Chem.*, **8**, 93 (1964).
(265) Parsons, R., and Devanathan, M. A. V., *Trans. Faraday Soc.*, **49**, 404 (1953).
(266) Parsons, R., and Devanathan, M. A. V., *Trans. Faraday Soc.*, **49**, 673 (1953).
(267) Pauling, L., "Nature of Chemical Bond," Cornell University Press, Ithaca, N. Y., 1960.
(268) Payne, R., *J. Electroanal. Chem.*, **7**, 343 (1964).
(269) Peries, P., M.Sc. Thesis, University of Ceylon, 1954.
(270) Petrii, O. A., reference quoted in (105).
(271) Philpot, L. St. J., *Phil. Mag.*, **13**, 775 (1932).
(272) Polianovskaya, N. S., reference quoted in (101).
(273) Popat, P. V., Ph.D. Thesis, University of Texas, 1958.
(274) Popat, P. V., and Hackerman, N., *J. Phys. Chem.*, **62**, 1198 (1958).
(275) Rampolla, R. W., Miller, R. C., and Smyth, C. P., *J. Chem. Phys.*, **30**, 566 (1959).
(276) Randles, J. E. B., reference quoted in (101).
(277) Randles, J. E. B., and White, W., *Z. Elektrochem.*, **59**, 666 (1955).
(278) Riney, J. S., Schmid, G. M., and Hackerman, N., *Rev. Sci. Instr.*, **32**, 588 (1961).
(279) Robertson, W. D., *J. Electrochem. Soc.*, **100**, 194 (1953).
(280) Ruetschi, P., and Delahay, P., *J. Chem. Phys.*, **23**, 697 (1955).
(281) Sams, J. R., Jr., Lees, C. W., and Grahame, D. C., *J. Phys. Chem.*, **63**, 2032 (1959).
(282) Sarmousakis, J. N., and Prager, M. J., *J. Electrochem. Soc.*, **104**, 454 (1957).
(283) Schapink, F. W., Oudeman, M., Leu, K. W., and Helle, J. N., *Trans. Faraday Soc.*, **56**, 415 (1960).
(284) Schmid, G. M., and Hackerman, N., *J. Electrochem. Soc.*, **110**, 440 (1963).
(285) Schuldiner, S., *J. Electrochem. Soc.*, **99**, 488 (1952).
(286) Schwartz, E., Damaskin, B. B., and Frumkin, A. N., *Zh. Fiz. Khim.*, **36**, 2419 (1962).
(287) Smyth, C. P., "Dielectric Behavior and Molecular Structure," McGraw-Hill Book Co., Inc., New York, N. Y., 1955.
(288) Staicopolus, D. N., *J. Electrochem. Soc.*, **108**, 900 (1961).
(289) Stern, O., *Z. Elektrochem.*, **30**, 508 (1924).
(290) Stifman, L. M., footnote 2 in ref. 103.
(291) Stillinger, J., and Kirkwood, J., *J. Chem. Phys.*, **33**, 1282 (1960).
(292) Stromberg, A., and Chukina, T., *Zh. Fiz. Khim.*, **18**, 234 (1944); *Chem. Abstr.*, **39**, 3193 (1945).
(293) Tsa, C.-S., and Iofa, Z. A., *Dokl. Akad. Nauk SSSR*, **131**, 137 (1960).
(294) Ukshe, E. A., and Bukun, N. G., *Zh. Fiz. Khim.*, **35**, 2689 (1961).
(295) Ukshe, E. A., Bukun, N. G., and Leikis, D. I., *Dokl. Akad. Nauk SSSR*, **135**, 1183 (1960).
(296) Ukshe, E. A., Bukun, N. G., and Leikis, D. I., *Zh. Fiz. Khim.*, **36**, 2322 (1962).
(297) Ukshe, E. A., Bukun, N. G., Leikis, D. I., and Frumkin, A. N., *Electrochim. Acta*, **9**, 431 (1964).
(298) Ukshe, E. A., and Levin, A., *Dokl. Akad. Nauk SSSR*, **105**, 119 (1955).
(299) Ukshe, E. A., and Tomshikh, I. V., *Dokl. Akad. Nauk SSSR*, **150**, 347 (1963).
(300) Vasenin, R. M., *Zh. Fiz. Khim.*, **27**, 878 (1953).
(301) Venstrom, E. K., and Rehbinder, P. A., *Dokl. Akad. Nauk SSSR*, **68**, 329 (1949).
(302) Volynskaya, M. P., Kuznetsov, V. A., and Balanova, S. Ya., *Zh. Fiz. Khim.*, **37**, 186 (1963).
(303) Voropajeva, T. N., Derjaguin, B. V., and Kabanov, B. N., *Dokl. Akad. Nauk SSSR*, **128**, 981 (1959).
(304) Vorsina, M. A., and Frumkin, A. N., *Zh. Fiz. Khim.*, **17**, 295 (1943).
(305) Watanabe, A., Tsuji, F., and Ueda, S., *Proc. Intern. Congr. Surface Activity, 2nd, London, 1957*, Vol. 3, p. 94.
(306) Watanabe, A., Tsuji, F., and Ueda, S., *Kolloid-Z.*, **191**, 147 (1963).
(307) Watts-Tobin, R. J., *Phil. Mag.*, **6**, 133 (1961).
(308) Wroblowa, H., and Green, M., *Electrochim. Acta*, **8**, 679 (1963).
(309) Zlata, K., personal communication, 1964.